FORMACIÓN DE LA CUENCA AMAZÓNICA DESDE LA BIOGEOGRAFÍA HISTÓRICA

KAREN ANDREA MÉNDEZ CAMACHO

UNIVERSIDAD INDUSTRIAL DE SANTANDER
FACULTAD DE CIENCIAS
ESCUELA DE BIOLOGÍA
BUCARAMANGA
2017

FORMACIÓN DE LA CUENCA AMAZÓNICA DESDE LA BIOGEOGRAFÍA HISTÓRICA

KAREN ANDREA MÉNDEZ CAMACHO

Trabajo de grado para optar el título de Bióloga

Director
Daniel Rafael Miranda Esquivel
PhD en Ciencias Naturales

UNIVERSIDAD INDUSTRIAL DE SANTANDER
FACULTAD DE CIENCIAS
ESCUELA DE BIOLOGÍA
BUCARAMANGA
2017

To my family for all the support, love, and understanding during all these years of personal growth

ACKNOWLEDGMENTS

We thank Omar Daniel Leon-Alvarado, Juan David Bayona-Serrano, Yelsin Méndez-Camacho, and Natalia Gonzales-Piñeres for the continuous revisions of the manuscript and language, which greatly improved the final version. We also thank all the members of the Laboratorio de Sistemática y Biogeografía who participated in each socialization and contributed feedback in each presentation.

CONTENT

FIGURE LIST

Pag

APPENDICES LIST

Pag

RESUMEN

T´ÍTULO: FORMACIÓN DE LA CUENCA AMAZÓNICA DESDE LA BIOGEOGRAFÍA HISTÓRICA[*]

AUTOR: KAREN ANDREA MÉNDEZ CAMACHO[**]

PALABRAS CLAVES: LACUSTRINO, FOSLIES, PRIORES, RÍOS AMAZÓNICOS, INFERENCIA BAYESIANA, CALIBRACIÓN.

DESCRIPCIÓN:

El objetivo de este estudio fue determinar el rango temporal para la transición de un sistema lacustre a un sistema fluvial como la cuenca Amazónica. Para llevar a cabo este análisis reconstruimos filogenias moleculares calibradas en el tiempo a partir de inferencia bayesiana usando 6 taxa pertenecientes a Amphibia, Aves, Insecta y Mammalia. Usamos datos de secuencias de DNA tanto mitocondrial como nuclear y fósiles como puntos de calibración. Asimismo llevamos a cabo una exploración de priores para cada punto de calibración. Determinamos las barreras de aislamiento para cada filogenia y llevamos cabo un análisis de reconstrucción ancestral usando áreas limitadas por los principales tributarios Amazónicos. Adicionalmente, evaluamos el efecto de diferentes tasas de dispersión a través del tiempo basados en información geológica y biogeográfica. Como resultado obtuvimos que los puntos de calibración para cada filogenia se ajustaron mejor a una distribución lognormal conllevando a una estimación de edad más precisa. Las primeras dispersiones a la cuenca Amazónica ocurrieron desde la Amazonia Occidental en un rango de 16.2 a 10.4 Ma, y los taxa abarcaron la mayoría de las áreas de la cuenca Amazónica entre 12.2 a 6.2 Ma. Adicionalmente, obtuvimos evidencia de 2 ríos -Tocantins y Madeira- actuando como barreras vicariantes. A partir de esto concluimos que la cuenca es una formación vieja ajustándose a una hipótesis de “Amazonas viejo”, sin embargo, nosotros proponemos un rango temporal más amplio que el propuesto en la literatura para el inicio y completa formación del sistema fluvial Amazónico.

---

*[*] Trabajo de Grado

**[**] Facultad de Ciencias. Escuela de Biología. Director: Daniel Rafael Miranda-Esquivel, PhD Ciencias Naturales.

ABSTRACT

TITLE: FORMATION OF THE AMAZON BASIN FROM HISTORICAL BIOGEOGRAPHY[*]

AUTHOR: KAREN ANDREA MÉNDEZ CAMACHO[**]

KEY WORDS: LACUSTRINE, FOSSILS, PRIORS, AMAZONIAN RIVERS, BAYESIAN INFERENCE, CALIBRATION

DESCRIPTION:

The object of this study was to determine the temporal range for the transition from a lacustrine to a fluvial system such as the “Amazon basin”. To carry out this analysis, we reconstructed time-calibrated molecular phylogenies through Bayesian inference for 6 taxa belonging to Amphibia, Aves, Insecta and Mammalia. We used both nuclear and mitochondrial DNA sequence data and fossils as calibration points. We explored the priors for each one. We detected the isolation barriers for each phylogeny and carried out an ancestral reconstruction analysis using areas bounded by major Amazonian rivers. Furthermore, we evaluated the effect of different dispersal rates through time based on geologic and biogeographic information. The results indicate that the calibration points for each phylogeny fitted to a lognormal distribution leading a more precise age estimation. The first dispersals to the Amazon basin occurred to Western Amazonia in a range of 16.2 to 10.4 Ma, and the taxa covered most of the areas of the Amazon basin between 12.2 to 6.2 Ma. Additionally, we obtained evidence of two rivers -Tocantins and Madeira- acting as vicariant barriers. We concluded that the basin is an old formation fitting the "Old Amazon hypothesis," however we propose a wider temporal range than the range proposed in the literature for the beginning and complete formation of the Amazon fluvial system.

---

*[*] Bachelor Thesis

**[**] Facultad de Ciencias. Escuela de Biología. Director: Daniel Rafael Miranda-Esquivel, PhD Ciencias Naturales.

INTRODUCTION

The Amazon basin is renowned for its high biodiversity which has been attributed to different geological events such as the formation of the rivers, in a scenario known as the “Riverine barrier hypothesis”, proposed by Alfred R. Wallace (1852). This hypothesis has been supported by different studies (Maldonado-Coelho et al 2013; dHorta et al 2013), in which the Amazon and its main tributaries have had a prominent role in the evolution of Amazonian biodiversity. Likewise, two geological models supporting this hypothesis have been proposed regarding the date of the formation of the Amazon basin. The “Old Amazon” model suggests that the fluvial system was established during the Late Miocene (10 to 7 Ma) (Hoorn et al 2010) whereas the “Young Amazon” model covers a wider temporal range, with studies agreeing that the basin was completely formed during the Plio-Pleistocene (2.5 Ma) (Horbe et al 2013; Figueiredo et al 2009). Both models have been evaluated using a biogeographical approach (Ribas et al 2011; Fernandes et al 2012), finding evidence that suggests the Amazon basin was formed in the Plio-Pleistocene, supporting the “Young Amazon" hypothesis (Alfaro et al 2015) and also proposed plausible dates for the formation of some of the main Amazonian rivers (Ribas et al 2011; Boubli et al 2015) providing a deeper understanding on how the basin reached its current configuration.

The changes in the Amazonian landscape that led to the formation of the current Amazon basin have been attributed to a series of geological events starting with the gradual uplift of the Eastern Cordillera in the Central Andes, which caused the closure of the Western Andean Portal and created a huge watershed in the Middle Miocene (Antonelli et al 2009) known as the Pebas mega-wetland system (PMWS). Located in Western Amazonia, the PMWS was connected with the Caribbean sea and bounded with the Purus Arch on the east (Figueiredo et al 2009), but many of its aspects are still a matter of discussion (Jaramillo et al 2017). During the Late Miocene the PMWS disappeared (Wesselingh et al 2002) due to the uplift of the Eastern Colombian Andes (15 to 3 Ma) (Mora et al 2008), and as a consequence, the Vaupes Arch was drawn close to the Andes, causing the Orinoco-Amazonas vicariance event (Olivares et al 2013) and gradually reducing the water flux towards the Caribbean (Lundberg et al 1998). Finally, the subsidence of the Purus Arch allowed the eastward extension of the Amazonas River from the Pliocene to the Pleistocene (Nogueira et al 2013). The role of these events in the formation of the modern Amazon basin has been highlighted in different studies (Matos-Maravi et al 2013; Horbe et al 2013). However, there is no agreement on the date in which each one of these events took place and therefore the formation time of the Amazon drainage system is still unresolved (Hoorn et al 2010; Figueiredo et al 2009). Likewise, there is no study that incorporates different taxa belonging to different taxonomic groups, and most studies that cover this question have used secondary calibrations (Buckner et al 2014) and analyses at the population level Ribas et al 2011), hence preventing the evaluation of a possible older formation for the Amazon basin. Therefore, the goal of the present study is to determine the transition date from a lacustrine to a fluvial system -“Amazon basin”-, using taxa from different taxonomic groups. We can establish the possible temporal range in which the disappearance of the Pebas system occurred -the event accepted as the first phase for the formation of the Amazonian river system (Wesselingh et al 2002)-, and the West-East formation of the Amazon fluvial system.

1. Methods

1.1 Selection of taxa

We selected the taxa using the following criteria: (1) We considered taxa with clades currently distributed in the Amazon basin. (2) The taxa must be monophyletic and have clades with divergences covering the temporal ranges proposed for the formation of the Amazon basin (1-11.8 Ma) (Hoorn et al 2010; Figueiredo et al 2009; Ribas et al 2011). (3) The phylogeny must include at least

60 % of its described species with a minimum of three genes using both mitochondrial and nuclear information. (4) The taxa must have fossil records available in the literature for each ingroup (see Appendix S3 in Supporting Information), excluding fossils with uncertain phylogenetic position (Hosner et al 2016; Kay 1997; Kay and Cozzuol 2006).

1.2 Molecular data

We downloaded all nucleotide gene sequences available in GenBank for each taxon (see Appendix S1). Each gene was aligned separately using the multiple sequence alignment (Edgar 2004a) as implemented in MUSCLE v3.8.31 (Edgar 2004b), and the models of nucleotide substitution were selected under the Akaike Information Criterion (AIC) (Akaike 1974) using the modelTest function in the R package 'phangorn' (Schliep 2011).

1.3 Distributional data

For the selected taxa, we obtained the species distributions from the available literature, along with occurrences from the Global Biodiversity Information Facility (GBIF) (www.gbif.org) database, which were reviewed using the distributional ranges described in the literature.

1.4 Phylogenetic reconstruction

We carried out a partitioned phylogenetic analysis under Bayesian Inference (BI) as implemented in MrBayes v3.2.6 (Ronquist et al 2012) via the CIPRES Science Gateway (Miller et al 2010). For each partition we applied the nucleotide model previously selected, and we tested whether the evolutionary rate was constant across the whole phylogeny or whether it varied on each branch. Then, we chose the model that best fitted our data through Bayes Factors (Kass and Raftery 1995). Furthermore, we modeled the relaxed clock using the Independent Gamma Rate model (IGR) (Lepage et al 2007; Bakiu et al 2015), and we applied a fossilized birth-death process (Heath et al 2014; Zhang et al 2016) to model the cladogenetic process.

1.5 Exploration of priors and clock dating

For each calibration point we tested two distributions (exponential and lognormal) and we chose the model that best fitted our data through Bayes Factors (Kass and Raftery 1995). Using the selected parameters, two independent runs were conducted by 30 million generations, sampling every 2000 generations with the first 25\% samples discarded. Both runs consisted of four Metropolis-coupled MCMC chains with default temperatures (delta of 0.09 between heated chains). Each analysis was carried out until the average standard deviation of split frequencies was below 0.05 (Ronquist et al 2012). The convergence between runs was assessed using the effective sample size as reported in Tracer (Rambaut et al 2014), and the potential scale reduction factor (Ronquist et al 2012). The final species tree with divergence times was visualized in Figtree v1.4 (Rambaut 2012). In addition, we also run the analyses without data to determine the impact of calibration points on the posterior estimates.

1.6 Infinite sites

We plotted the posterior means against the 95\% posterior credibility intervals (CI) (Yang and Rannala 2006) for each phylogeny.

1.7 Isolation barriers and ancestral area inference

We determined the potential isolation barriers for each clade following Hovenkamp (1997, 2001) ideas, implemented in the Vicariance Inference Program (VIP) (Arias et al 2011). Furthermore, we performed the reconstruction of the ancestral distribution using areas bounded by major Amazonian rivers (Alfaro et al 2015) (see Appendix S2) and under the Dispersal-Extinction-Cladogenesis (DEC) model (Ree et al 2005; Ree and Smith 2008) as implemented in the R package 'BioGeoBears' (Matzke 2013).

For the reconstruction of ancestral area, we assessed two different biogeographic models, the base model with a constant dispersal rate, and the stratified model with different dispersal rates through time (Ree and Smith 2008). We used the default dispersion rate for all areas in the base model, while for the stratified model we created three models, with three time slices for each one and we designed the dispersal rate matrices based on geologic and biogeographic evidence (Ribas et al 2011; Hoorn et al 2010). The first stratified model was based on the "Young Amazon" hypothesis in which the dispersal rates were low before 11.8 Ma (0.25), and started to increase (0.50) during the temporal range in which the Amazon system began forming (11.8 to 2.5 Ma), and the rates became maximum when the Amazon basin reached its current form and size (after 2.5 Ma). Moreover, the second stratified model was based on the "Old Amazon" hypothesis, in which the rates were intermediate (0.5) in the range of 10-7 Ma, suggesting that the system was mostly formed during this range, and the Amazon basin was completely established after 7 Ma (1). For the third stratified model we used the ranges in which there were changes in the diversification rates according to the lineage-through-time (LTT) plot for all taxa together (see Appendix S9), then we assumed that the rates were low until 17 Ma (0.25), and became intermediate (0.5) between 17-10 Ma, in which a system of great magnitude existed (MWPS). Finally, the rates were maximum in the last 10 Ma to the present, showing that the MWPS drained and the Amazon basin reached its present form during this temporal range. To compare models, we used a log-likelihood difference of two units (Edwards 1992).

1.8 Congruence between events

After obtaining the vicariant events associated with the formation of rivers for each clade through isolation barriers and reconstruction of the ancestral distribution, we checked whether for two or more taxa the same river acted as a vicariant barrier, and also if they shared similar divergence times for that event. The congruence was evaluated for each method separately, and once obtained the clades that matched the two requirements mentioned above, we could propose a date for the formation of a particular river, in order to understand the configuration process of the Amazon basin through years. Finally, we verified if both methodological approaches were congruent in the vicariant events associated with the formation of rivers that each one recovered.

2. Results

2.1 Taxa

The dataset was composed by taxa from four different taxonomic groups: Rhinella (Bufonidae, Amphibia), Cracidae (Aves), Melipona (Apidae, Insecta), Cebidae, Echimyidae, and Stenodermatinae (Mammalia).

2.2 Calibration points

For Mammals, there were fossil information for the ingroup and for the remaining phylogenies we used the fossils available for the outgroup (Cracidae, Melipona and Rhinella).

2.3 Molecular clock

The strict molecular clock was rejected for all genes, except for two ATP7 and COI genes (Stenodermatinae), which showed strong evidence favouring a strict clock model (log difference of 3-5) (see Appendix S4). In order to see the overall impact of these genes on the final topology, we checked the individual topologies of both genes. We found that they produced unresolved topologies, in which COI did not present common nodes and ATP7 presented 2 % of common nodes with respect to the total evidence. Nonetheless, when we removed the ATP7A and COI genes from the complete dataset, it turned out in a less resolved topology (50 % of common nodes) with lower PP (<0.7) than the total evidence analysis.

2.4 Prior and posterior estimates

Although, there was no difference in the obtained topologies, without branch lengths, under both distributions, all calibration points for each phylogeny fitted best to a lognormal distribution, showing the narrowest 95 % confidence intervals (Figure 1). Furthermore, for most of the calibration points, there was overlap between the prior and the posterior distributions with different overlap percentages. For 16 calibration points, the prior overlapped considerably with the posterior (80-100 %). Within of these 16 calibration points, the posterior was narrower for 9 calibration points, the posterior were highly similar to the prior for 3 calibration points, and the posterior was wider, leading to older ages, for 4 calibration points. For the remaining calibration points of this study, the overlap percentage between the prior and posterior was low (30-45 %), leading the posterior to older ages (see Appendix S5). The only exception in which the prior and posterior did not overlap was Pampamys emmonsae (Echimyidae), where the posterior distribution was older and out of the prior with a difference of ~3 Myr (median:17.58 CI95 %: 21.58-14.09 Ma) (see Appendix S5). The absence of this fossil in the analysis led to a wider CI95 % with a difference of 1 Myr (median: 18.84 CI95 %: 23.35-14.68 Ma) than the analysis including this calibration point. The PP did not change between both analyses (100 %). On the other hand, the incorporation of the new fossil record in the Cebuella lineage (Cebidae) led to CI95 % narrower (10-10.9 Ma) and PP higher (100\%) than the analysis without this calibration point (CI95 %: 8.7-4.5 Ma and PP: 73 %). Finally, the analyses without data resulted in unresolved topologies (results not shown).

The posterior age means and confidence intervals fitted best to a straight line under the exponential fossil prior (gray colour), and led to older ages and CI95 % larger than lognormal distribution (red colour) (Figure 1). The taxa with the widest posterior density intervals (low precision) and oldest ages were Melipona (R^2 = 0.76), Rhinella (R^2 = 0.27), followed by Cracidae which has the highest regression value (R^2 = 0.91). On the other hand, the taxon with the highest precision and more recent ages of the entire dataset was Cebidae, presenting the lowest regression value (R^2 = 0.03) (Figure 1). Additionally, Melipona presented the largest slope value (w = 0.44) among all taxa, and Cebidae the lowest value (w = 0.05).

2.5 Isolation barriers and Ancestral reconstruction

In total, we obtained 55 isolation barriers registered for all the analyzed clades (264), which were mostly concentrated in Echimyidae and Melipona. 9 of these 55 isolation barriers were associated with some Amazonian rivers (Tocantins, Madeira, Amazonas, Marañón and Ucayali). However, only two of these nine barriers were congruent between different taxa, matching with the Tocantins (range of 10.85-9.75 Ma) and Madeira rivers (range of 10.40-8.27 Ma). On the other hand, the reconstruction of the ancestral distribution only reported one vicariant event associated with the Negro river. However, this vicariant barrier was not congruent among different taxa, and there was not congruence between both methodological approaches (see Appendix S6).

Although all taxa fitted stratified models, four of them fitted more than one stratified model with a log-likelihood difference of 0.1 to 0.77 (see Appendix S7). Otherwise, Cracidae and Stenodermatinae only fitted the model in which the dispersal rates were intermediate between 11.8 to a 2.5 and the dispersal rates were maximum after 2.5 Ma. For most taxa Rhinella, Melipona, Echimyidae and Cebidae), the first dispersals to the Amazon basin occurred from the Atlantic Forest to some areas of Western Amazonia (Napo, Marañón, and Ucayali) in a temporal range of 16.2 to

10.4 Ma, and all taxa covered most of the areas of the Amazon basin between 12.2 to 6.2 Ma. Nevertheless, for Cebidae and Echimyidae, the first dispersals involved all areas of the Amazon basin, and then they experimented contraction of the ancestral range, but there was not congruence in the temporal range in which this event took place. After the contraction of the ancestral range to the Atlantic Forest and the Andes respectively, both taxa experimented expansions to some areas of Western Amazonia (Ucayali and Napo). For the remaining two taxa, Cracidae and Stenodermatinae, the first dispersals to the Amazon basin occurred from Central America and the Andes respectively in different temporal ranges and out of the suggested ranges for the taxa mentioned above (CI95 %: 3.3-0.99 Ma and 7-3 Ma respectively). Additionally, our data suggests the temporal range for another geological event such as the closure of the Isthmus, which allows colonizations from and toward South America in range between 9.23 to 4.73 Ma.

3. Discussion

3.1 Age estimates

According to the analysis without data, the set of fossils for each phylogeny are not dominating the analysis, and the uncertainty in posterior age estimates is mainly due to limited molecular data, as suggested by the infinite-sites plot (Yang and Rannala 2006) (Figure 1). One exception to this fact was Cracidae with the highest regression value, indicating that the amount of sequence data is very high, and the uncertainties in the posterior estimates are mostly due to uncertainties in the fossil calibrations (Yang and Rannala 2006). The other exception was Melipona with an intermediate regression value suggesting that the most plausible explanation is that the uncertainty is due to fossil data, which is also supported by the fact that the taxon presents the most imprecise fossil calibrations from all taxa, although the value is still low. Therefore, it is not ruled out that both an increased density of taxon-sampling at genome scale and fossil sampling could improve the age estimates (Yang and Rannala 2006) (Figure 1). Although the chosen priors are reasonable for modelling our data; the cases where there is similarity between prior and posterior indicate that the data contain little information about the parameters, and when the prior and posterior did not overlap properly there might be a conflict between the prior and the data (see Appendix S5) (Nascimento et al 2017). However, we noted that the incorporation of the fossil for the clade in which the posterior is older and out of the prior (Foote et al 1999; Smith and Peterson 2002; Sytsma et al 2014), led to a more precise age estimation. Therefore, the fossil records used in the present study are informative (Xie et al 2010) and their incorporation along with the available molecular data increases the precision in posterior time estimates and the support for the clades. Despite that, there is evidence of the effect of limited data. Accordingly adding more genes which fit either a relaxed or strict molecular clock model along with the whole dataset provides more resolved topologies with narrower 95\% confidence intervals, indicating that more genomic information is more suitable for date estimation analysis (Yang and Yoder 2003).

Furthermore, the molecular clock model used here does not incorporate uneven fossil sampling (Drummond et al 2012; Zhang et al 2015), which could have an impact on the posterior age estimates. Thus, the ancient and less precise ages produced in the present study could be due to a lack of internal node constraints which leads to ancient ages (Arcila et al 2015), and this could be highlighted by the fact that the taxon with more fossils and even fossil sampling (Cebidae), presents the more precise date estimates of the entire dataset \citep{bibi2013} and the amount of uncertainty added in the posterior CI is less (Figure 1). On the other hand, our results show that the use of an exponential distribution for calibration points generates older and less precise posterior estimates (Figure 1) (Sauquet et al 2012; Arcila et al 2015), which contrasts with Heads (2012), who suggested that the exponential distribution is useful for generating younger ages than any other distributions, because it has the fewest possible parameters (a single rate parameter). Additionally, our findings are in concordance with Heath (2012) who suggested that the use of exponential distribution can place much higher probabilities on excessively old divergences (exponential distributions have a "fatter tail") (Figure 1).

3.2 Historical Amazon

We found that the Amazon basin began forming between 16.2 to 10.4 Ma with the first dispersals to Western Amazonia. This pattern suggests that possibly the MWPS disappeared for that time, allowing colonization of these areas, which is in concordance with Shephard et al (2010) who by mean of palaeo-geographic maps suggest that the MWPS was reduced greatly in the Middle-late Miocene. Hence, we propose that the Amazon fluvial system probably reached its shape and size in a range from 12.2 to 6.2 Ma (Figure 2), when the taxa extended their distribution to Eastern Amazonia. In general, the temporal range proposed here agrees with the "Old Amazon hypothesis", but we suggest a wider temporal range than the proposed by Hoorn et al (2010). In the same way, our results are not affected by the impact of the number of time slices and different probabilities of dispersal on the range-inheritance scenarios (Ree and Smith 2008) (see Appendix S8), and consequently, we cannot establish the temporal ranges in which there is a change in the dispersal rates according to the geological ranges proposed for the two hypotheses aforementioned (see Appendix S7). Moreover, we demonstrated that large Amazonian rivers can limit species distribution ranges (Moraes et al 2016; Oliveira et al 2017), and we suggest the temporal range for the formation of two of the major Amazonian rivers. The dates proposed here differ from Ribas et al (2011) and Alfaro et al (2015), who suggested that the Tocantins river was formed between 0.8-0.3 Ma and Buckner et al (2014) who suggested that the Madeira river was formed about 5 Ma. It is worth noting that the methods used in this study to identify rivers as vicariant barriers are based on different algorithms, then they provided different results. The main differences between our findings and other authors who propose recent dates for rivers are the type of analyses and the implemented data. Some authors incorporate both, populations and species (Ribas et al 2011; Buckner et al 2014) and some others only took into account mitochondrial genes (Alfaro et al 2015) or secondary calibrations (Buckner et al 2014, Alfaro et al 2015), and did not carry out an exploration of priors. Despite the differences with other studies, we found that both rivers are old formations and they fit the pattern proposed here.

The temporal range proposed here for the formation of the Amazon fluvial system agrees with geological processes that occurred during that time: as Hoorn et al (1995, 2010) who suggest that the formation of the Amazon river has been attributed to Andean uplift and our findings are in concordance with stratigraphic studies about the emergence of the Eastern Cordillera of the Colombian Andes (Mora et al 2008), and with paleobotanic observations, which suggest that elevations of the eastern Colombian Andes were homogeneous between Early-Middle Miocene and Pliocene times (Gregory-Wodzicki 2000), and also with studies about the sedimentary flux of the Foz do Amazonas, which show increasing efflux through time with higher values since Mid-Miocene times (Rodríguez Tribaldos et al 2017; Macgregor 2012}. Besides, our results are in discordance with other geological events like: the date of the activation of the Vaupes arch in the Late Miocene (Olivares et al 2013) and the subsidence of the Purus Arch that allowed the Amazon to flow to the east. Although in the present study we cannot establish the exact range of its subsidence we can say that it was in the Middle Miocene, which contrasts with the proposals to date (Nogueira et al 2013; Figueiredo et al 2009). The performance of these geological events together has been broadly accepted to be the main causes of the disappearance of the MWPS. Notwithstanding, we were unable to establish whether it was the result of several marine transgressions (Jaramillo et al 2017) or if it was a continuous event covering a wide temporal range (Hoorn et al 2010). In addition, our data describes a pattern for the possible temporal range of the closure of the Panama isthmus, which covers the ranges proposed by Bacon et al (2015), and it is in discordance with Montes et al (2015) and ODea et al (2016). Furthermore, our biogeographic reconstructions and divergence time estimates support a scenario where cracids colonized and diversified in South America following uplift of the Panamanian Isthmus (Hosner et al 2016; Mayr 1946), which happened in a more recent temporal range than the proposed for the remaining taxa. The other exception was Stenodermatinae where the dispersals to the Amazon basin also happened in a more recent date but we cannot establish the involved event in this scenario, and therefore there is not a general pattern found for both taxa.

REFERENCES

Akaike, H. (1974). A new look at the statistical model identification. *IEEE transactions on automatic control*, *19*(6), 716-723.

Alfaro, J. W. L., Boubli, J. P., Paim, F. P., Ribas, C. C., da Silva, M. N. F., Messias, M. R., ... & Pinho, G. M. (2015). Biogeography of squirrel monkeys (genus Saimiri): South-central Amazon origin and rapid pan-Amazonian diversification of a lowland primate. *Molecular phylogenetics and evolution*, *82*, 436-454.

Wallace, A. R. (1854). On the monkeys of the Amazon. *Journal of Natural History*, *14*(84), 451-454.

Ali, J. R. (2012). Colonizing the Caribbean: is the GAARlandia land-bridge hypothesis gaining a foothold?. *Journal of Biogeography*, *39*(3), 431-433.

Antonelli, A., Nylander, J. A., Persson, C., & Sanmartín, I. (2009). Tracing the impact of the Andean uplift on Neotropical plant evolution. *Proceedings of the National Academy of Sciences*, *106*(24), 9749-9754.

Arcila, D., Pyron, R. A., Tyler, J. C., Ortí, G., & Betancur-R, R. (2015). An evaluation of fossil tip-dating versus node-age calibrations in tetraodontiform fishes (Teleostei: Percomorphaceae). *Molecular Phylogenetics and Evolution*, *82*, 131-145.

Arias, J. S., Szumik, C. A., & Goloboff, P. A. (2011). Spatial analysis of vicariance: a method for using direct geographical information in historical biogeography. *Cladistics*, *27*(6), 617-628.

Bacon, C. D., Silvestro, D., Jaramillo, C., Smith, B. T., Chakrabarty, P., & Antonelli, A. (2015). Biological evidence supports an early and complex emergence of the Isthmus of Panama. *Proceedings of the National Academy of Sciences*, *112*(19), 6110-6115.

Bakiu, R., Korro, K., & Santovito, G. (2015). Positive selection effects on the biochemical properties of mammal pyroglutamylated RFamide peptide receptor (QRFPR). *Italian journal of zoology*, *82*(3), 309-326.

Bibi, F. (2013). A multi-calibrated mitochondrial phylogeny of extant Bovidae (Artiodactyla, Ruminantia) and the importance of the fossil record to systematics. *BMC Evolutionary Biology*, *13*(1), 166.

Boubli, J. P., Ribas, C., Alfaro, J. W. L., Alfaro, M. E., da Silva, M. N. F., Pinho, G. M., & Farias, I. P. (2015). Spatial and temporal patterns of diversification on the Amazon: A test of the riverine hypothesis for all diurnal primates of Rio Negro and Rio Branco in Brazil. *Molecular Phylogenetics and Evolution*, *82*, 400-412.

Buckner, J. C., Alfaro, J. W. L., Rylands, A. B., & Alfaro, M. E. (2015). Biogeography of the marmosets and tamarins (Callitrichidae). *Molecular phylogenetics and evolution*, *82*, 413-425.

Drummond, A. J., Suchard, M. A., Xie, D., & Rambaut, A. (2012). Bayesian phylogenetics with BEAUti and the BEAST 1.7. *Molecular biology and evolution*, *29*(8), 1969-1973.

d’Horta, F. M., Cuervo, A. M., Ribas, C. C., Brumfield, R. T., & Miyaki, C. Y. (2013). Phylogeny and comparative phylogeography of Sclerurus (Aves: Furnariidae) reveal constant and cryptic diversification in an old radiation of rain forest understorey specialists. *Journal of Biogeography*, *40*(1), 37-49.

Edgar, R. C. (2004a). MUSCLE: a multiple sequence alignment method with reduced time and space complexity. *BMC bioinformatics*, *5*(1), 113.

Edgar, R. C. (2004b). MUSCLE: multiple sequence alignment with high accuracy and high throughput. *Nucleic acids research*, *32*(5), 1792-1797.

Edwards, A. W. F. (1992). Likelihood Johns Hopkins University Press. *Baltimore, Maryland, USA*.

Fernandes, A. M., Wink, M., & Aleixo, A. (2012). Phylogeography of the chestnut-tailed antbird (Myrmeciza hemimelaena) clarifies the role of rivers in Amazonian biogeography. *Journal of Biogeography*, *39*(8), 1524-1535.

Figueiredo, J. J. J. P., Hoorn, C., Van der Ven, P., & Soares, E. (2009). Late Miocene onset of the Amazon River and the Amazon deep-sea fan: Evidence from the Foz do Amazonas Basin. *Geology*, *37*(7), 619-622.

Foote, M., Hunter, J. P., Janis, C. M., & Sepkoski, J. J. (1999). Evolutionary and preservational constraints on origins of biologic groups: divergence times of eutherian mammals. *Science*, *283*(5406), 1310-1314.

Gregory-Wodzicki, K. M. (2000). Uplift history of the Central and Northern Andes: a review. *Geological Society of America Bulletin*, *112*(7), 1091-1105.

Heads, M. (2012). Bayesian transmogrification of clade divergence dates: a critique. *Journal of Biogeography*, *39*(10), 1749-1756.

Heath, T. A. (2012). A hierarchical Bayesian model for calibrating estimates of species divergence times. *Systematic biology*, *61*(5), 793-809.

Hoorn, C., Guerrero, J., Sarmiento, G. A., & Lorente, M. A. (1995). Andean tectonics as a cause for changing drainage patterns in Miocene northern South America. *Geology*, *23*(3), 237-240.

Hoorn, C., Wesselingh, F. P., Ter Steege, H., Bermudez, M. A., Mora, A., Sevink, J., ... & Jaramillo, C. (2010). Amazonia through time: Andean uplift, climate change, landscape evolution, and biodiversity. *Science*, *330*(6006), 927-931.

Horbe, A. M. C., Motta, M. B., de Almeida, C. M., Dantas, E. L., & Vieira, L. C. (2013). Provenance of Pliocene and recent sedimentary deposits in western Amazônia, Brazil: Consequences for the paleodrainage of the Solimões-Amazonas River. *Sedimentary Geology*, *296*, 9-20.

Hosner, P. A., Braun, E. L., & Kimball, R. T. (2016). Rapid and recent diversification of curassows, guans, and chachalacas (Galliformes: Cracidae) out of Mesoamerica: Phylogeny inferred from mitochondrial, intron, and ultraconserved element sequences. *Molecular phylogenetics and evolution*, *102*, 320-330.

Hovenkamp, P. (1997). Vicariance events, not areas, should be used in biogeographical analysis. *Cladistics*, *13*(1-2), 67-79.

Hovenkamp, P. (2001). A direct method for the analysis of vicariance patterns. *Cladistics*, *17*(3), 260-265.

Jaramillo, C., Romero, I., D'Apolito, C., Bayona, G., Duarte, E., Louwye, S., ... & Mora, A. (2017). Miocene flooding events of western Amazonia. *Science Advances*, *3*(5), e1601693.

Kass, R. E., & Raftery, A. E. (1995). Bayes factors. *Journal of the american statistical association*, *90*(430), 773-795.

Kay, R. F. (1997). A new small platyrrhine and the phyletic position of Callitrichinae. *Vertebrate paleontology in the neotropics*.

Kay, R. F., & Cozzuol, M. A. (2006). New platyrrhine monkeys from the Solimões formation (late Miocene, Acre State, Brazil). *Journal of Human Evolution*, *50*(6), 673-686.

Lepage, T., Bryant, D., Philippe, H., & Lartillot, N. (2007). A general comparison of relaxed molecular clock models. *Molecular biology and evolution*, *24*(12), 2669-2680.

Lundberg, J. G., Marshall, L. G., Guerrero, J., Horton, B., Malabarba, M. C. S. L., & Wesselingh, F. (1998). The stage for Neotropical fish diversification: a history of tropical South American rivers. *Phylogeny and classification of Neotropical fishes*, *603*, 14-48.

Macgregor, D. S. (2013). Late Cretaceous–Cenozoic sediment and turbidite reservoir supply to South Atlantic margins. *Geological Society, London, Special Publications*, *369*(1), 109-128.

Maldonado-Coelho, M., Blake, J. G., Silveira, L. F., Batalha-Filho, H., & Ricklefs, R. E. (2013). Rivers, refuges and population divergence of fire-eye antbirds (Pyriglena) in the Amazon Basin. *Journal of evolutionary biology*, *26*(5), 1090-1107.

Matos-Maravi, P. F., Pena, C., Willmott, K. R., Freitas, A. V., & Wahlberg, N. (2013). Systematics and evolutionary history of butterflies in the “Taygetis clade”(Nymphalidae: Satyrinae: Euptychiina): towards a better understanding of Neotropical biogeography. *Molecular Phylogenetics and Evolution*, *66*(1), 54-68.

Matzke, N. J. (2013). BioGeoBEARS: BioGeography with Bayesian (and likelihood) evolutionary analysis in R Scripts. *R package, version 0.2*, *1*, 2013.

Mayr, E. (1946). History of the North American bird fauna. *The Wilson Bulletin*, *58*(1), 3-41.

Miller, M. A., Pfeiffer, W., & Schwartz, T. (2010, November). Creating the CIPRES Science Gateway for inference of large phylogenetic trees. In *Gateway Computing Environments Workshop (GCE), 2010* (pp. 1-8). Ieee.

Montes, C., Cardona, A., Jaramillo, C., Pardo, A., Silva, J. C., Valencia, V., ... & Niño, H. (2015). Middle Miocene closure of the Central American seaway. *Science*, *348*(6231), 226-229.

Mora, A., Parra, M., Strecker, M. R., Sobel, E. R., Hooghiemstra, H., Torres, V., & Jaramillo, J. V. (2008). Climatic forcing of asymmetric orogenic evolution in the Eastern Cordillera of Colombia. *Geological Society of America Bulletin*, *120*(7-8), 930-949.

Moraes, L. J., Pavan, D., Barros, M. C., & Ribas, C. C. (2016). The combined influence of riverine barriers and flooding gradients on biogeographical patterns for amphibians and squamates in south-eastern Amazonia. *Journal of Biogeography*, *43*(11), 2113-2124.

Nascimento, F. F., dos Reis, M., & Yang, Z. (2017). A biologist’s guide to Bayesian phylogenetic analysis. *Nature Ecology & Evolution*, *1*(10), 1446.

Nogueira, A. C. R., Silveira, R., & Guimarães, J. T. F. (2013). Neogene–Quaternary sedimentary and paleovegetation history of the eastern Solimões Basin, central Amazon region. *Journal of South American Earth Sciences*, *46*, 89-99.

Olivares, A. M., Hrbek, T., Escobar, M. D., & Caballero, S. (2013). Population structure of the black arowana (Osteoglossum ferreirai) in Brazil and Colombia: implications for its management. *Conservation genetics*, *14*(3), 695-703.

Oliveira, U., Vasconcelos, M. F., & Santos, A. J. (2017). Biogeography of Amazon birds: rivers limit species composition, but not areas of endemism. *Scientific Reports*, *7*.

O’Dea, A., Lessios, H. A., Coates, A. G., Eytan, R. I., Restrepo-Moreno, S. A., Cione, A. L., ... & Stallard, R. F. (2016). Formation of the Isthmus of Panama. *Science Advances*, *2*(8), e1600883.

Rambaut, A. (2012). FigTree v. 1.4. Molecular evolution, phylogenetics and epidemiology. Edinburgh, UK: University of Edinburgh, Institute of Evolutionary Biology.

Rambaut, A., Suchard, M., Xie, D., & Drummond, A. (2014). Tracer v1. 6 http://beast. bio. ed. ac. uk. *Tracer>(Online 2015, May 29)*.

Ree, R. H., Moore, B. R., Webb, C. O., & Donoghue, M. J. (2005). A likelihood framework for inferring the evolution of geographic range on phylogenetic trees. *Evolution*, *59*(11), 2299-2311.

Ree, R. H., & Smith, S. A. (2008). Maximum likelihood inference of geographic range evolution by dispersal, local extinction, and cladogenesis. *Systematic Biology*, *57*(1), 4-14.

Ribas, C. C., Aleixo, A., Nogueira, A. C., Miyaki, C. Y., & Cracraft, J. (2011). A palaeobiogeographic model for biotic diversification within Amazonia over the past three million years. *Proceedings of the Royal Society of London B: Biological Sciences*, rspb20111120.

Rodríguez Tribaldos, V., White, N. J., Roberts, G. G., & Hoggard, M. J. (2017). Spatial and temporal uplift history of South America from calibrated drainage analysis. *Geochemistry, Geophysics, Geosystems*.

Ronquist, F., Teslenko, M., Van Der Mark, P., Ayres, D. L., Darling, A., Höhna, S., ... & Huelsenbeck, J. P. (2012). MrBayes 3.2: efficient Bayesian phylogenetic inference and model choice across a large model space. *Systematic biology*, *61*(3), 539-542.

Sauquet, H., Ho, S. Y., Gandolfo, M. A., Jordan, G. J., Wilf, P., Cantrill, D. J., ... & Lee, D. M. (2011). Testing the impact of calibration on molecular divergence times using a fossil-rich group: the case of Nothofagus (Fagales). *Systematic Biology*, *61*(2), 289-313.

Schliep, K. P. (2010). phangorn: phylogenetic analysis in R. *Bioinformatics*, btq706.

Shephard, G. E., Müller, R. D., Liu, L., & Gurnis, M. (2010). Miocene drainage reversal of the Amazon River driven by plate-mantle interaction. *Nature Geoscience*, *3*(12), 870-875.

Smith, A. B., & Peterson, K. J. (2002). Dating the time of origin of major clades: molecular clocks and the fossil record. *Annual Review of Earth and Planetary Sciences*, *30*(1), 65-88.

Sytsma, K. J., Spalink, D., & Berger, B. (2014). Calibrated chronograms, fossils, outgroup relationships, and root priors: re-examining the historical biogeography of Geraniales. *Biological Journal of the Linnean Society*, *113*(1), 29-49.

Wesselingh, F. P., Räsänen, M. E., Irion, G., Vonhof, H. B., Kaandorp, R., Renema, W., ... & Gingras, M. (2002). Lake Pebas: A palaeoecological reconstruction of a Miocene, long-lived lake complex in western Amazonia: Cainozoic Research, v. 1.

Xie, W., Lewis, P. O., Fan, Y., Kuo, L., & Chen, M. H. (2010). Improving marginal likelihood estimation for Bayesian phylogenetic model selection. *Systematic biology*, *60*(2), 150-160.

Yang, Z., & Rannala, B. (2006). Bayesian estimation of species divergence times under a molecular clock using multiple fossil calibrations with soft bounds. *Molecular biology and evolution*, *23*(1), 212-226.

Yang, Z., & Yoder, A. D. (2003). Comparison of likelihood and Bayesian methods for estimating divergence times using multiple gene loci and calibration points, with application to a radiation of cute-looking mouse lemur species. *Systematic biology*, *52*(5), 705-716.

Zhang, C., Stadler, T., Klopfstein, S., Heath, T. A., & Ronquist, F. (2016). Total-evidence dating under the fossilized birth–death process. *Systematic Biology*, *65*(2), 228-249.

Figure 1

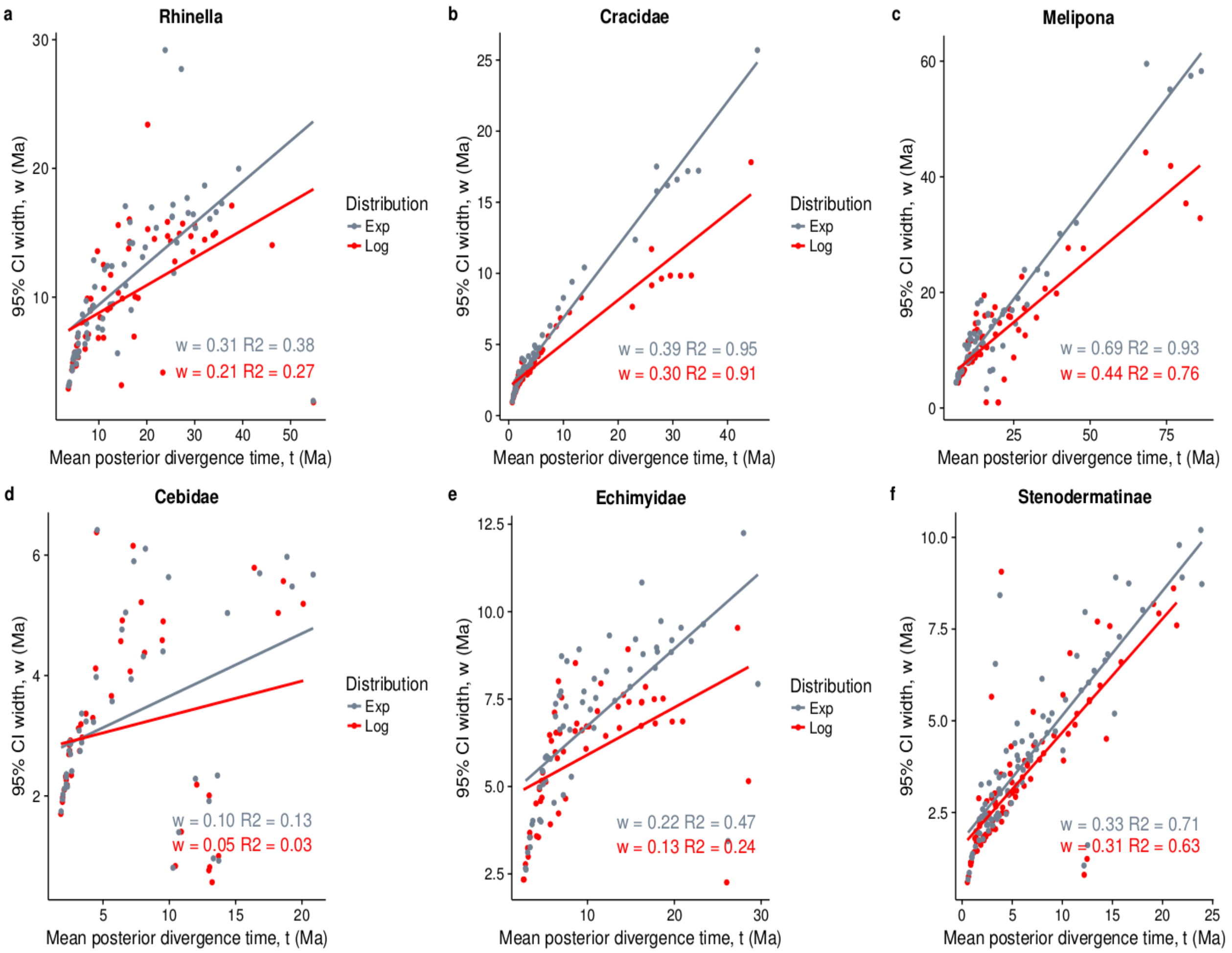

THE INFINITE-SITES PLOT FOR ALL TAXA UNDER LOGNORMAL AND EXPONENTIAL DISTRIBUTIONS. The x-axis are the posterior means of the each node age, and the y-axis are the 95 % posterior CI widths. The slope (w) is a measure of fossil precision and presents the direct relationship between divergence time and uncertainty in the posterior CI (Yang and Rannala 2006).

Figure 2

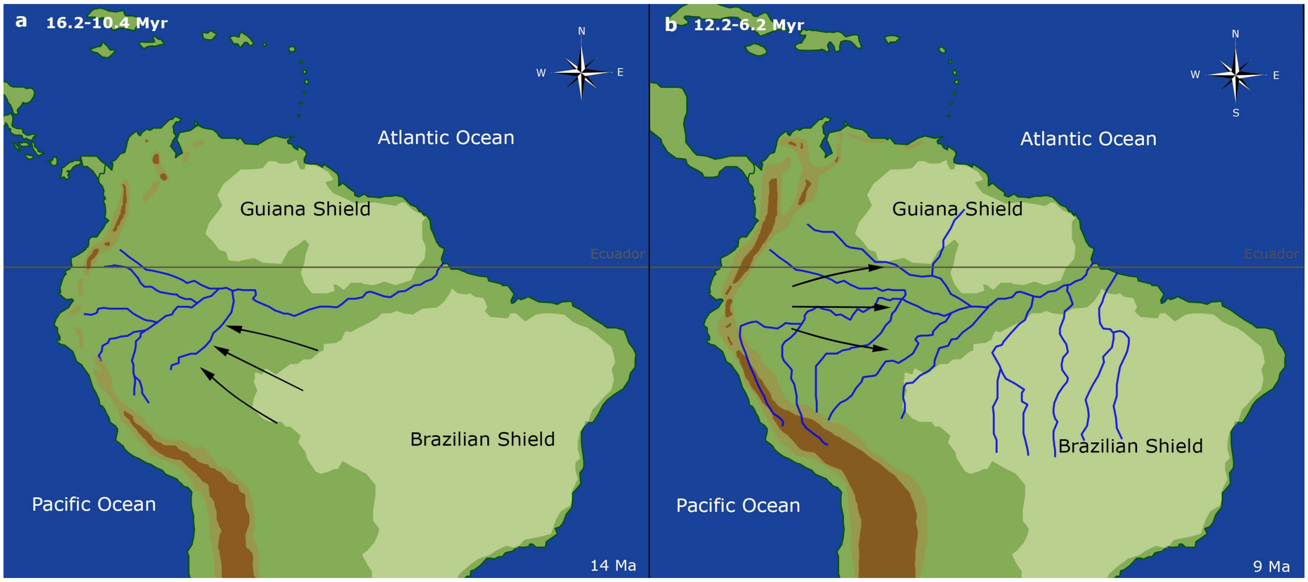

BIOGEOGRAPHICAL PATTERN FOR THE FORMATION OF THE AMAZON BASIN. Maps are modified from Hoorn et al (2010). (a) The first dispersals to Western Amazonia. (b) Expansion of the distributional range from Western Amazonia to Eastern Amazonia and the possible range for the establishment of the Amazon fluvial system. Closure of the Panama isthmus according to Bacon et al (2015), and Caribbean islands based on Ali (2012). The numbers at the right bottom correspond to Andean uplift.

APPENDICES

Appendix A

Rhinella

Specie	Cytb	Rhod	16s	12s-trna-val-16s	Rag1	Pomc
Anaxyrus_americanus	AB159264	NA	KF665122	DQ158426	KJ609650	DQ158268
Anaxyrus_woodhousii	AY288067	NA	NA	DQ158498	KJ609653	DQ158339
Anaxyrus_cognatus	NA	NA	NA	DQ158444	KJ609656	DQ158285
Anaxyrus_exsul	NA	NA	NA	AY325990	DQ158372	DQ158291
Cranopsis_coccifer	HM563944	NA	AY927856	DQ158443	KJ609669	DQ158284
Cranopsis_coniferus	HM563945	NA	FJ784601	DQ158445	HM563988	DQ158286
Cranopsis_valliceps	AY008230	NA	AY008229	DQ158493	KJ609665	DQ158334
Cranopsis_alvarius	HM563933	NA	HM563860	DQ158425	KJ609663	DQ158267
Bufo_bufo	AB159262	NA	AY555021	DQ158438	AY583336	KT239445
Bufo_andrewsi	AF174502	NA	AF160782	DQ158428	DQ158353	DQ158270
Amietophrynus_gracilipes	NA	NA	NA	DQ158456	DQ158378	DQ158297
Amietophrynus_regularis	NA	NA	KX671722	DQ158485	KJ609677	DQ158326
Amietophrynus_maculatus	NA	NA	NA	DQ158469	KJ609678	DQ158311
Duttaphrynus_melanostictus	AY247259	NA	NA	DQ158475	KJ609681	KU183158
Schismaderma_carens	NA	NA	KF665363	DQ158424	KF666220	DQ158266
Ingerophrynus_macrotis	NA	NA	NA	DQ158468	KF666244	KU183150
Peltophryne_lemur	NA	NA	U52787	DQ158465	DQ158386	DQ158306
Rhaebo_haematiticus	HM563930	NA	KR863345	DQ158461	KJ609683	DQ158302
Rhaebo_nasicus	NA	NA	NA	DQ158477	DQ158396	DQ158319
Nannophryne_cophotis	NA	NA	NA	DQ158446	DQ158369	DQ158287
Dendrophryniscus	KX025647	NA	KU495200	AY326000	DQ503337	AY819081
Melanophryniscus_klappenbachi	DQ502444	DQ283765	NA	AY843699	AY844478	KP295580
Melanophryniscus_stelzneri	NA	NA	U52782	DQ158421	KF666223	DQ158263
Rhinella_achavali	KC567990	HM159237	GU178798	GU178787	NA	NA
Rhinella_amboroensis	NA	DQ284003	NA	DQ283386	NA	NA
Rhinella_arenarum	HM159228	AY844547	GU178796	DQ158429	AY844370	DQ158271
Rhinella_arequipensis	NA	NA	NA	DQ158430	DQ158355	DQ158272
Rhinella_arunco	KC817199	NA	NA	DQ158442	DQ158365	DQ158283
Rhinella_atacamensis	KC778243	NA	NA	DQ158433	JX442329	DQ158275
Rhinella_azarai	KP684987	KP685164	NA	KP685186	KP685115	KP685079
Rhinella_bergi	KP684990	KP685165	NA	KP685189	KP685118	KP685084
Rhinella_bernardoi	KP684991	KP685166	NA	KP685194	KP685120	KP685086
Rhinella_castaneotica	NA	NA	KU495498	DQ158440	DQ158364	DQ158282
Rhinella_centralis	KP684992	KP685167	JN021325	KP685195	KP685122	KP685087

Rhinella_cerradensis	HM159232	HM159238	NA	NA	NA	NA
Rhinella_crucifer	HM159226	KC199966	KU495502	DQ158447	KJ609675	KJ532293
Rhinella_dapsilis	NA	NA	KR012641	DQ158448	DQ158370	NA
Rhinella_dorbignyi	KP684994	KP685168	NA	KP685199	KP685123	KP685090
Rhinella_fernandezae	KP684997	KP685169	NA	KP685202	KP685124	KP685092
Rhinella_festae	NA	NA	KR012624	DQ158423	DQ158349	DQ158265
Rhinella_granulosa	KP685002	KP685172	GU178800	KP685209	KP685129	KP685098
Rhinella_henseli	NA	KC199854	NA	KP685183	KP685113	KP685077
Rhinella_humboldti	NA	KP685173	KP149488	KP685211	KP685131	KP685099
Rhinella_icterica	HM159230	HM159240	KU495510	DQ158462	NA	DQ158303
Rhinella_jimi	HM159234	HM159241	GU178795	GU178784	NA	NA
Rhinella_limensis	NA	NA	NA	DQ158466	NA	DQ158307
Rhinella_major	KP685008	KP685175	JF790180	KP685219	KP685135	KP685105
Rhinella_manu	NA	NA	NA	NA	DQ404395	DQ404396
Rhinella_margaritifera	JX298409	HM159242	KR012628	NA	HM563975	AY819080
Rhinella_marina	KR011949	DQ283789	KR012644	DQ158474	DQ158392	DQ158316
Rhinella_merianae	KP685010	KP685176	NA	KP685222	KP685137	KP685107
Rhinella_mirandaribeiroi	KP685012	KP685177	KF723018	KP685228	KP685140	KP685109
Rhinella_nesiotes	NA	NA	NA	DQ158478	DQ158397	DQ158320
Rhinella_ocellata	NA	NA	JN867572	DQ158479	DQ158398	DQ158321
Rhinella_ornata	NA	KC199963	KU495531	NA	NA	NA
Rhinella_poeppigii	HM159233	HM159243	GU178790	DQ158481	KJ609674	KJ532292
Rhinella_pygmaea	KP685013	KP685181	NA	KP685229	KP685141	KP685110
Rhinella_rubescens	HM159229	HM159244	NA	DQ158486	NA	DQ158327
Rhinella_schneideri	HM159235	NA	JQ627202	DQ158480	KJ609673	DQ158322
Rhinella_spinulosa	NA	DQ283775	NA	DQ158487	KJ609676	DQ158328
Rhinella_sternosignata	NA	KP685163	NA	KP685184	KP685144	KP685078
Rhinella_vellardi	NA	NA	NA	DQ158495	DQ158411	DQ158336
Rhinella_veraguensis	NA	NA	NA	DQ158496	DQ158412	DQ158338
Rhinella_veredas	HM159231	HM159245	NA	NA	NA	NA

Cracidae

Specie	Nd2	Cytb	Coi	Nd5	Cltcl1	Eef2	Tfb5	Rho	Serpinb14	Cltc
Numida_meleagris	NA	KF833637	NA	NA	EU302774	EU738650	NA	EU737246	KC749887	KC749599
Megapodius_layardi	NA	KF833615	NA	NA	KF833495	FJ881844	NA	NA	KC749932	KC749598
Ptilopachus_petrosus	DQ768289	AM236886	NA	KR732873	NA	KR732890	NA	NA	KR732792	KR732672
Rollulus_rouloul	KR732854	EF571185	NA	NA	JF497007	EU738688	NA	EU737280	KC749947	NA

Tympanuchus_phasianellus	AF230127	AF230181	DQ434206	NA	KC749662	KC749714	NA	NA	KC749906	KC749617
Coturnix_japonica	NA	DQ515818	GQ481652	NA	KC749626	KC749691	NA	DQ402463	KC749869	KC749581
Callipepla_californica	KR732836	AB120131	JN850719	KR732862	NA	KR732885	NA	KR732764	KR732783	KR732687
Colinus_virginianus	KR732833	EU372675	NA	KR732859	KC749627	KR732887	NA	KR732765	KR732785	KR732685
Gallus_gallus	KF792740	EU839454	JF498860	NA	EU302770	EU738569	NA	AB496228	NM_205152	KC749587
Meleagris_gallopavo	AF222556	HQ122602	DQ433017	NA	KC749642	FJ881856	NA	NA	NM_001303190	KC749597
Oreophasis_derbianus	NA	AY659805	AF165495	AY140759	KX345905	KX356290	KX356206	KX356149	KX356174	KX345877
Ortalis_vetula	KX356238	L08384	KX356279	KX356262	KX345911	NA	KX356214	KX356156	KX356180	KC749601
Ortalis_leucogastra	NA	NA	NA	NA	KX345908	KX356306	KX356211	KX356153	KX356177	KX345880
Ortalis_poliocephala	KX356257	AY659784	KX356278	KX356261	KX345910	KX356293	KX356213	KX356155	KX356179	NA
Ortalis_wagleri	KX356239	NA	KX356280	NA	KF833519	KX356296	KX356215	NA	KX356181	KX345883
Chamaepetes_unicolor	KX356231	AY659796	JQ174405	NA	KX345897	NA	KX356198	NA	KX356168	NA
Penelopina_nigra	NA	AY354492	AF165499	AY140757	KX345923	KX356302	KX356227	KX356164	KX356192	NA
Chamaepetes_goudotii	AY140741	AY659795	JN801554	AY140755	NA	NA	KX356197	NA	NA	NA
Penelope_argyrotis	NA	AY659803	NA	NA	NA	NA	NA	NA	NA	NA
Penelope_barbata	KX356252	NA	JN801892	NA	NA	NA	NA	NA	NA	NA
Penelope_montagnii	KX356245	AY659802	KX356283	KX356267	KX345918	KX356305	KX356222	KX356161	KX356188	KX345890
Penelope_marail	KX356244	KX356277	JQ175713	KX356266	KX345917	NA	KX356221	KX356160	KX356187	KX345889
Penelope_superciliaris	AY367090	AY659804	KX356284	NA	KX345922	NA	KX356226	KX356163	KX356191	KX345892
Penelope_jacquacu	NA	AY659801	JQ175710	NA	NA	NA	NA	NA	NA	NA
Penelope_purpurasc	AY3670	AY6598	JQ1757	KX3562	KF8335	KF8336	KX356	NA	KX356190	NA

ens	97	00	18	69	21	95	225			
Penelope_albipennis	KX356240	NA	JN801891	NA	KX345914	KX356297	KX356217	NA	KX356183	KX345885
Penelope_obscura	AY140742	AF165474	JQ175715	AY140756	KX345919	KX356301	KX356223	NA	NA	NA
Penelope_pileata	KX356247	NA	JQ175717	KX356268	KX345920	KX356300	KX356224	KX356162	KX356189	KX345891
Penelope_ochrogaster	AY367089	AY367101	NA	NA	NA	NA	NA	NA	NA	NA
Penelope_dabbenei	KX356241	KX356275	KX356281	KX356263	KX345915	KX356303	KX356218	KX356158	KX356184	KX345886
Penelope_jacucaca	KX356243	KX356276	KX356282	KX356265	KX345916	KX356298	KX356219	KX356159	KX356185	KX345887
Pipile_pipile	AY367094	AY367106	JQ175861	NA	KX345925	KX356299	KX356229	KX356166	KX356195	KX345895
Pipile_cumanensis	AY367099	AY659798	NA	KX356271	KX345924	NA	NA	NA	KX356194	KX345894
Pipile_cujubi	AY367092	AY659799	NA	KX356270	NA	NA	KX356228	KX356165	KX356193	KX345893
Pipile_jacutinga	AY140744	AF165476	AF165500	AY140758	NA	NA	NA	NA	NA	NA
Aburria_aburri	AY140740	AY354489	JN801479	AY140754	KX345896	NA	KX356196	KX356143	KX356167	NA
Ortalis_cinereiceps	KX356253	KX356273	KF799991	KX356258	KX345907	KX356295	KX356209	KX356151	KX356176	KX345879
Ortalis_garrula	NA	AY659780	NA	NA	NA	NA	NA	NA	NA	NA
Ortalis_ruficauda	NA	AY659781	NA	NA	NA	NA	NA	NA	NA	NA
Ortalis_canicollis	AY140746	AF165472	AF165496	AY140760	KX345906	KX356291	KX356208	KX356150	KX356175	KX345878
Ortalis_guttata	KX356237	AY659782	NA	KX356259	NA	KX356292	KX356210	KX356152	NA	NA
Ortalis_motmot	NA	AY659778	KF446138	KX356260	KX345909	KX356307	KX356212	KX356154	KX356178	KX345881
Ortalis_erythroptera	KX356256	NA	NA	NA	NA	NA	NA	NA	NA	NA
Nothocrax_urumutum	AY140749	AY354488	KM896479	AY140763	KX345904	KX356289	KX356205	NA	NA	KX345876
Crax_rubra	AY952746	AY659793	AY141915	AY141965	KX345902	KX356308	KX356203	KX356147	KX356172	KC749583

Crax_alberti	AY141930	AY141920	AY141910	AY141960	KX345898	NA	KX356199	KX356144	KX356169	KX345872
Crax_daubentoni	AY141932	AY141922	AY141912	AY141962	KX345899	KX356285	KX356200	KX356145	KX356170	NA
Crax_alector	AY141931	EF571188	JQ174569	AY141961	EU302762	EU738611	NA	EU737204	NA	EU302719
Crax_globulosa	AY141934	AY141924	AY141914	NA	KX345901	NA	KX356202	KX356146	KX356171	KX345873
Crax_fasciolata	AY141933	AY659790	JQ174570	NA	KX345900	KX356286	KX356201	NA	NA	NA
Crax_blumenbachii	AY140747	AY659791	AF165492	AY140761	NA	NA	NA	NA	NA	NA
Mitu_tomentosum	AY141938	AY659787	JQ175400	AY141968	NA	NA	NA	NA	NA	NA
Mitu_salvini	AY141937	AY659785	EU525438	AY141967	NA	NA	NA	NA	NA	NA
Mitu_tuberosum	AY140748	AY354484	EU525441	AY140762	KX345903	KX356287	KX356204	KX356148	KX356173	KX345875
Mitu_mitu	AY141936	AY098552	AY141916	AY141966	NA	NA	NA	NA	NA	NA
Pauxi_pauxi	AY140750	AY354486	AF165497	AY140764	NA	KX356288	KX356216	KX356157	KX356182	KX345884
Pauxi_unicornis	AY141939	AY659786	AY141919	AY141969	NA	NA	NA	NA	NA	NA

Melipona

Specie	Coi	16s	Rna-pol2	Ef1-alpha	Argk
Melipona_costaricaensis	EU163129	EU162954	EU162885	EU163207	EU163048
Melipona_solari	EU163160	EU162994	EU162915	EU163247	EU163079
Melipona_ogilviei	EU163140	EU162974	EU162896	EU163227	EU163059
Melipona_micheneri	EU163139	EU162973	EU162895	EU163226	EU163058
Melipona_quadrifasciata	EU163150	AF343100	EU162887	EU163218	EU163069
Melipona_mandacaia	EU163156	EU162990	EU162911	EU163243	EU163075
Melipona_asilvai	EU163157	EU162991	EU162912	EU163244	EU163076
Melipona_melanopleura	EU163113	EU162946	EU162866	EU163197	EU163029
Melipona_panamica	EU163096	EU162928	EU162848	EU163179	EU163012
Melipona_rufiventris	EU163132	EU162966	EU162888	EU163219	EU163051
Melipona_scutellaris	EU163152	EU162986	EU162907	EU163239	EU163071

Melipona_seminigra	EU163138	EU162972	EU162894	EU163225	EU163057
Melipona_fuscopilosa	EU163136	EU162970	EU162892	EU163223	EU163055
Melipona_fulva	EU163125	EU162959	EU162881	EU163212	EU163044
Melipona_lateralis	EU163144	EU162978	EU162900	EU163231	EU163063
Melipona_nebulosa	EU163146	EU162980	NA	EU163233	EU163065
Melipona_illota	EU163167	EU163001	EU162921	EU163254	FJ042220
Melipona_crinita	EU163164	EU162998	EU162919	EU163251	EU163052
Melipona_melanoventer	EU163135	EU162969	EU162891	EU163222	EU163054
Melipona_captiosa	EU163142	EU162976	EU162898	EU163229	EU163061
Melipona_fuliginosa	EU163141	EU162975	EU162897	EU163228	EU163037
Melipona_marginata	EU163153	EU162987	EU162908	EU163240	EU163072
Melipona_bicolor	EU163158	EU162992	FJ041919	EU163245	FJ042195
Melipona_amazonica	EU163166	EU163000	NA	EU163253	EU163085
Melipona_favosa	EU163127	EU162961	EU162883	EU163214	EU163046
Melipona_compressipes	EU163137	AF181589	EU162893	EU163224	EU163056
Melipona_grandis	EU163169	EU163003	EU162886	EU163256	EU163088
Melipona_triplaridis	EU163154	EU162988	EU162909	EU163241	EU163073
Melipona_quinquefasciata	EU163155	EU162989	EU162910	EU163242	EU163074
Melipona_beecheii	EU163126	EU162960	EU162882	EU163213	EU163045
Melipona_illustris	EU163145	EU162979	EU162901	EU163232	EU163064
Melipona_bradleyi	NA	FJ041921	NA	FJ042298	FJ042197
Melipona_capixaba	JN315064	NA	NA	NA	NA
Melipona_colimana	JX869619	JX869598	NA	NA	NA
Melipona_eburnea	NA	FJ041935	NA	FJ042312	FJ042211
Melipona_fasciata	JX869623	JX869600	NA	FJ042323	FJ042222
Melipona_fasciculata	NA	FJ041946	NA	FJ042324	FJ042223
Melipona_flavolineata	KP708582	NA	NA	NA	NA
Melipona_orbignyi	FJ975767	NA	NA	NA	NA
Scaptotrigona	JQ783156	L22900	EU162854	GU244963	EU163018
Trigona	AF214669	L22901	EU162858	EU049789	EU184829
Cephalotrigona	EU163161	EU162995	EU162916	EU184771	EU184830
Geotrigona	EU163112	EU162945	EU162865	DQ813116	EU163028
Plebeia_franki	EU163098	EU162930	EU162850	EU163181	EU163014
Friesella_schrotkyii	EU163103	EU162936	EU162856	EU163187	EU163020
Frieseomelitta	EU163104	FJ041924	EU162857	EU163188	EU163021
Lestrimelitta	EU163111	EU162944	EU162864	AY208287	EU163027
Tetragonisca	KF224897	FJ042001	EU162849	EU163180	EU163013
Nannotrigona	EU163100	FJ041953	EU162853	EU163184	EU163017
Nogueirapis_mirandula	NA	EU162947	EU162867	EU163198	EU163030
Meliwillea_bivea	EU163114	AF343108	EU162868	EU163199	EU163031
Meliponula	EU163118	EU162951	EU162873	EU163204	EU163036
Bombus	JQ769073	AF364824	NA	NA	AY739533
Apis_cerana	KJ755628	HQ318940	NA	EU184774	EU163040
Apis_koschevnikovi	AY754732	EU162942	EU162863	EU163193	EU163025

Apis_mellifera	KR793809	JF825886	NA	NA	NA
Apis_dorsata	KT960840	KU752359	NA	NA	AY267178
Apis_andreniformis	AB284158	KU212301	EU162879	AY721702	EU163042
Apis_florea	AB284150	KU752357	NA	NA	EU184831
Euglossa_asarophora	EU421496	NA	EU421248	EU163171	EU421628
Euglossa_mixta	EU163094	NA	EU421309	EU421436	NA
Euglossa_villosa	EU421556	NA	EU421301	EU421428	EU163009
Euglossa_decorata	EU421505	NA	EU162841	EU163172	EU421636
Aglae_caerulea	EU421542	EU162926	EU421289	EU421413	EU163007
Eufriesea_caerulescens	EU421584	NA	EU162847	AY208283	EU421711
Eulaema_peruviana	AJ581111	AJ581092	EU421290	EU421414	EU163008
Exaerete_azteca	EU421557	EU162927	EU421302	EU421429	EU163010
Centris	DQ225328	EU162948	EU162869	EU163200	EU163032
Epicharis	EU163115	NA	GU245359	EU163201	EU163033

Cebidae

Specie	Sry	Bdnf	Rag1	Rag2	16s	Mc1r	Cytb	Beta2-microglobulin	Coii	Dmrt1	Fbn1	Abca1	Adora3	Aff2
Aotus	AF338375	HM763844	HM759104	HM758932	AB107211	AY205129	HQ005496	AF042145	AF352260	HM762509	HM761928	HM765414	HM765178	HM765068
Lagothrix	HM757996	HM763833	HM759086	HM758914	U39005	NA	KR902423	AH006721	HM057599	HM762589	HM761911	HM765336	HM765159	HM764984
Brachyteles	NA	NA	HM759084	HM758912	DQ078115	NA	AY065906	AH006720	AF216253	HM762519	NA	HM765272	HM765157	HM764912
Ateles	DQ976605	HM763850	AY065918	HM758938	AB116026	AB296241	KR902384	AH006727	AF216249	HM762505	HM761933	HM765262	HM765184	HM764897
Cacajao	HM758004	HM763852	HM759113	HM758943	NA	NA	EU560418	AH006724	NA	HM762530	HM761935	HM765283	HM765187	HM764926
Chiropotes	NA	HM763856	HM759121	HM758950	NA	NA	FJ531667	AH006723	NA	HM762677	NA	HM765295	HM765195	HM765071
Pithecia	NA	FJ648367	HM759140	HM758971	U39007	NA	KR902426	AH006729	JN161059	HM762634	HM761960	HM765380	HM765215	HM765029
Callicebus	HM758005	HM763866	HM759137	HM758970	AB107212	NA	AF289988	AH006728	JN161057	HM762527	HM761959	HM765284	HM765210	HM764941
Alouatta	DQ875683	HM763841	AY065919	HM758927	U38997	AY205132	AY374376	AH006717	AF054296	HM762515	HM761922	HM765267	HM765171	HM764906

Cebus_albifrons	AF338385	JN633376	HM759115	HM758944	NA	AY205128	FJ529109	AH006509	NA	HM762675	HM761936	HM765415	KU694339	HM765069
Cebus_apella	AF338387	NA	HM759116	HM758945	U39003	NA	FJ529104	AH006508	AF181088	HM762524	HM761937	HM765278	HM765190	HM764920
Cebus_capucinus	AF338388	HM763853	NA	HM758946	NA	NA	FJ529110	NA	JF735240	HM762532	HM761938	HM765285	HM765191	HM764928
Cebus_nigritus	NA	NA	HM759118	HM758948	NA	NA	KR528406	NA	AF181088	NA	HM761940	HM765308	NA	HM764953
Cebus_olivaceus	AF338389	HM763854	HM759117	HM758947	NA	NA	FJ529107	AH006733	NA	HM762551	HM761939	HM765303	HM765192	HM764948
Cebus_xanthosternos	NA	NA	HM759119	NA	NA	NA	JN835288	NA	NA	NA	NA	NA	NA	NA
Saimiri_boliviensis	HM758016	NA	HM759129	HM758961	DQ334826	NA	NA	NA	AF396460	HM762645	HM761953	NA	HM765204	HM765040
Saimiri_oerstedii	HM758017	HM763864	HM759130	HM758962	NA	AY205127	KM234547	NA	NA	HM762657	HM761954	HM765400	HM765205	HM765052
Saimiri_sciureus	HM758018	HM763865	HM759131	HM758963	AB107214	AB296239	HQ005511	AH007458	U36848	HM762658	HM761955	HM765401	HM765206	HM765053
Saimiri_ustus	NA	NA	NA	NA	NA	NA	EU232707	NA	NA	NA	NA	NA	NA	NA
Saimiri_vanzolinii	NA	NA	NA	NA	NA	NA	KM234514	NA	NA	NA	NA	NA	NA	NA
Leontopithecus_chrysomelas	AF338370	HM763839	HM759094	HM758923	NA	AY205116	KR528398	NA	NA	HM762585	HM761918	HM765332	HM765168	HM764980
Leontopithecus_chrysopygus	AF338371	NA	NA	NA	NA	AY205115	NA	AH006736	NA	NA	NA	NA	NA	NA
Leontopithecus_rosalia	AF338373	HM763840	HM759095	HM758924	U39006	AY205114	KR528404	NA	NA	HM762590	HM761919	HM765337	HM765169	HM764985
Callimico_goeldii	AF338383	AY011480	HM759087	HM758915	U39000	AY205121	NA	AH006734	AY118175	HM762538	HM761912	HM765291	HM765160	HM764934
Callithrix_aurita	AF338392	NA	NA	HM758917	NA	NA	KR528400	AH008973	AY118188	NA	NA	NA	HM765162	HM764917
Callithrix_geoffroyi	AF338378	HM763835	HM759089	HM758918	NA	AY205119	KU253509	NA	AY118192	HM762537	HM761914	HM765290	HM765163	HM764933
Callithrix_kuhlii	AF338380	NA	HM759091	HM758920	NA	NA	KU253511	AH006715	AY118193	NA	NA	HM765297	HM765165	HM764940
Callithrix_penicillata	AF338381	HM763837	HM759092	HM758921	NA	NA	NA	AH007459	AY118196	HM762552	HM761916	HM765304	HM765166	HM764949
Callithrix_jacchus	AF338379	HM763836	HM759090	HM758919	U39001	AY205120	AY434079	AH008974	AY321457	HM762543	HM761915	HM765296	NM_001302791	XM_017968309
Cebuella_pygm	AF33	HM76	HM75	HM75	U290	NA	NA	AH006	NA	NA	NA	NA	NA	NA

aea	8382	3838	9093	8922	02			726						
Mico_argentatus	NA	HM763834	HM759088	HM758916	NA	AY205118	AF245065	NA	AY118183	HM762525	HM761913	HM765279	HM765161	HM764921
Mico_emiliae	NA	NA	NA	NA	FJ769146	NA	L44587	AH006735	AY118178	NA	NA	NA	NA	NA
Mico_humeralifer	NA	NA	HM759096	HM758925	NA	NA	AF245052	AH007460	AY118184	NA	NA	HM765345	HM765170	HM764994
Mico_mauesi	NA	NA	NA	NA	FJ769147	NA	AF245051	NA	AY118187	NA	NA	NA	NA	NA
Mico_saterei	NA	NA	NA	NA	NA	NA	NA	NA	AY118180	NA	NA	NA	NA	NA
Mico_chrysoleuca	NA	NA	NA	NA	NA	NA	KR528411	NA	NA	NA	NA	NA	NA	NA
Saguinus_nigricollis	NA	NA	NA	NA	NA	NA	HM368075	NA	NA	NA	NA	NA	NA	NA
Saguinus_fuscicollis	HM758012	HM763858	HM759123	HM758953	NA	AY205123	NA	AH008977	NA	HM762648	NA	HM765391	HM765197	HM765043
Saguinus_tripartitus	NA	NA	NA	NA	NA	NA	HM368006	NA	NA	NA	NA	NA	NA	NA
Saguinus_imperator	NA	NA	NA	HM758955	EU497287	AY205122	HM368020	AH006731	NA	HM762651	HM761946	HM765394	NA	HM765046
Saguinus_labiatus	NA	HM763860	HM759125	HM758956	EU497289	NA	HM367998	NA	NA	HM762652	HM761947	HM765395	NA	HM765047
Saguinus_inustus	NA	NA	NA	NA	NA	NA	KM370859	NA	NA	NA	NA	NA	NA	NA
Saguinus_mystax	HM758014	HM763862	HM759127	HM758959	EU497294	NA	HM367983	AH008978	NA	HM762655	HM761951	HM765398	HM765202	HM765050
Saguinus_leucopus	NA	NA	NA	NA	EU497286	NA	NA	NA	NA	NA	NA	NA	NA	NA
Saguinus_oedipus	HM758015	HM763863	HM759128	HM758960	EU497296	AY205125	HM368007	AH006510	NA	HM762656	HM761952	HM765399	HM765203	HM765051
Saguinus_niger	NA	NA	NA	NA	EU497246	NA	NA	AH006193	NA	NA	NA	NA	NA	NA
Saguinus_midas	AF338391	HM763861	HM759126	HM758958	EU497273	AY205126	AJ489760	AH006716	NA	HM762653	HM761950	HM765396	HM765200	HM765048
Saguinus_bicolor	HM758011	HM763857	HM759122	HM758952	EU497280	NA	NA	AH008975	NA	HM762644	HM761944	HM765388	HM765196	HM765039
Saguinus_martinsi	NA	NA	NA	NA	EU497276	NA	NA	AH008976	NA	HM762659	HM761948	HM765402	NA	HM765054
Saguinus_geoffroyi	NA	HM763859	NA	NA	U39008	AY205124	NA	NA	NA	NA	NA	NA	NA	NA

Saguinus_graellsi	NA	NA	NA	NA	NA	NA	HM368035	NA	NA	NA	NA	NA	NA	NA
Saguinus_melanoleucus	NA	NA	NA	NA	NA	NA	HM368078	NA	NA	NA	NA	NA	NA	NA
Callibella_humilis	NA	NA	NA	NA	FJ769145	NA	NA	NA	NA	NA	NA	NA	NA	NA

Echimyidae

Specie	Cytb	Rag1	16s	12s	Ghr	Coi	Vwf
Capromys_pilorides	AF422915	KM013988	KM013971	KM013959	AF433950	NA	AJ251142
Myocastor_coypus	EU544663	JN414955	AY011155	AY012123	NA	NA	AJ251140
Chinchilla_lanigera	AF244382	KF590658	AY062170	AF520696	AY701337	GU130595	NA
Ctenomys_boliviensis	AF007040	NA	NA	U12446	JN414757	JQ341048	NA
Octodontomys_gliroides	AF370706	KF590663	NA	AF520684	AF520664	GQ121084	KF590672
Octodon_bridgesi	KJ742651	KJ742676	NA	AF520677	AF520646	NA	KJ742611
Abrocoma_cinerea	AF244388	NA	NA	AF520666	AF520643	NA	NA
Abrocoma_bennettii	AF244387	NA	NA	NA	FJ855213	NA	JN415073
Dactylomys_boliviensis	L23339	EU313299	AF422909	AF422875	KF590679	NA	AJ849307
Dactylomys_dactylinus	L23335	EU313301	AF422908	AF422874	KF590681	NA	KF590667
Dactylomys_peruanus	EU313207	NA	NA	NA	NA	NA	NA
Kannabateomys_amblyonyx	AF422917	NA	AF422884	AF422850	NA	NA	AJ849310
Olallamys_albicauda	KF590697	NA	NA	NA	KF590691	NA	KF590673
Callistomys_pictus	KJ742659	KJ742677	NA	KJ742594	KJ742627	NA	KJ742614
Diplomys_labilis	KJ742660	KJ742685	NA	NA	KJ742636	NA	KJ742613
Diplomys_rufodorsalis	KJ742664	NA	NA	NA	NA	NA	NA
Echimys_chrysurus	L23341	EU313303	AF422911	AY093663	FJ855215	JF458603	AJ251141
Echimys_semivillosus	KJ742662	KJ742687	NA	NA	NA	JF458604	KJ742616
Isothrix_bistriata	L23355	EU313311	AF422907	AF422873	FJ855216	NA	AJ849308
Isothrix_negrensis	EU313221	NA	NA	NA	NA	NA	NA
Isothrix_pagurus	EU313226	KF590661	NA	KF590703	KF590684	NA	KF590670
Isothrix_sinnamariensis	AY745734	EU313313	NA	KF590704	KF590686	JF458606	AJ849309
isothrix_barbarabrownae	EU313214	EU313304	NA	KF590701	KF590682	NA	KF590668
Isothrix_orinoci	EU313225	KF590660	NA	KF590702	KF590683	NA	KF590669
Makalata_didelphoides	L23363	EU313320	AF422912	KJ742600	KJ742639	JF458629	JF297707
Makalata_grandis	KF590699	EU313336	NA	NA	KF590694	NA	KF590676
Makalata_macrura	EU302703	EU313330	AF422913	AF422879	KF590687	NA	AJ849312
Makalata_occasius	KJ742661	NA	NA	NA	KJ742637	NA	NA
Makalata_rhipidura	KJ742663	KJ742686	NA	NA	KJ742638	NA	KJ742617
Phyllomys_blainvillii	JF297836	KF590664	NA	KF590706	KF590692	JF297686	JF297735
Phyllomys_brasiliensis	EF608182	NA	NA	AY093666	NA	JF297680	JF297729
Phyllomys_dasythrix	EF608185	KJ742689	NA	KJ742605	KJ742641	JF297660	JF297709

Phyllomys_lamarum	EF608181	NA	NA	NA	NA	JF297682	JF297731
Phyllomys_lundi	EF608183	NA	NA	NA	NA	JF297672	JF297721
Phyllomys_mantiqueirensis	EF608179	NA	NA	NA	NA	JF297671	JF297720
Phyllomys_nigrispinus	EF608184	NA	NA	NA	NA	JF297666	JF297719
Phyllomys_pattoni	EF608187	KJ742690	NA	KJ742606	KJ742642	JF297704	JF297754
Phyllomys_unicolor	EF608188	NA	NA	NA	NA	NA	NA
Carterodon_sulcidens	KJ742666	KJ742678	NA	KJ742596	KJ742640	NA	KJ742615
Clyomys_laticeps	AF422918	KJ742679	AF422885	KJ742597	KJ742628	NA	AJ849306
Euryzygomatomys_spinosus	EU544667	KJ742680	NA	NA	KJ742629	GU938885	AJ849319
Hoplomys_gymnurus	AF422922	JN414965	AF422896	AF520668	JN414758	NA	JN415080
Lonchothrix_emiliae	EU313229	NA	AF422891	AF422857	NA	NA	NA
Mesomys_hispidus	KF590696	EU313322	AF422895	KF590705	KF590688	HQ919652	KF590671
Mesomys_occultus	NA	EU313331	AF422893	AF422859	KF590689	NA	NA
Mesomys_stimulax	KJ742667	KJ742674	NA	KJ742603	KJ742630	NA	KJ742618
Proechimys_cuvieri	AY206633	KF590665	NA	KF590707	KF590693	JF458720	KF590675
Proechimys_guyannensis	NA	NA	NA	KX381547	NA	EU096897	NA
Proechimys_hoplomyoides	NA	NA	NA	NA	NA	EU095484	NA
Proechimys_longicaudatus	NA	KJ742681	NA	U12447	KJ742643	NA	KJ742619
Proechimys_quadruplicatus	AF308435	NA	NA	NA	NA	EU095487	AJ849313
Proechimys_roberti	EU544666	NA	NA	NA	NA	NA	NA
Proechimys_simonsi	U35414	EU313333	AF422898	AF422864	KJ742631	EU095486	AJ849320
Proechimys_steerei	NA	NA	NA	NA	NA	JF459060	NA
Thrichomys_apereoides	EU544668	EU313335	AF422890	AF422856	JX515325	NA	AJ849315
Thrichomys_inermis	JX459887	NA	NA	NA	NA	NA	NA
Thrichomys_pachyurus	AY083340	NA	NA	NA	NA	NA	NA
Trinomys_albispinus	KM014008	KM013992	KM013976	KM013964	KM013987	NA	KM014003
Trinomys_dimidiatus	AF194296	KJ742682	AF422901	AF422867	NA	NA	KJ742620
Trinomys_eliasi	KJ707247	NA	AF422903	AF422869	NA	NA	NA
Trinomys_gratiosus	KJ707248	NA	NA	NA	NA	NA	NA
Trinomys_iheringi	EU544664	EU313338	AF422902	AF422868	KF590695	NA	KF590677
Trinomys_moojeni	KF562097	NA	NA	NA	NA	NA	NA
Trinomys_paratus	U35165	NA	AF422900	AF422866	JX515330	NA	AJ849316
Trinomys_setosus	AF422924	NA	AF422906	AF422872	JX515329	NA	AJ849317
Trinomys_yonenagae	AF194295	NA	AF422899	AF422865	JX515328	NA	AJ849318

Stenodermatinae

Specie	Cytb	Rag2	Nd2	Coi	Plcb4	Atp7	Bdnf	Thy
Rhinophylla_alethina	AF187027	NA	NA	JF449072	NA	NA	NA	NA
Rhinophylla_fischerae	AF18703	KF56935	NA	JF44911	KF56932	NA	NA	KF56945

	2	1		0	9			5
Carollia_subrufa	AF187024	NA	NA	JF448015	KM362009	NA	NA	NA
Carollia_castanea	AF512006	FN641676	NA	JF448773	KF569314	NA	KF569466	KF569450
Glyphonycteris_sylvestris	AY380746	AF316471	NA	KX910802	KM362017	NA	NA	NA
Trinycteris_nicefori	AY380749	AF316469	NA	JF456028	KC783108	NA	KC783000	KC783252
Lonchophylla_hesperia	KF815310	KM362062	NA	NA	KM362022	NA	KM361983	NA
Lonchophylla_dekeyseri	NA	NA	NA	NA	KM362021	KM361948	KM361982	NA
Lionycteris_spurrelli	KF815304	AF316455	NA	JF454738	KC783075	NA	KC782968	KC783226
Platalina_genovensium	KF815311	NA	NA	NA	NA	NA	NA	NA
Lonchophylla_chocoana	AF423092	NA	NA	JF448854	KF569321	NA	KF569473	KF569453
Lonchophylla_mordax	AF423095	KC783116	NA	JF448855	KM362020	NA	NA	NA
Centurio_senex	AY604444	AF316438	NA	JF447241	KF569315	NA	NA	KM362119
Sturnira_lilium	DQ312398	KC754302	KC753968	JF459281	KC783105	KC783048	KC782996	KC783248
Sturnira_tildae	KC753897	DQ903847	NA	JF455952	KF569331	KF569434	KF569480	KF569452
Sturnira_ludovici	KC753807	KC754272	KC753925	JN659773	KF569334	KF569432	NA	NA
Sturnira_luisi	KC753815	KC754280	KC753933	JN659882	KM362042	NA	KM361996	KM362139
Sturnira_erythromos	FJ154179	FJ154377	FJ154245	JN659617	NA	NA	NA	NA
Sturnira_parvidens	KC753873	KC754337	KC753994	KX756039	NA	NA	NA	NA
Sturnira_magna	KC753820	KC754283	KC753938	JN659896	KF569332	KF569433	NA	NA
Sturnira_bidens	AF435200	NA	KC753900	JN659567	NA	NA	NA	NA
Sturnira_oporaphilum	KC753855	KC754318	KC753975	NA	KM362043	KM361963	KM361997	KM362140

Sturnira_hondurensis	KC753827	KC754288	KC753946	NA	NA	NA	NA	NA
Sturnira_bogotensis	KC753787	KC754252	KC753905	NA	KF569333	KF569431	NA	KF569451
Sturnira_mordax	KC753824	KC754287	KC753943	NA	NA	NA	NA	NA
Sturnira_burtonlimi	NA	NA	NA	KX814421	NA	NA	NA	NA
Sturnira_adrianae	KY366229	NA	NA	NA	NA	NA	NA	NA
Sturnira_perla	NA	NA	NA	JN659911	NA	NA	NA	NA
Sturnira_aratathomasi	AF435252	NA	KC753899	NA	NA	NA	NA	NA
Sturnira_nana	AF435252	NA	KC753899	NA	NA	NA	NA	NA
Uroderma_bilobatum	L28941	AF316491	NA	JF456031	NA	KC783052	NA	NA
Uroderma_magnirostris	AY169957	FJ154378	FJ154246	JF456032	KF569335	KF569435	KF569481	KF569449
Vampyriscus_bidens	FJ154181	FJ154379	FJ154247	JF456128	KM362046	NA	KM361999	KM362142
Vampyriscus_nymphaea	DQ312418	KF569357	NA	JF448146	KF569336	KF569436	KF569482	NA
Vampyriscus_brocki	DQ312421	KM362070	NA	JF456129	KM362047	KM361967	NA	NA
Vampyressa_thyone	DQ312431	KF569358	NA	JN312368	KF569337	KF569437	KF569483	KF569448
Vampyressa_melissa	FJ154185	FJ154383	FJ154251	NA	NA	NA	NA	EU371980
Vampyressa_pusilla	DQ312428	DQ903844	NA	JF448148	KM362048	KM361968	KM362000	EU371990
Chiroderma_villosum	L28943	FJ154319	FJ154187	JF454586	NA	NA	NA	EU371975
Chiroderma_trinitatum	L28942	KF569345	NA	JF454562	KF569316	NA	NA	NA
Chiroderma_doriae	AY169958	KM362056	NA	JF448016	KM362010	KM361941	KM361977	NA
Chiroderma_salvini	L28939	KM362058	NA	JF446777	KM362012	KM361943	KM361979	KM362121
Chiroderma_improvisum	L28938	KM36205	NA	NA	KM36201	KM36194	KM36197	KM36212

		7			1	2	8	0
Mesophylla_macconnelli	FJ154122	FJ154320	AY504555	JF454947	KF569324	NA	NA	EU371977
Vampyrodes_caraccioli	FJ154184	FJ154382	FJ154250	JF456147	KC783110	KC783053	KC783002	EU371991
Vampyrodes_major	HQ637422	NA	NA	NA	NA	NA	NA	NA
Platyrrhinus_helleri	FJ154141	FJ154339	FJ154206	JF455411	KC783100	KC783043	KC782991	KC783244
Platyrrhinus_aurarius	FJ154129	FJ154327	FJ154195	JF455410	KM362031	KM361955	KM361988	KM362131
Platyrrhinus_lineatus	FJ154173	FJ154358	FJ154226	JF446382	KM362035	KM361959	KM361991	KF569447
Platyrrhinus_infuscus	FJ154151	FJ154349	FJ154217	JF449066	KF569326	NA	NA	NA
Platyrrhinus_dorsalis	FJ154139	FJ154337	FJ154205	NA	KM362032	KM361956	KM361989	KM362132
Platyrrhinus_recifinus	FJ154176	FJ154374	FJ154242	JF446385	KM362036	KM361960	KM361992	KM362136
Platyrrhinus_brachycephalus	FJ154132	FJ154330	FJ154198	JF447853	KF569327	KF569428	KF569477	KF569446
Platyrrhinus_guianensis	KJ576932	KJ576959	KJ576941	NA	NA	NA	NA	NA
Platyrrhinus_ismaeli	FJ154155	FJ154353	FJ154221	NA	KM362034	KM361958	KM361990	KM362134
Platyrrhinus_matapalensis	FJ154168	FJ154366	FJ154234	NA	NA	NA	NA	KM362135
Platyrrhinus_masu	FJ154164	FJ154362	FJ154230	NA	NA	NA	NA	NA
Platyrrhinus_albericoi	FJ154124	FJ154322	FJ154190	NA	KM362030	KM361954	KM361987	KM362130
Platyrrhinus_vittatus	FJ154178	FJ154376	FJ154243	JF446602	KM362037	NA	NA	NA
Platyrrhinus_incarum	FJ154147	FJ154344	FJ154213	NA	KM362033	KM361957	KM381957	KM362133
Platyrrhinus_nigellus	FJ154173	FJ154371	FJ154239	NA	KM362035	KM361959	KM361991	NA
Enchisthenes_hartii	EU160972	AF316449	NA	JF447409	KC783070	KC783016	KC782964	KC783222
Ectophylla_alba	DQ312404	AF316448	NA	JF446595	NA	KF569420	KF569469	KF569445

Sphaeronycteris_toxophyllum	AY604452	AF316486	NA	NA	KF569330	KF569430	KF569479	NA
Pygoderma_bilabiatum	AY604438	DQ903839	NA	NA	KC783103	KC783046	KC782994	KC783247
Ametrida_centurio	AY604446	AF316430	NA	JF452119	KF569308	KF569409	NA	NA
Ardops_nichollsi	KJ024748	AF316434	NA	NA	NA	NA	NA	KF569438
Ariteus_flavescens	KJ024703	AF316435	NA	NA	KM362003	KF569410	NA	KM362113
Stenoderma_rufum	DQ312400	AF316487	NA	NA	NA	NA	NA	EU371963
Phyllops_falcatus	DQ211651	AY604453	NA	NA	NA	NA	NA	NA
Artibeus_lituratus	EU160833	DQ985529	NA	EU161033	KC783061	NA	KC782955	EU371964
Artibeus_jamaicensis	DQ869504	FN641674	NA	JF459376	KC783060	AY011419	KC782954	AJ865664
Artibeus_planirostris	AY684720	NA	NA	EU161056	NA	NA	NA	NA
Artibeus_obscurus	EU160865	NA	NA	EU161044	KC783062	NA	KC782956	KC783217
Artibeus_glaucus	EU160970	KF569339	NA	EU160995	KF569310	KF569414	KF569463	KF569444
Artibeus_cinereus	EU160687	AF316443	NA	EU160983	KM362004	KF569412	KF569461	KF569440
Artibeus_schwartzi	DQ869521	NA	NA	NA	NA	NA	NA	NA
Artibeus_intermedius	FJ179231	KM362055	NA	JF447942	KM362008	KM361940	KM361976	KM362118
Artibeus_phaeotis	FJ179248	KF569340	NA	JF498954	KF569313	KF569415	KF569464	KF569442
Artibeus_concolor	EU160951	AF316432	NA	EU160986	KF569309	KF569413	KF569462	KF569443
Artibeus_bogotensis	EU805596	NA	NA	JN312365	NA	NA	NA	NA
Artibeus_fimbriatus	EU160723	DQ985533	NA	EU160992	KM362005	KM361937	KM361973	KM362114
Artibeus_toltecus	FJ179258	NA	NA	KX814389	KM362013	NA	NA	KM362143
Artibeus_amplus	EU16094	NA	NA	EU16097	NA	NA	NA	NA

	7			4				
Artibeus_anderseni	EU160967	NA	NA	EU160976	KF569311	KF569411	KF569460	KF569439
Artibeus_fraterculus	EU160955	KM362052	NA	EU160994	KM362006	KM361938	KM361974	KM362115
Artibeus_aztecus	FJ179238	NA	NA	JF447913	NA	NA	NA	NA
Artibeus_hirsutus	FJ179226	AF316433	NA	NA	NA	KC783007	NA	NA
Artibeus_inopinatus	FJ179229	NA	NA	NA	NA	NA	NA	KM362117
Artibeus_incomitata	NA	KM362054	NA	NA	KM362007	KM361939	KM361975	KM362116
Rhinophylla_pumilio	AF187031	AF316484	NA	JF455665	KC783104	KC783047	KC782995	EU371960

Appendix B

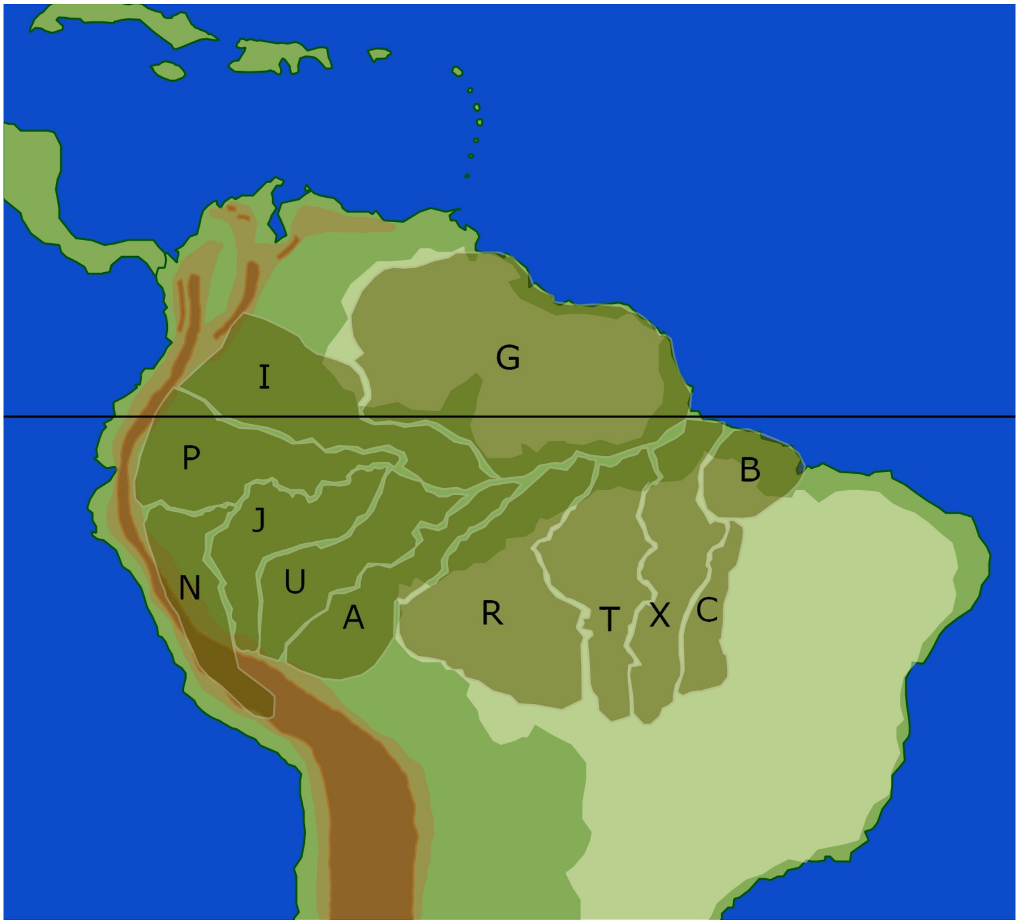

G = Guiana, I = Imeri, P = Napo, N = Marañón, J = Ucayali, U = Jurua, A = Purus, R = Rondonia, T = Tapajos, X = Xingu, C = Araguaia, B = Belem, M = Atlantic forest, Y, O = Andes.

Appendix C

Taxon	Fossil	Age
Melipona	*Melittosphex*	Early Cretaceous
	oldest stem bee fossil	Upper Albian
	(Poinar and Danforth, 2006)	
	Proplebeia dominicana	Miocene
	Iturralde-Vinent 1996	
	Apis lithohermaea	Middle Miocene
	Engel, 2006	
	Euglossa moronei	Miocene
	Engel, 1999	
Echimyidae	*Draconomys verai*	Early Oligocene
		pre Deseadan SALMA
	Sallamys	Deseadan, Late oligocene,
	Kay et al (1998)	
	Paradelphomys	Early Miocene
	Patterson & Pascual, 1968	Colhuehuapian SALMA
	Pampamys emmonsae	Late Miocene
	(Olivares 2012)	Chasicoan-Huayquerian SALMA
Cebidae	*Branisella boliviana*	Deseadan SALMA
	Takai et al, 2000	
	Cebupithecia sarmientoi	Middle Miocene
	Stirton, 1951	
	Neosaimiri fieldsi	Middle miocene
	Stirton, 1951	
	Stirtonia spp.	Middle Miocene
	(Hershkovitz, 1970)	
	Lagonimico conclucatus	Middle miocene
	Kay, 1994	
	Cebuella	Mayoan SALMA
	Marivaux et al 2016	
Rhinella	oldest fossil of Bufonidae	Late Paleocene
	Baéz and Gasparini, 1979	
	oldest fossil of *Rhinella marina*	Middle Miocene
	Estes and Wassersug, 1963;	
	Sanchíz, 1998	
Stenodermatinae	*Cubanycteris silvai*	Quaternary

	Czaplewski et al (2003)	
	Phyllops vetus	Quaternary
	Teeling et al (2005);	
	Dávalos (2007)	
	Palynephyllum antimaster	Middle Miocene
Cracidae	*Gallinuloides wyomingensis*	Early Eocene
	Eastman, 1900; Dyke, 2003; Mayr and Weidig, 2004	
	Palaeortyx gallica	Late Oligocene
	Mayr et al 2006	
	Schaubortyx keltica	Oligocene
	Rodkorb,1964	
	Rhegminornis calobates	Early Miocene
	Olson and Farrand, 1974	
	Callipepla shotwelli	Middle Pliocene
	Holman,1961	

Appendix D

Taxon	Gene	Strict	Relaxed	Delta
Stenodermatinae	Thy	-2.99E+003	-2.98E+003	-11.933
	Rag2	-4.38E+003	-4.37E+003	-12.917
	Plcb4	-1.78E+003	-1.70E+003	-83.752
	Nd2	-1.11E+004	-1.09E+004	-215.26
	Cytb	-2.05E+004	-2.04E+004	-82.47
	coi	-1.29E+004	-1.36E+004	676.21
	bdnf	-1.49E+003	-1.49E+003	-5.819
	atp7	-2.26E+003	-2.27E+003	4.743
Echimyidae	12s	-9.91E+003	-9.82E+003	-89.5
	cytb	-2.15E+004	-2.13E+004	-238.26
	ghr	-7.42E+003	-7.19E+003	-228.412
	rag1	-8.27E+003	-7.02E+003	-1253.132
	vwf	-8.13E+003	-7.94E+003	-191.062
Cebidae	16s	-5.82E+003	-5.80E+003	-15.684
	abca1	-5.17E+003	-5.05E+003	-119.114
	adora3	-3.67E+003	-3.66E+003	-10
	aff2	-1.90E+004	-1.90E+004	-9.31
	bdnf	-1.27E+003	-1.25E+003	-20
	beta2	-6.46E+003	-6.45E+003	-10
	cytb	-1.16E+004	-1.16E+004	-8.44
	D-loop	-1.14E+004	-1.14E+004	-31.63
	dmrt1	-1.31E+003	-1.31E+003	-6.887
	fbn1	-1.41E+003	-1.40E+003	-10
	rag1	-3.15E+003	-3.15E+003	-6
	rag2	-1.55E+003	-1.54E+003	-6.278
	sry	-3.25E+003	-3.23E+003	-13.668
Rhinella	12s-trna-val-16s	-2.69E+004	-2.68E+004	-100
	16s	-4.87E+003	-4.84E+003	-30
	cytb	-10543.52	-10502.04	-41
	pomc	-2.90E+003	-2.89E+003	-12.117
	rag1	-1.13E+004	-1.09E+004	-400
	rhod	-1.10E+003	-1.09E+003	-10
Cracidae	cltc1	-4.77E+003	-4.38E+003	-386.003
	cltc	-6.93E+003	-6.17E+003	-757.934
	coi	-9.58E+003	-8.68E+003	-905.836

	cytb	-1.05E+004	-9.73E+003	-805.309
	eff2	-8.41E+003	-7.82E+003	-588.553
	nd2	-1.56E+004	-1.36E+004	-2008.82
	nd5	-7.91E+003	-7.43E+003	-473.938
	rhod	-9.91E+003	-8.39E+003	-1514.413
	serpinb14	-1.03E+004	-9.09E+003	-1204.605
	tfb5	-1.87E+003	-1.83E+003	-40.824
Melipona	16s	-9.09E+003	-8.24E+003	-852.724
	argk	-1.08E+004	-9.46E+003	-1340
	coi	-1.48E+004	-1.35E+004	-1300
	ef1-alpha	-1.46E+004	-1.20E+004	-2600
	Rna-pol2	-7.73E+003	-6.13E+003	-1600

Appendix E

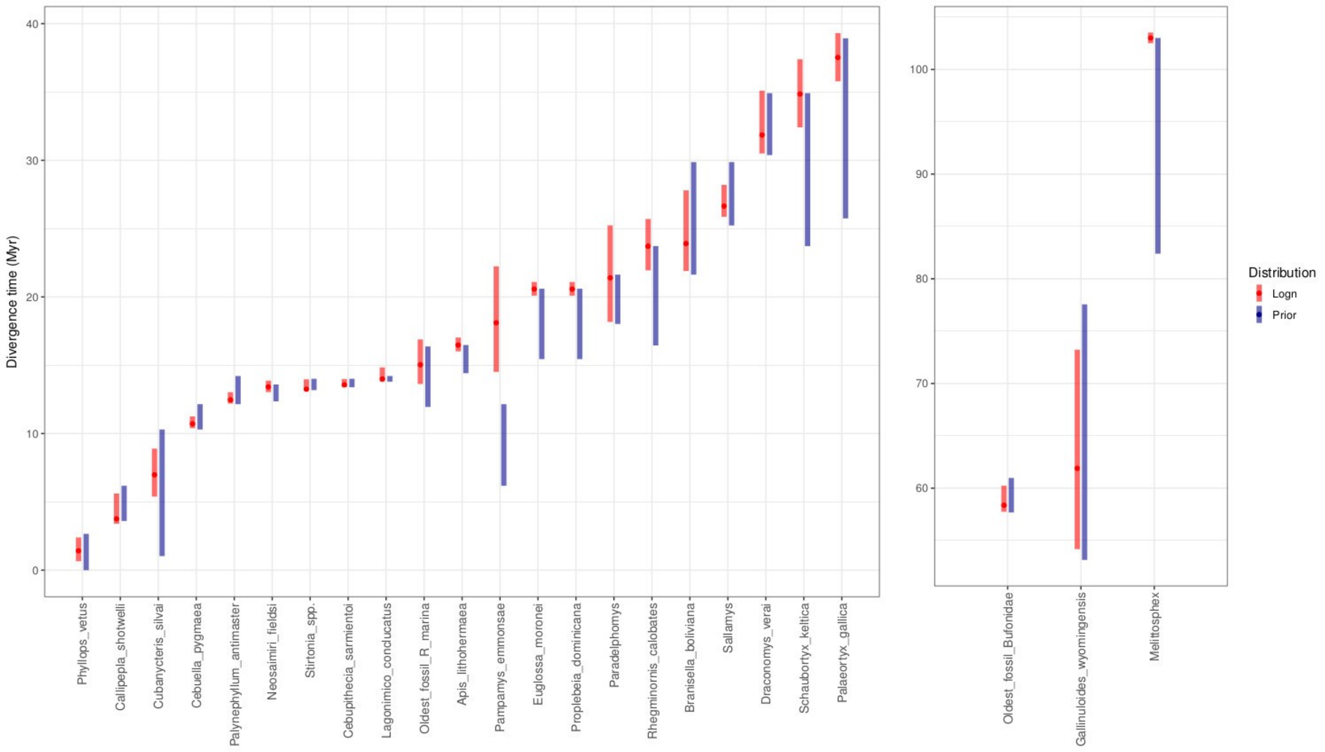

Red bars indicate the 95 % posterior CI under a lognormal distribution, and the points represent the posterior median values. Blue bars correspond to the temporal range for each prior.

Appendix F

Taxa	Barrier	VIP
Cebidae	Tocantins	10.23-11.64 Median=10.85
	Madeira	10.09-10.92 median=10.40
Rhinella	Ucayali	2.74-10.79 median=5.97
	Marañon	8.35-24.39 median=16.26
Echimyidae	Tocantins	6.81-12.89 Median=9.75
Melipona	Madeira	5.39-12.33 median=8.27 mean=8.54
Stenodermatinae	Madeira	0.24-0.84 median=0.5 mean=0.52
Cracidae	Tocantins	0.54-2.22 1.23 mean=1.30
	Amazonas-madeira	0.38-2.14 1.15 mean=1.22

Taxa	Barrier	BioGeoBears
Echyimidae	Negro	3.8-9.6 Median=6.40

Appendix G

Phylogeny	Modelo	Timeperiods (Myr)	dispersal rates	DEC Likelihood
Stenodermatinae	M0	no	1	-457.84
	M1	Root-10-7 →	0.25-0.50-1	-441.55
	M2	Root-11.8-2.5 →	0.25-0.50-1	-439
	M3	Root-17-10 →	0.25-0.50-1	-448.61
	M4	Root-10-7 →	0.25-0.50-0.25	-465.11
Cracidae	M0	no	1	-228.86
	M1	Root-10-7 →	0.25-0.50-1	-225.14
	M2	Root-11.8-2.5 →	0.25-0.50-1	-221.97
	M3	Root-10 →	0.25-1	-227.12
	M4	Root-10-7 →	0.25-0.50-0.25	-233.38
Echimyidae	M0	no	1	-220.48
	M1	Root-10-7 →	0.25-0.50-1	-221.73
	M2	Root-11.8-2.5 →	0.25-0.50-1	-219.47
	M3	Root-17-10 →	0.25-0.50-1	-219.86
	M4	Root-10-7 →	0.25-0.50-0.25	-221.02
Cebidae	M0	no	1	-151.63
	M1	Root-10-7 →	0.25-0.50-1	-154.46
	M2	Root-11.8-2.5 →	0.25-0.50-1	-154.23
	M3	Root-17-10 →	0.25-0.50-1	-153.04
	M4	Root-10-7 →	0.25-0.50-0.25	-152.85
Rhinella	M0	no	1	-133.37
	M1	Root-10-7 →	0.25-0.50-1	-130.83
	M2	Root-11.8-2.5 →	0.25-0.50-1	-130.73
	M3	Root-17-10 →	0.25-0.50-1	-131.36
	M4	Root-10-7 →	0.25-0.50-0.25	-133.39
Melipona	M0	no	1	-210.41
	M1	Root-10-7 →	0.25-0.50-1	-212.55
	M2	Root-11.8-2.5 →	0.25-0.50-1	-211.18
	M3	Root-17-10 →	0.25-0.75-1	-215.67
	M4	Root-10-7 →	0.25-0.50-0.25	-211.89

Appendix H

Cebidae M0

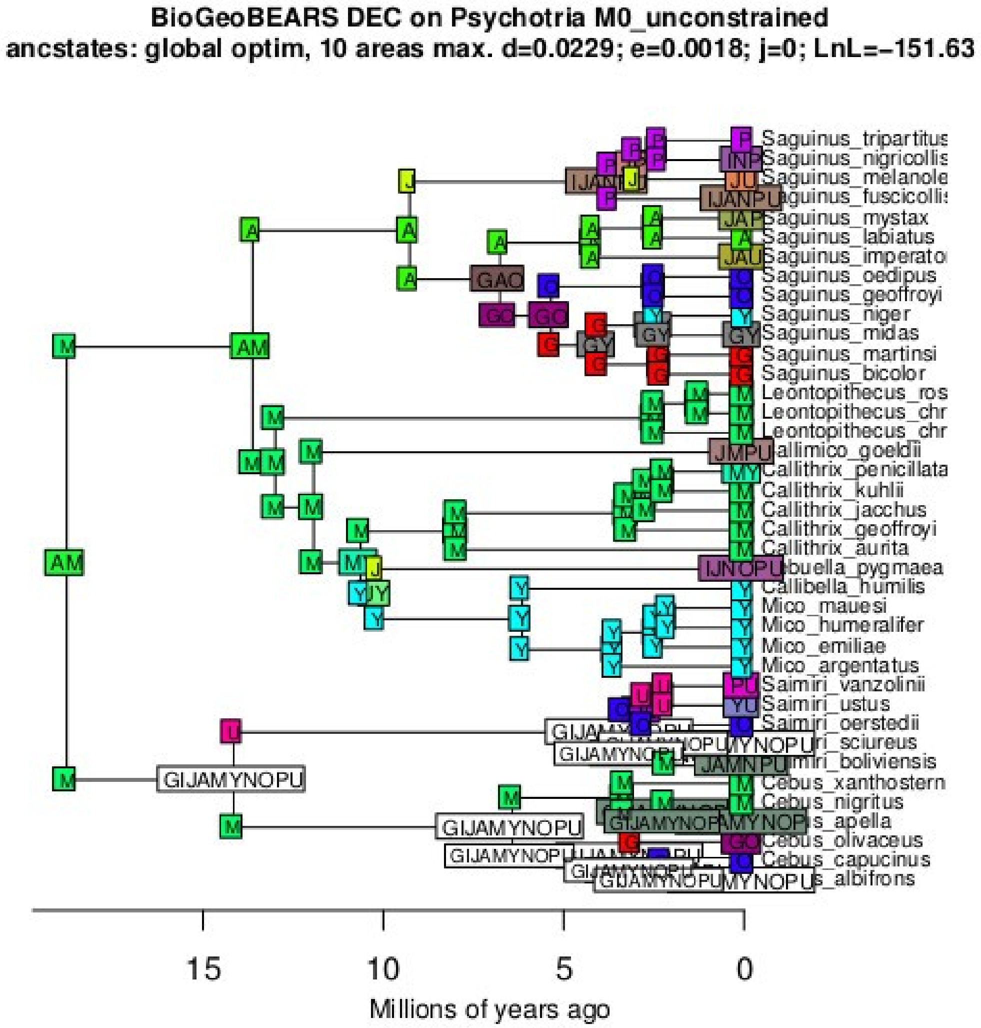

Cebidae M1

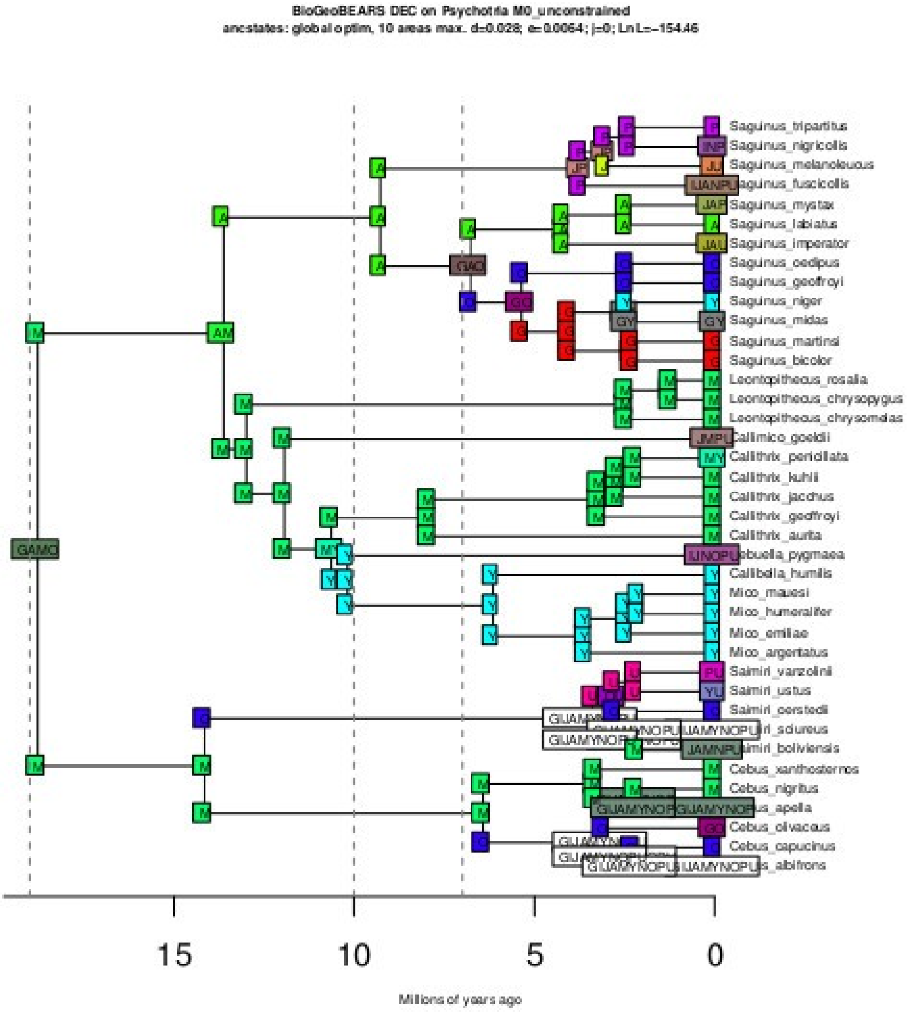
BioGeoBEARS DEC on Psychotria M0_unconstrained
ancstates: global optim, 10 areas max. d=0.028; e=0.0064; j=0; LnL=-154.46
Saguinus_tripartitus
Saguinus_nigricollis
Saguinus_melanoleucus
agunus_fuscicollis
Saguinus_mystax
Saguinus_labiatus
Saguinus_imperator
Saguinus_oedipus
Saguinus_geoffroyi
Saguinus_niger
Saguinus_midas
Saguinus_martinsi
Saguinus_bicolor
Leontopithecus_rosalia
Leontopithecus_chrysopygus
Leontopithecus_chrysomelas
Callimico_goeldii
Callithrix_penicillata
Callithrix_kuhlii
Callithrix_jacchus
Callithrix_geoffroyi
Callithrix_aurita
ebuella_pygmaea
Callibella_humilis
Mico_mauesi
Mico_humeralifer
Mico_emiliae
Mico_argentatus
Saimiri_vanzolinii
Saimiri_ustus
Saimiri_oerstedii
iri_sciureus
imiri_boliviensis
Cebus_xanthosternos
Cebus_nigritus
us_apella
Cebus_olivaceus
Cebus_capucinus
s_albifrons
GAMO
AM
GIJAMYNOPU
JAMNPU
IJNOPU
JMPU
IJANPU
15
10
5
0
Millions of years ago

Cebidae M2

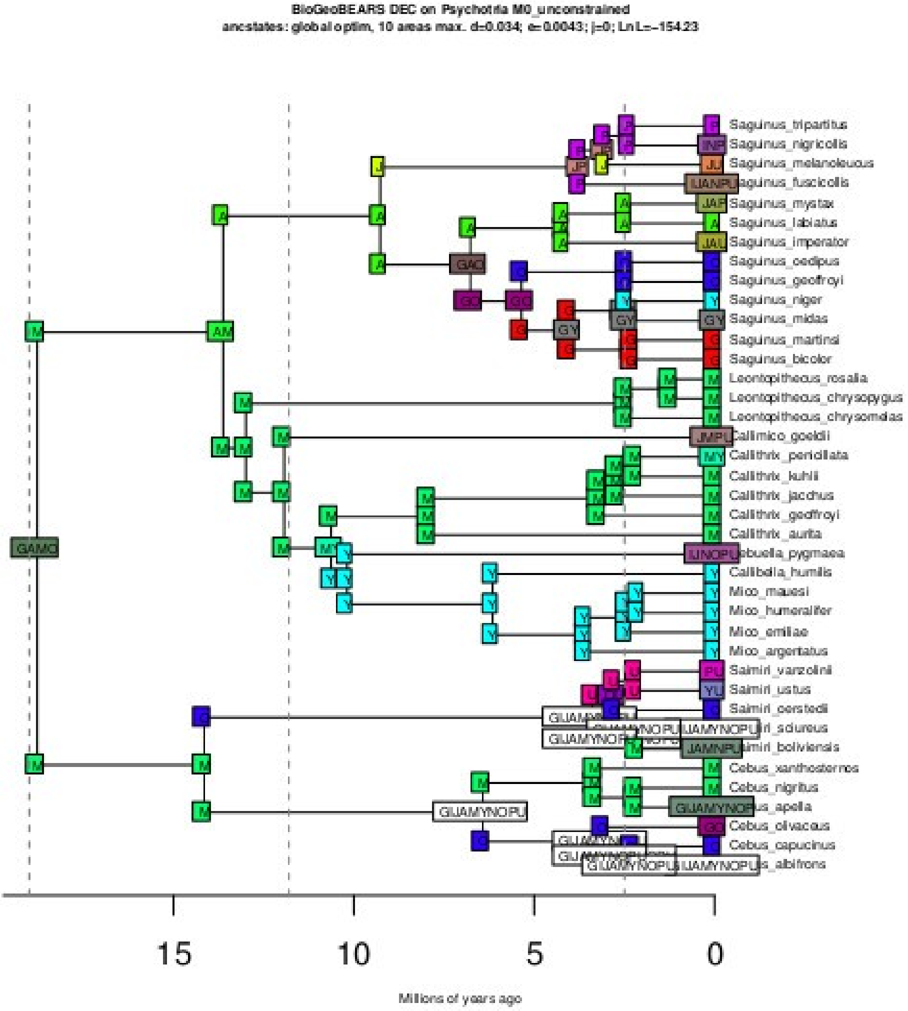
BioGeoBEARS DEC on Psychotria M0_unconstrained
ancstates: global optim, 10 areas max. d=0.034; e=0.0043; j=0; LnL=-154.23
Saguinus_tripartitus
Saguinus_nigricollis
Saguinus_melanoleucus
aguinus_fuscicollis
Saguinus_mystax
Saguinus_labiatus
Saguinus_imperator
Saguinus_oedipus
Saguinus_geoffroyi
Saguinus_niger
Saguinus_midas
Saguinus_martinsi
Saguinus_bicolor
Leontopithecus_rosalia
Leontopithecus_chrysopygus
Leontopithecus_chrysomelas
Callimico_goeldii
Callithrix_penicillata
Callithrix_kuhlii
Callithrix_jacchus
Callithrix_geoffroyi
Callithrix_aurita
ebuella_pygmaea
Callibella_humilis
Mico_mauesi
Mico_humeralifer
Mico_emiliae
Mico_argentatus
Saimiri_vanzolinii
Saimiri_ustus
Saimiri_oerstedii
iri_sciureus
imiri_boliviensis
Cebus_xanthosternos
Cebus_nigritus
us_apella
Cebus_olivaceus
Cebus_capucinus
s_albifrons
GAMO
AM
GIJAMYNOPU
15
10
5
0
Millions of years ago

Cebidae M3

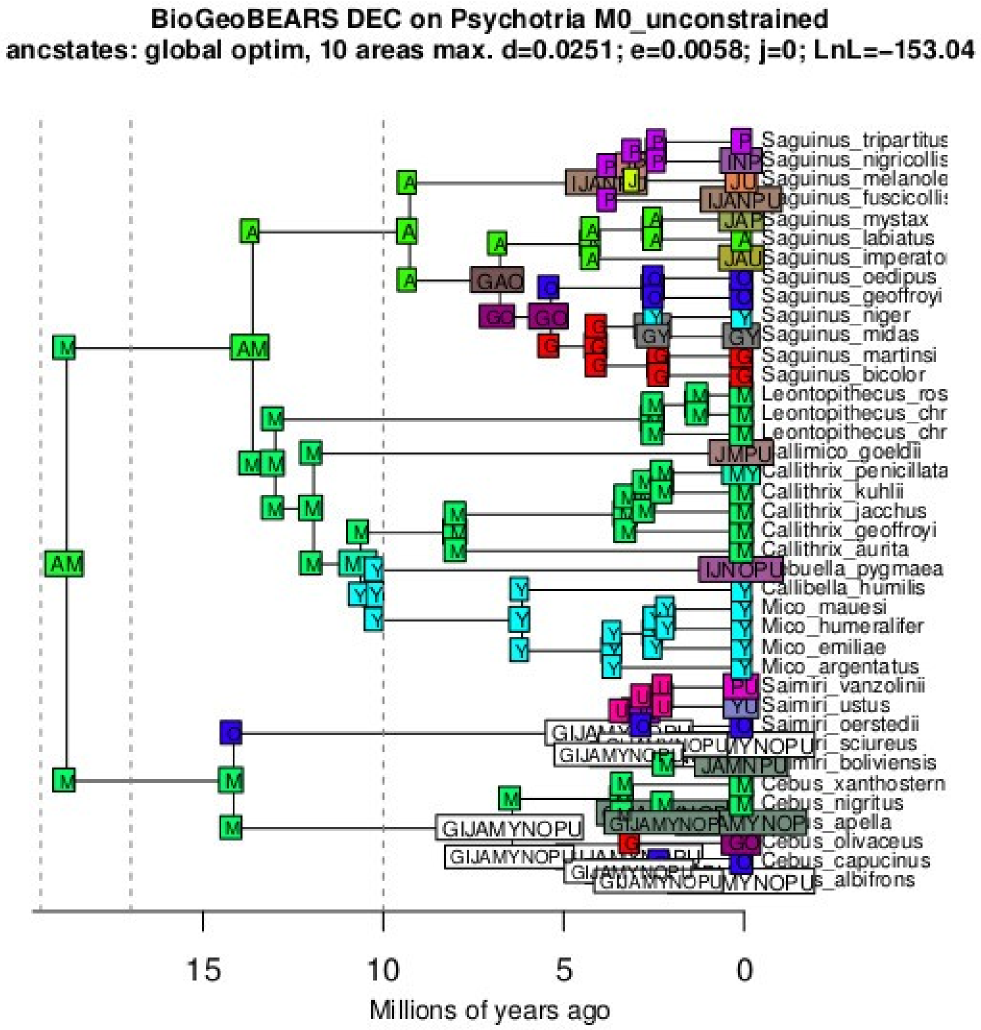
BioGeoBEARS DEC on Psychotria M0_unconstrained
ancstates: global optim, 10 areas max. d=0.0251; e=0.0058; j=0; LnL=-153.04
Saguinus_tripartitus
Saguinus_nigricollis
Saguinus_melanole
aguinus_fuscicollis
Saguinus_mystax
Saguinus_labiatus
Saguinus_imperato
Saguinus_oedipus
Saguinus_geoffroyi
Saguinus_niger
Saguinus_midas
Saguinus_martinsi
Saguinus_bicolor
Leontopithecus_ros
Leontopithecus_chr
Leontopithecus_chr
allimico_goeldii
Callithrix_penicillata
Callithrix_kuhlii
Callithrix_jacchus
Callithrix_geoffroyi
Callithrix_aurita
ebuella_pygmaea
Callibella_humilis
Mico_mauesi
Mico_humeralifer
Mico_emiliae
Mico_argentatus
Saimiri_vanzolinii
Saimiri_ustus
Saimiri_oerstedii
ri_sciureus
imiri_boliviensis
Cebus_xanthostern
Cebus_nigritus
s_apella
Cebus_olivaceus
Cebus_capucinus
s_albifrons
AM
M
GIJAMYNOPU
15
10
5
0
Millions of years ago

Cebidae M4

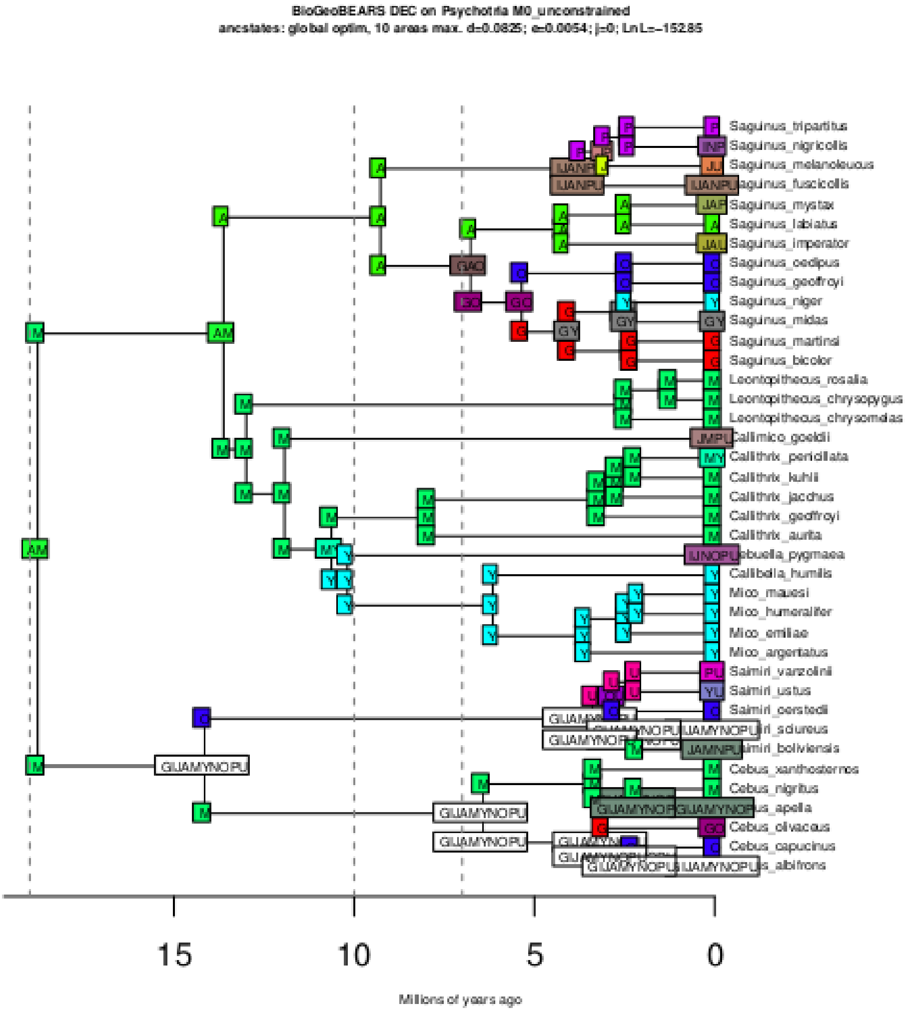
BioGeoBEARS DEC on Psychotria M0_unconstrained
ancstates: global optim, 10 areas max. d=0.0825; e=0.0054; j=0; LnL=-152.85
Saguinus_tripartitus
Saguinus_nigricollis
Saguinus_melanoleucus
aguinus_fuscicollis
Saguinus_mystax
Saguinus_labiatus
Saguinus_imperator
Saguinus_oedipus
Saguinus_geoffroyi
Saguinus_niger
Saguinus_midas
Saguinus_martinsi
Saguinus_bicolor
Leontopitheous_rosalia
Leontopitheous_chrysopygus
Leontopitheous_chrysomelas
allimico_goeldii
Callithrix_penicillata
Callithrix_kuhlii
Callithrix_jacchus
Callithrix_geoffroyi
Callithrix_aurita
ebuella_pygmaea
Callibella_humilis
Mico_mauesi
Mico_humeralifer
Mico_emiliae
Mico_argentatus
Saimiri_vanzolinii
Saimiri_ustus
Saimiri_oerstedii
iri_sciureus
imiri_boliviensis
Cebus_xanthosternos
Cebus_nigritus
us_apella
Cebus_olivaceus
Cebus_capucinus
s_albifrons
15
10
5
0
Millions of years ago

Cracidae M0

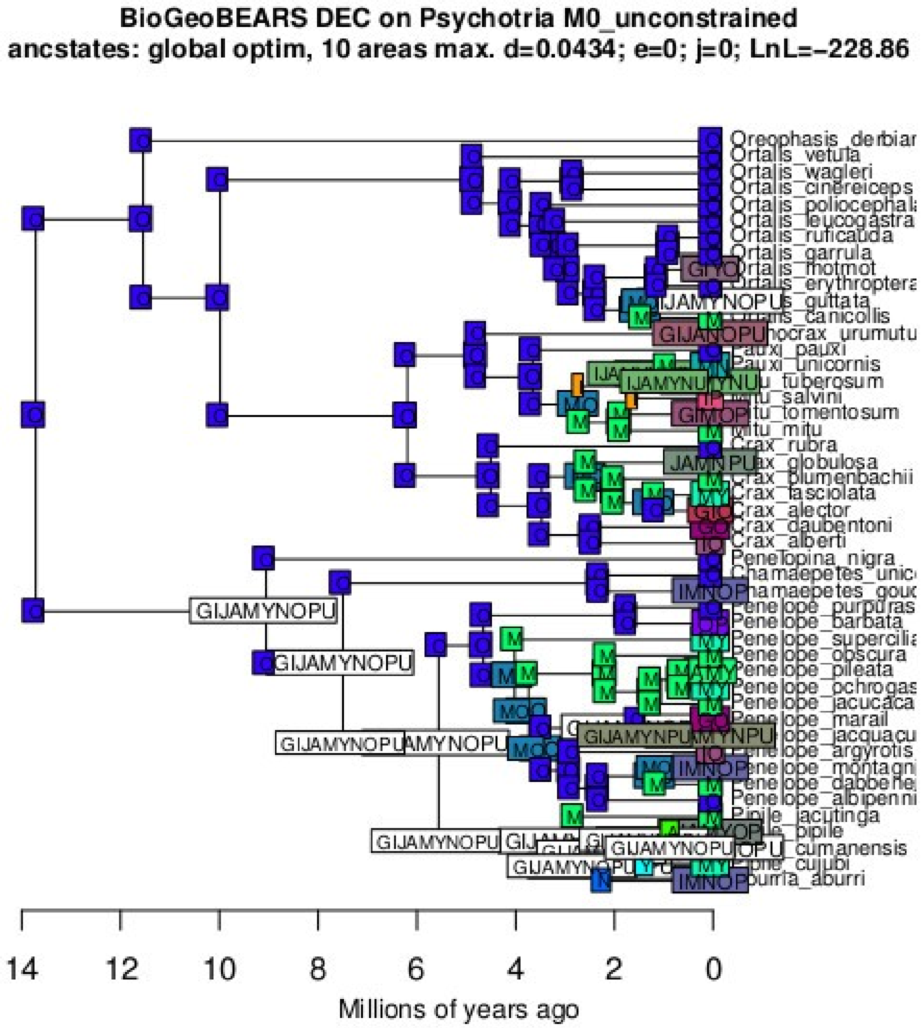
BioGeoBEARS DEC on Psychotria M0_unconstrained
ancstates: global optim, 10 areas max. d=0.0434; e=0; j=0; LnL=-228.86
Oreophasis_derbiar
Ortalis_vetula
Ortalis_wagleri
Ortalis_cinereiceps
Ortalis_poliocephala
Ortalis_leucogastra
Ortalis_ruficauda
Ortalis_garrula
Ortalis_motmot
Ortalis_erythroptera
s_guttata
Ortalis_canicollis
nocrax_urumutu
Pauxi_pauxi
Pauxi_unicornis
u_tuberosum
Mitu_salvini
itu_tomentosum
Mitu_mitu
Crax_rubra
ax_globulosa
Crax_blumenbachii
Crax_fasciolata
Crax_alector
Crax_daubentoni
Crax_alberti
Penelopina_nigra
Chamaepetes_unic
hamaepetes_gouc
Penelope_purpuras
Penelope_barbata
Penelope_supercilia
Penelope_obscura
Penelope_pileata
Penelope_ochrogas
Penelope_jacucaca
Penelope_marail
lope_jacquacu
lope_argyrotis
enelope_montagni
enelope_dabbene
Penelope_albipenni
Pipile_jacutinga
le_pipile
_cumanensis
Pipile_cujubi
burria_aburri
GIJAMYNOPU
IJAMYNOPU
GIJANOPU
GIMOP
JAMNPU
IMNOP
GIJAMYNPU
14
12
10
8
6
4
2
0
Millions of years ago

Cracidae M1

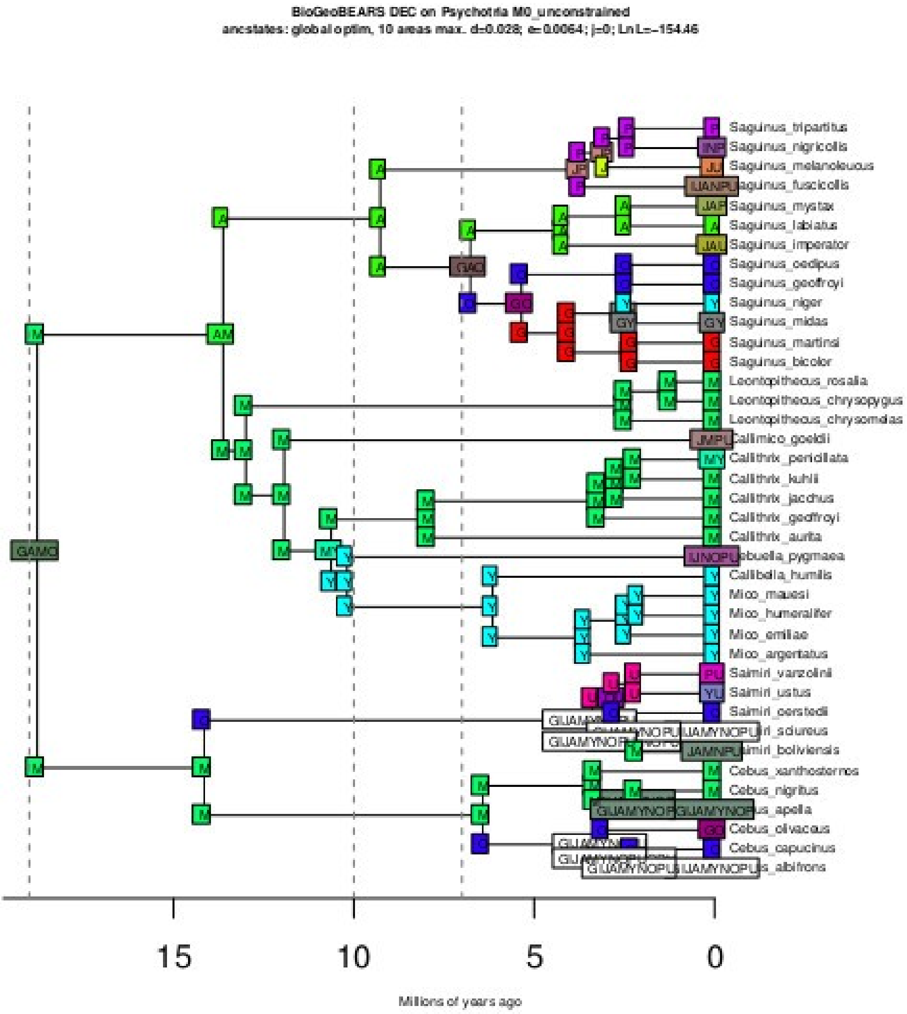
BioGeoBEARS DEC on Psychotria M0_unconstrained
ancstates: global optim, 10 areas max. d=0.028; e=0.0064; j=0; LnL=-154.46
Saguinus_tripartitus
Saguinus_nigricollis
Saguinus_melanoleucus
aguinus_fuscicollis
Saguinus_mystax
Saguinus_labiatus
Saguinus_imperator
Saguinus_oedipus
Saguinus_geoffroyi
Saguinus_niger
Saguinus_midas
Saguinus_martinsi
Saguinus_bicolor
Leontopitheous_rosalia
Leontopitheous_chrysopygus
Leontopitheous_chrysomelas
Callimico_goeldii
Callithrix_penicillata
Callithrix_kuhlii
Callithrix_jacchus
Callithrix_geoffroyi
Callithrix_aurita
ebuella_pygmaea
Callibella_humilis
Mico_mauesi
Mico_humeralifer
Mico_emiliae
Mico_argentatus
Saimiri_vanzolinii
Saimiri_ustus
Saimiri_oerstedii
iri_sciureus
imiri_boliviensis
Cebus_xanthosternos
Cebus_nigritus
us_apella
Cebus_olivaceus
Cebus_capucinus
s_albifrons
GAMC
AM
GAC
GY
JMPU
MY
IJNOPU
IJANPU
JAMNPU
GIJAMYNOPU
15
10
5
0
Millions of years ago

Cracidae M2

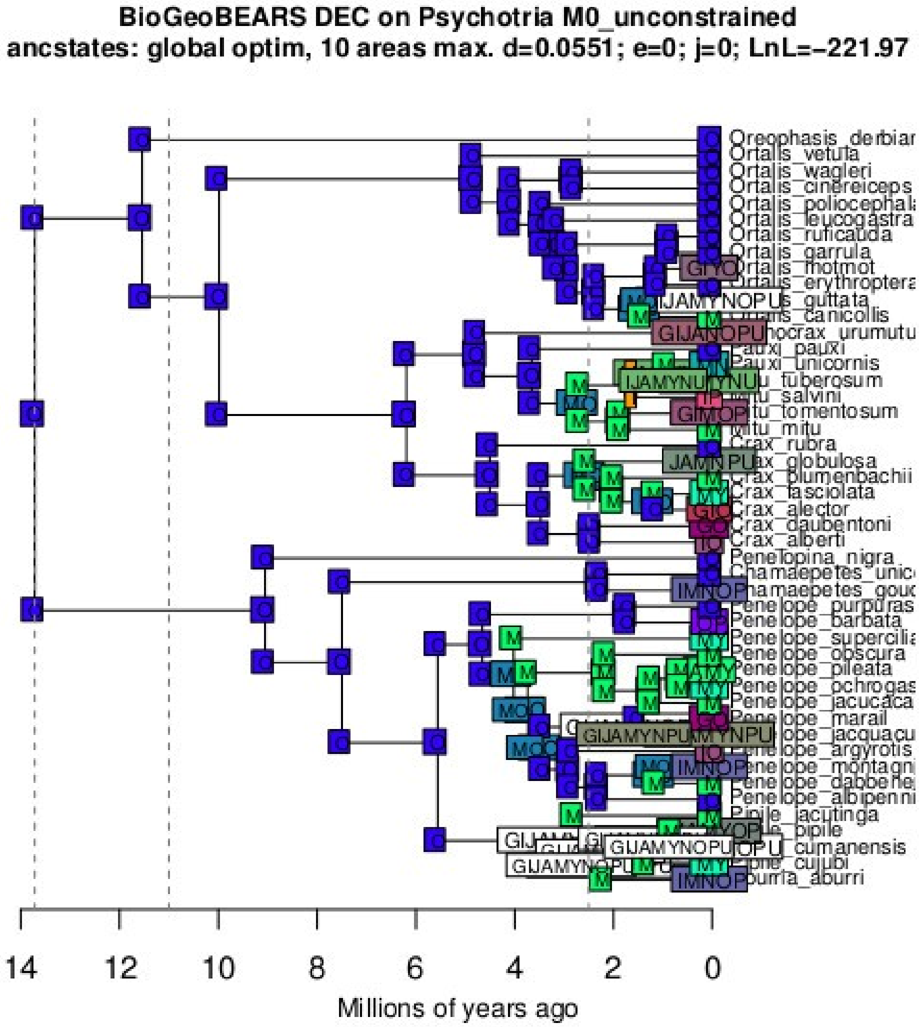
BioGeoBEARS DEC on Psychotria M0_unconstrained
ancstates: global optim, 10 areas max. d=0.0551; e=0; j=0; LnL=-221.97
Oreophasis_derbiar
Ortalis_vetula
Ortalis_wagleri
Ortalis_cinereiceps
Ortalis_poliocephala
Ortalis_leucogastra
Ortalis_ruficauda
Ortalis_garrula
Ortalis_motmot
Ortalis_erythroptera
s_guttata
Ortalis_canicollis
nocrax_urumutu
Pauxi_pauxi
Pauxi_unicornis
u_tuberosum
Mitu_salvini
itu_tomentosum
Mitu_mitu
Crax_rubra
ax_globulosa
Crax_blumenbachii
Crax_fasciolata
Crax_alector
Crax_daubentoni
Crax_alberti
Penelopina_nigra
Chamaepetes_unic
hamaepetes_gouc
Penelope_purpuras
Penelope_barbata
Penelope_supercilia
Penelope_obscura
Penelope_pileata
Penelope_ochrogas
Penelope_jacucaca
Penelope_marail
elope_jacquacu
Penelope_argyrotis
enelope_montagni
Penelope_dabbeneı
Penelope_albipenni
Pipile_jacutinga
ile_pipile
_cumanensis
Pipile_cujubi
burria_aburri
GIYO
GIJAMYNOPU
GIJANOPU
IJAMYNU
YNU
GIMOP
JAMNPU
GIO
GO
IO
IMNOP
OP
MY
AMY
GIJAMYNPU
MYNPU
MO
YOP
OPU
GIJAMYNOPU
14
12
10
8
6
4
2
0
Millions of years ago

Cracidae M3

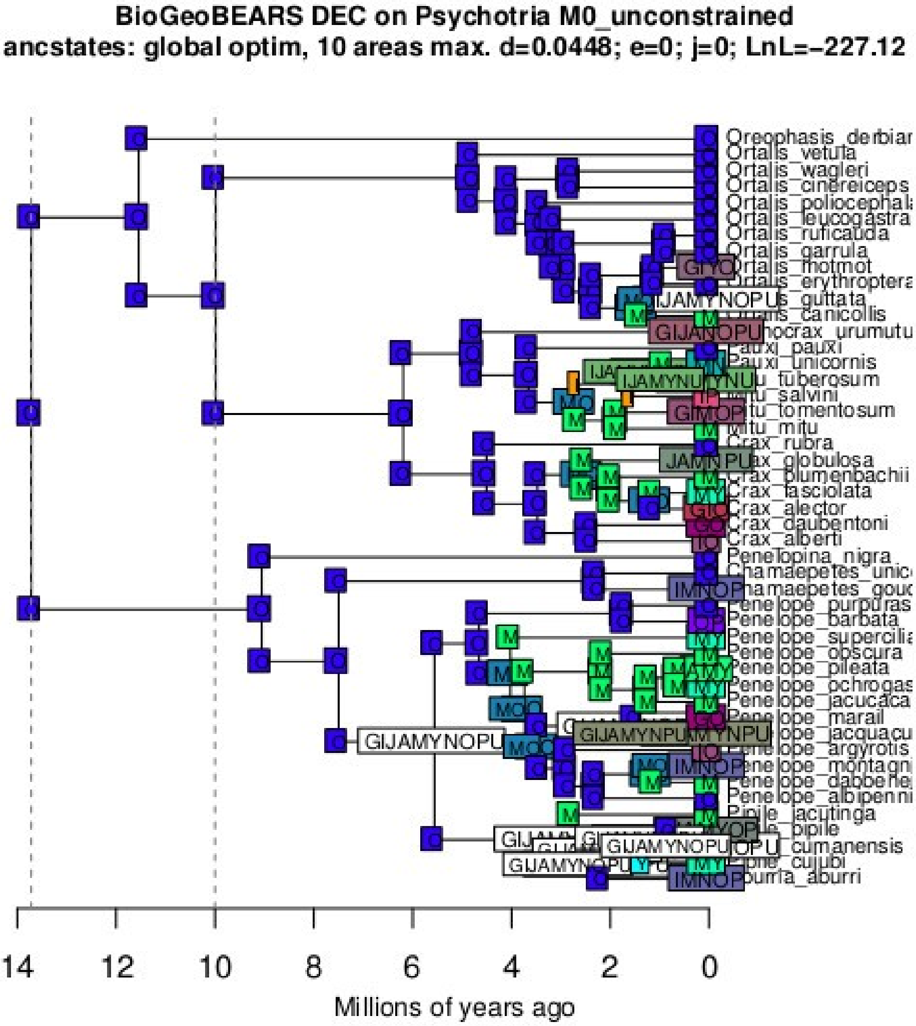
BioGeoBEARS DEC on Psychotria M0_unconstrained
ancstates: global optim, 10 areas max. d=0.0448; e=0; j=0; LnL=-227.12
Oreophasis_derbiar
Ortalis_vetula
Ortalis_wagleri
Ortalis_cinereiceps
Ortalis_poliocephal
Ortalis_leucogastra
Ortalis_ruficauda
Ortalis_garrula
Ortalis_motmot
Ortalis_erythropter
s_guttata
Ortalis_canicollis
ocrax_urumutu
Pauxi_pauxi
Pauxi_unicornis
u_tuberosum
itu_salvini
itu_tomentosum
itu_mitu
Crax_rubra
ax_globulosa
Crax_blumenbachii
Crax_fasciolata
Crax_alector
Crax_daubentoni
Crax_alberti
Penelopina_nigra
Chamaepetes_unic
hamaepetes_gouc
Penelope_purpuras
Penelope_barbata
Penelope_supercilia
Penelope_obscura
Penelope_pileata
Penelope_ochrogas
Penelope_jacucaca
Penelope_marail
ope_jacquacu
ope_argyrotis
enelope_montagni
enelope_dabbene
Penelope_albipenni
Pipile_jacutinga
le_pipile
_cumanensis
pile_cujubi
burria_aburri
GIJAMYNOPU
GIJAMYNPU
IJAMYNOPU
GIJANOPU
IJAMYNU
GIMOP
JAMNPU
IMNOP
GIYO
MOO
14
12
10
8
6
4
2
0
Millions of years ago

Cracidae M4

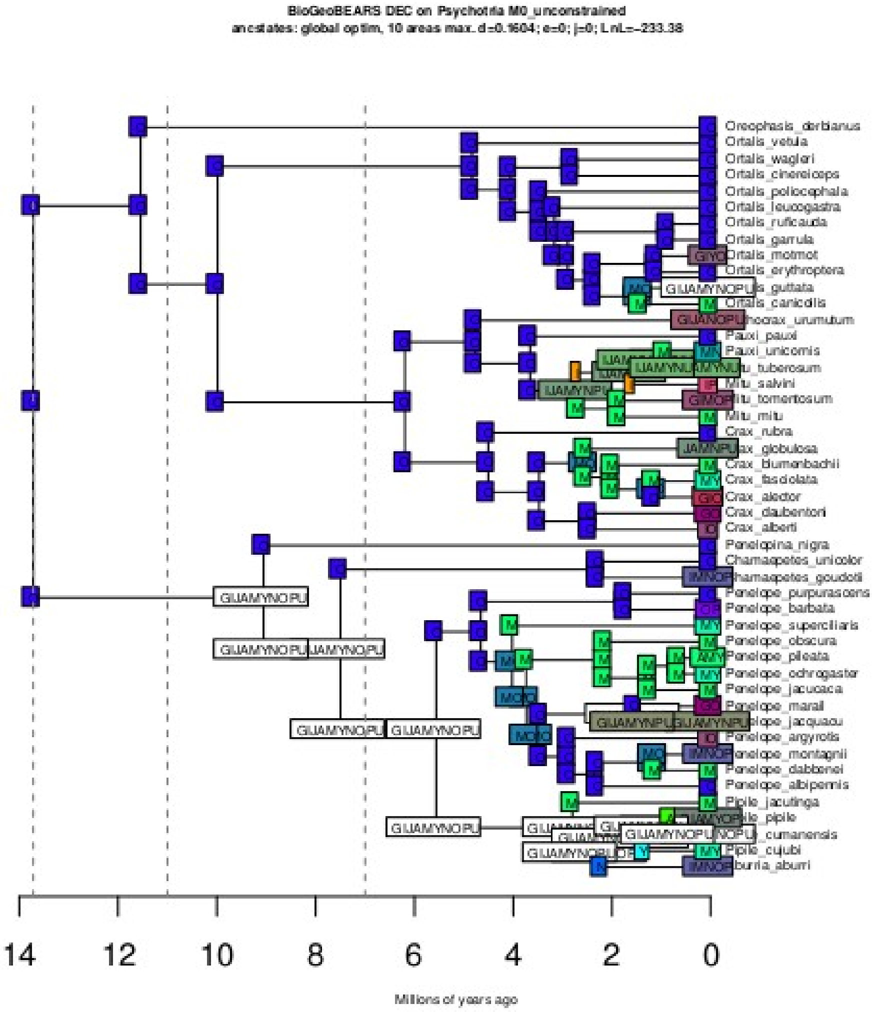
BioGeoBEARS DEC on Psychotria M0_unconstrained
ancstates: global optim, 10 areas max. d=0.1604; e=0; j=0; LnL=-233.38
Oreophasis_derbianus
Ortalis_vetula
Ortalis_wagleri
Ortalis_cinereiceps
Ortalis_poliocephala
Ortalis_leucogastra
Ortalis_ruficauda
Ortalis_garrula
Ortalis_motmot
Ortalis_erythroptera
s_guttata
Ortalis_canicollis
hocrax_urumutum
Pauxi_pauxi
Pauxi_unicornis
tu_tuberosum
Mitu_salvini
itu_tomentosum
Mitu_mitu
Crax_rubra
ax_globulosa
Crax_blumenbachii
Crax_fasciolata
Crax_alector
Crax_daubentoni
Crax_alberti
Penelopina_nigra
Chamaepetes_unicolor
hamaepetes_goudotii
Penelope_purpurascens
Penelope_barbata
Penelope_superciliaris
Penelope_obscura
Penelope_pileata
Penelope_ochrogaster
Penelope_jacucaca
Penelope_marail
elope_jacquacu
Penelope_argyrotis
enelope_montagnii
Penelope_dabbenei
Penelope_albipennis
Pipile_jacutinga
ile_pipile
_cumanensis
Pipile_cujubi
burria_aburri
GIUAMYNOPU
GIUAMYNOPU
GIUAMYNOPU
14
12
10
8
6
4
2
0
Millions of years ago

Rhinella M0

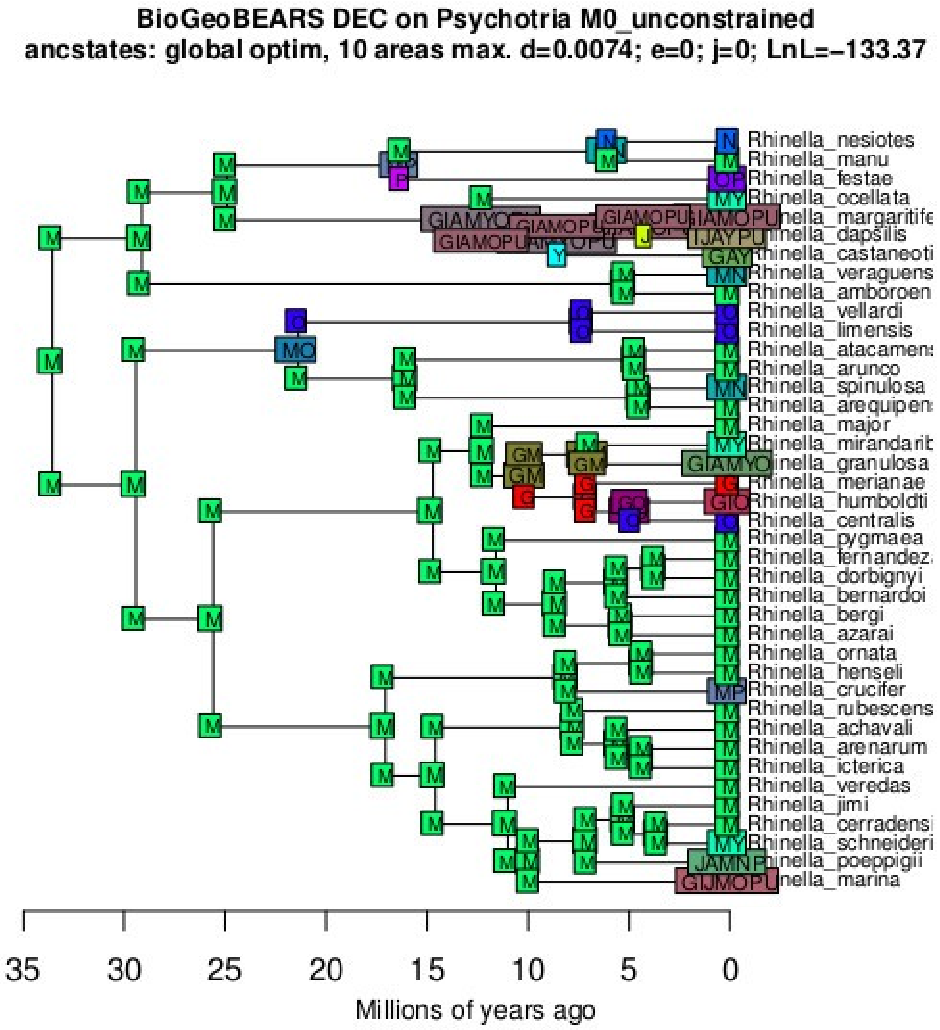
BioGeoBEARS DEC on Psychotria M0_unconstrained
ancstates: global optim, 10 areas max. d=0.0074; e=0; j=0; LnL=-133.37
Rhinella_nesiotes
Rhinella_manu
Rhinella_festae
Rhinella_ocellata
nella_margaritife
nella_dapsilis
hinella_castaneoti
Rhinella_veraguens
Rhinella_amboroen
Rhinella_vellardi
Rhinella_limensis
Rhinella_atacamens
Rhinella_arunco
Rhinella_spinulosa
Rhinella_arequipens
Rhinella_major
Rhinella_mirandarib
inella_granulosa
hinella_merianae
Rhinella_humboldti
Rhinella_centralis
Rhinella_pygmaea
Rhinella_fernandeza
Rhinella_dorbignyi
Rhinella_bernardoi
Rhinella_bergi
Rhinella_azarai
Rhinella_ornata
Rhinella_henseli
Rhinella_crucifer
Rhinella_rubescens
Rhinella_achavali
Rhinella_arenarum
Rhinella_icterica
Rhinella_veredas
Rhinella_jimi
Rhinella_cerradensi
Rhinella_schneideri
hinella_poeppigii
nella_marina
35
30
25
20
15
10
5
0
Millions of years ago

Rhinella M1

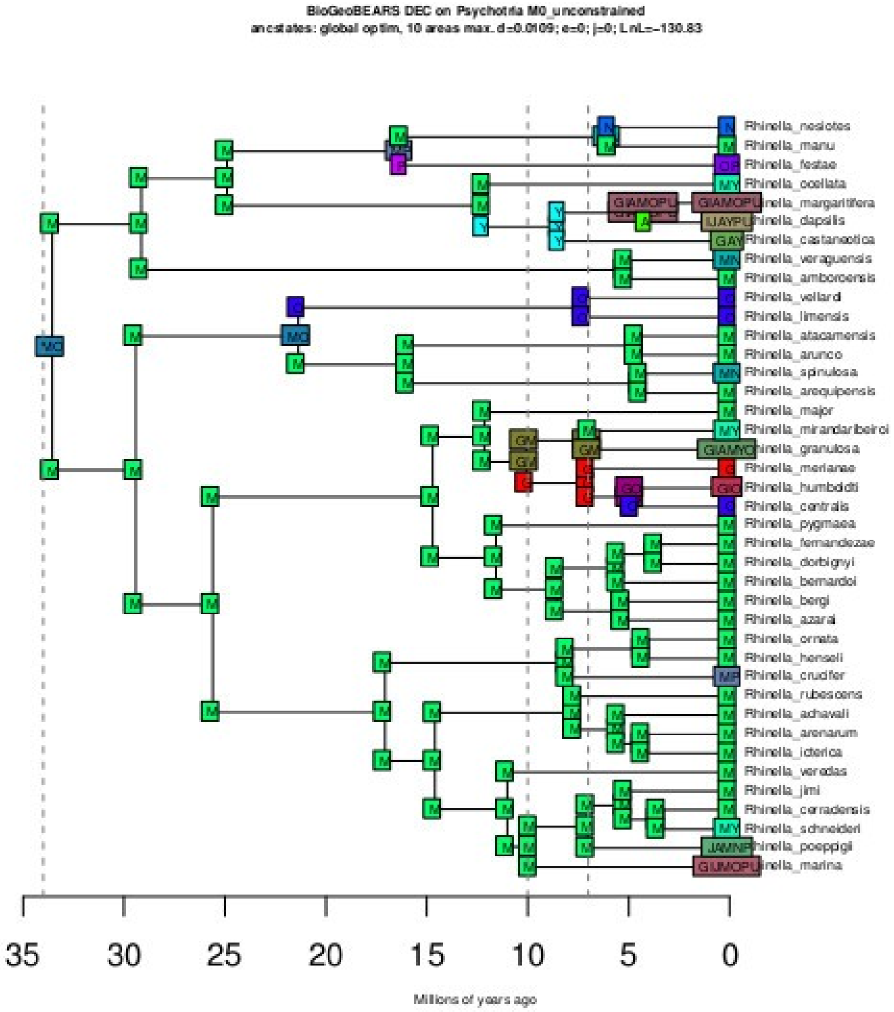
BioGeoBEARS DEC on Psychotria M0_unconstrained
ancstates: global optim, 10 areas max. d=0.0109; e=0; j=0; LnL=-130.83
Rhinella_nesiotes
Rhinella_manu
Rhinella_festae
Rhinella_ocellata
inella_margaritifera
hinella_dapsilis
Rhinella_castaneotica
Rhinella_veraguensis
Rhinella_amboroensis
Rhinella_vellardi
Rhinella_limensis
Rhinella_atacamensis
Rhinella_arunco
Rhinella_spinulosa
Rhinella_arequipensis
Rhinella_major
Rhinella_mirandaribeiroi
hinella_granulosa
Rhinella_merianae
Rhinella_humboldti
Rhinella_centralis
Rhinella_pygmaea
Rhinella_fernandezae
Rhinella_dorbignyi
Rhinella_bernardoi
Rhinella_bergi
Rhinella_azarai
Rhinella_ornata
Rhinella_henseli
Rhinella_crucifer
Rhinella_rubescens
Rhinella_achavali
Rhinella_arenarum
Rhinella_icterica
Rhinella_veredas
Rhinella_jimi
Rhinella_cerradensis
Rhinella_schneideri
hinella_poeppigii
inella_marina
35
30
25
20
15
10
5
0
Millions of years ago

Rhinella M2

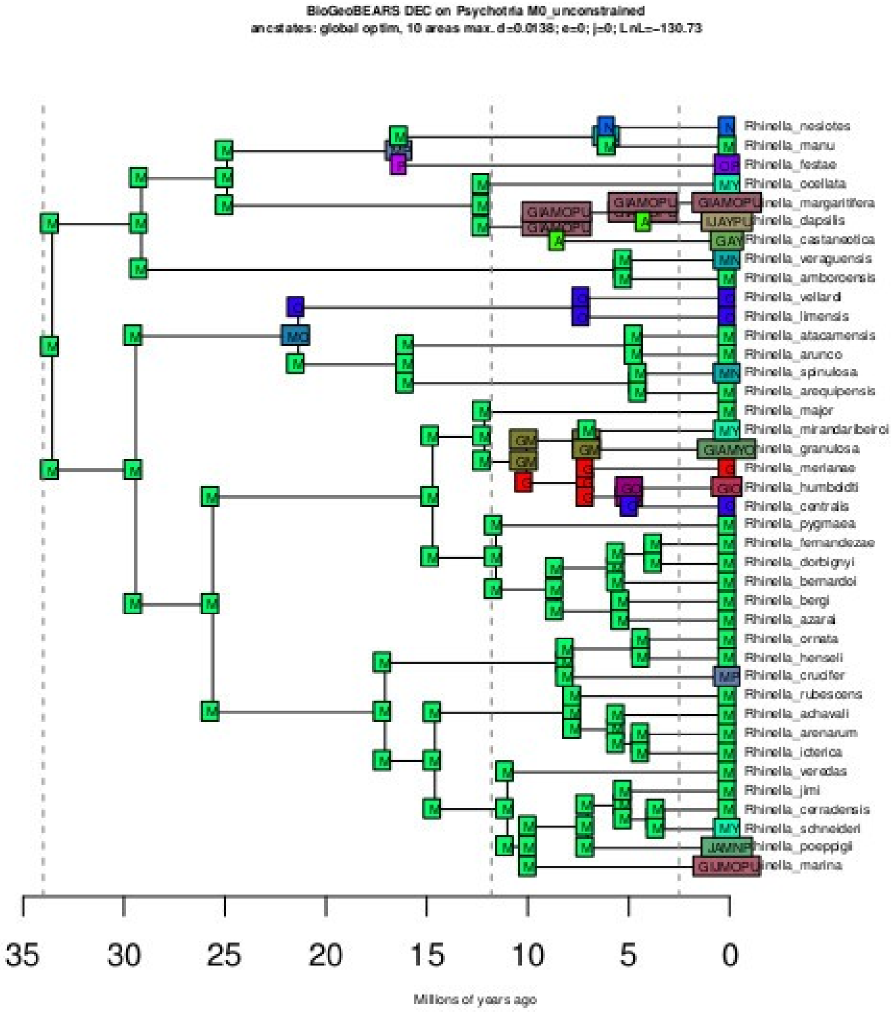
BioGeoBEARS DEC on Psychotria M0_unconstrained
ancstates: global optim, 10 areas max. d=0.0138; e=0; j=0; LnL=-130.73
Rhinella_nesiotes
Rhinella_manu
Rhinella_festae
Rhinella_ocellata
inella_margaritifera
hinella_dapsilis
Rhinella_castaneotica
Rhinella_veraguensis
Rhinella_amboroensis
Rhinella_vellardi
Rhinella_limensis
Rhinella_atacamensis
Rhinella_arunco
Rhinella_spinulosa
Rhinella_arequipensis
Rhinella_major
Rhinella_mirandaribeiroi
hinella_granulosa
Rhinella_merianae
Rhinella_humboldti
Rhinella_centralis
Rhinella_pygmaea
Rhinella_fernandezae
Rhinella_dorbignyi
Rhinella_bernardoi
Rhinella_bergi
Rhinella_azarai
Rhinella_ornata
Rhinella_henseli
Rhinella_crucifer
Rhinella_rubescens
Rhinella_achavali
Rhinella_arenarum
Rhinella_icterica
Rhinella_veredas
Rhinella_jimi
Rhinella_cerradensis
Rhinella_schneideri
hinella_poeppigii
inella_marina
N
M
GP
MY
GIAMOPU
IJAYPU
GAY
MN
GIAMYO
G
GIO
MP
JAMNP
GIJMOPU
MO
GM
A
35
30
25
20
15
10
5
0
Millions of years ago

Rhinella M3

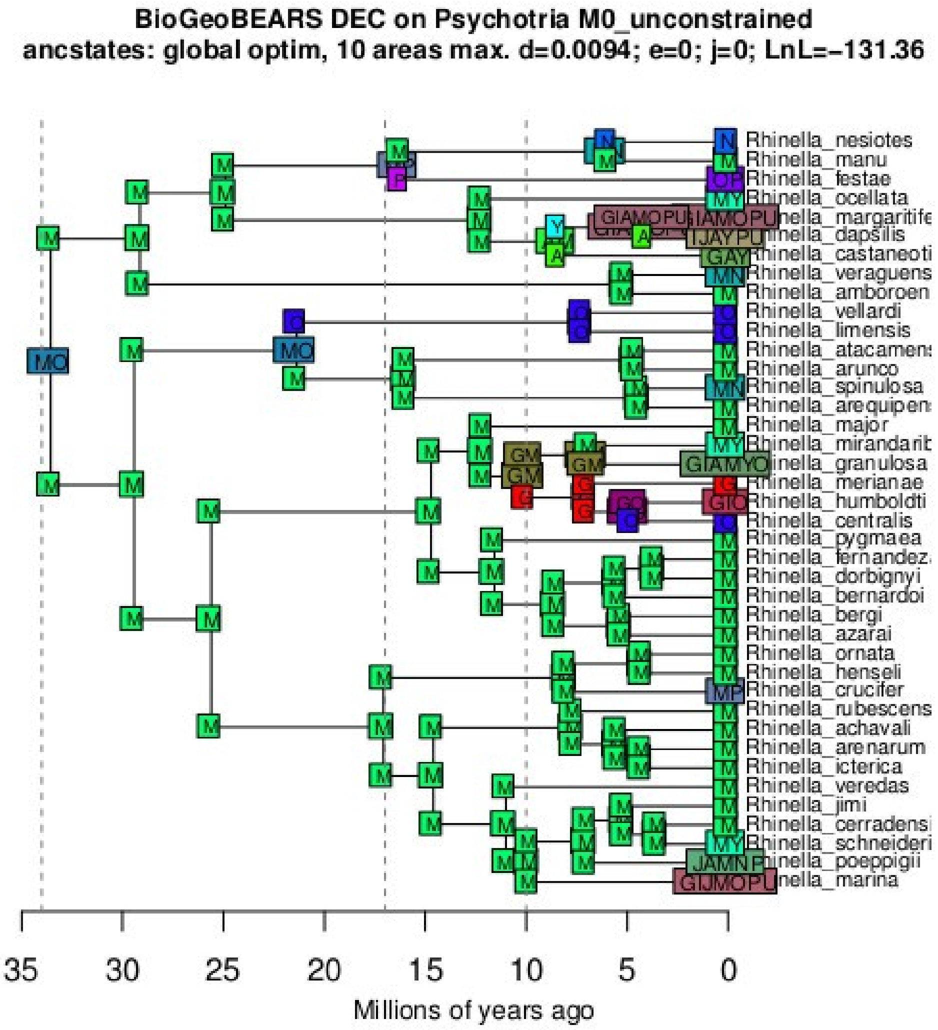
BioGeoBEARS DEC on Psychotria M0_unconstrained
ancstates: global optim, 10 areas max. d=0.0094; e=0; j=0; LnL=-131.36
Rhinella_nesiotes
Rhinella_manu
Rhinella_festae
Rhinella_ocellata
nella_margaritife
nella_dapsilis
Rhinella_castaneoti
Rhinella_veraguens
Rhinella_amboroen
Rhinella_vellardi
Rhinella_limensis
Rhinella_atacamens
Rhinella_arunco
Rhinella_spinulosa
Rhinella_arequipen
Rhinella_major
Rhinella_mirandarib
inella_granulosa
Rhinella_merianae
Rhinella_humboldti
Rhinella_centralis
Rhinella_pygmaea
Rhinella_fernandez
Rhinella_dorbignyi
Rhinella_bernardoi
Rhinella_bergi
Rhinella_azarai
Rhinella_ornata
Rhinella_henseli
Rhinella_crucifer
Rhinella_rubescens
Rhinella_achavali
Rhinella_arenarum
Rhinella_icterica
Rhinella_veredas
Rhinella_jimi
Rhinella_cerradensi
Rhinella_schneideri
inella_poeppigii
nella_marina
35
30
25
20
15
10
5
0
Millions of years ago

Rhinella M4

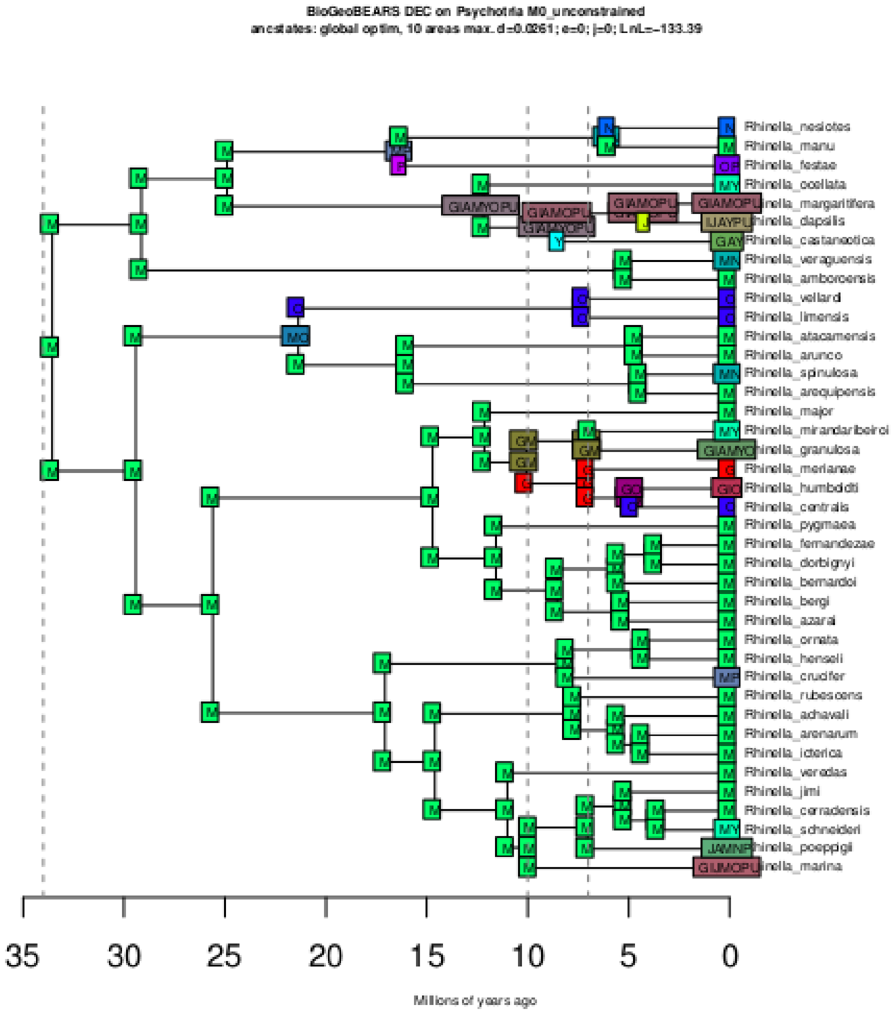
BioGeoBEARS DEC on Psychotria M0_unconstrained
ancstates: global optim, 10 areas max. d=0.0261; e=0; j=0; LnL=-133.39
Rhinella_nesiotes
Rhinella_manu
Rhinella_festae
Rhinella_ocellata
inella_margaritifera
hinella_dapsilis
Rhinella_castaneotica
Rhinella_veraguensis
Rhinella_amboroensis
Rhinella_vellardi
Rhinella_limensis
Rhinella_atacamensis
Rhinella_arunco
Rhinella_spinulosa
Rhinella_arequipensis
Rhinella_major
Rhinella_mirandaribeiroi
hinella_granulosa
Rhinella_merianae
Rhinella_humboldti
Rhinella_centralis
Rhinella_pygmaea
Rhinella_fernandezae
Rhinella_dorbignyi
Rhinella_bernardoi
Rhinella_bergi
Rhinella_azarai
Rhinella_ornata
Rhinella_henseli
Rhinella_crucifer
Rhinella_rubescens
Rhinella_achavali
Rhinella_arenarum
Rhinella_icterica
Rhinella_veredas
Rhinella_jimi
Rhinella_cerradensis
Rhinella_schneideri
hinella_poeppigii
inella_marina
35
30
25
20
15
10
5
0
Millions of years ago

Melipona M0

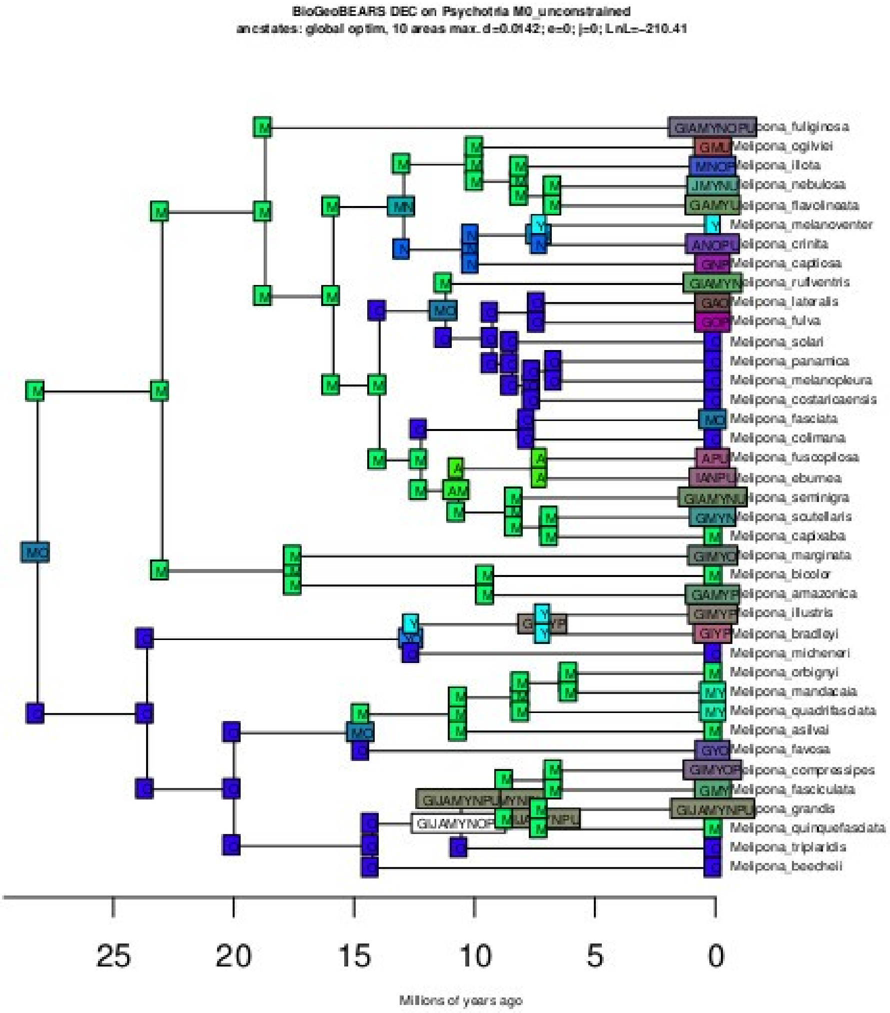

BioGeoBEARS DEC on Psychotria M0_unconstrained
ancstates: global optim, 10 areas max. d=0.0142; e=0; j=0; LnL=-210.41

Melipona M1

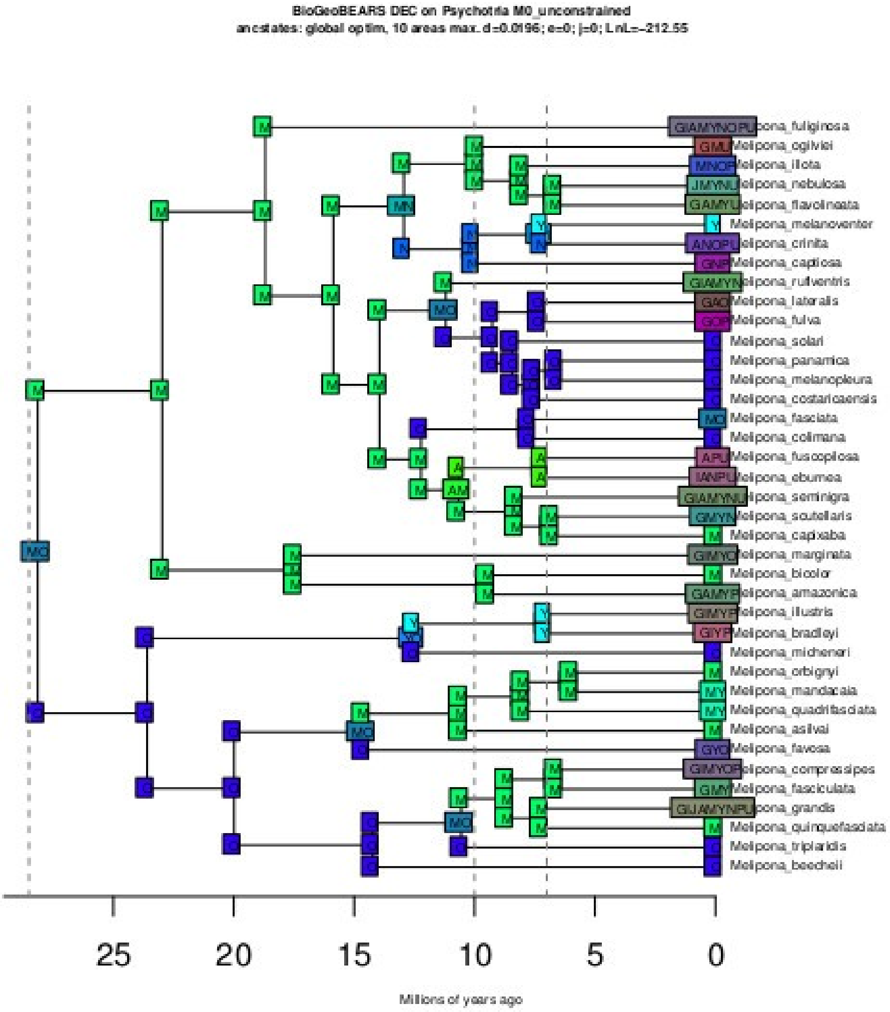
BioGeoBEARS DEC on Psychotria M0_unconstrained
ancstates: global optim, 10 areas max. d=0.0196; e=0; j=0; LnL=-212.55
GIAMYNOPU pona_fuliginosa
GMU Melipona_ogilviei
MNOP elipona_illota
JMYNU elipona_nebulosa
GAMYU elipona_flavolineata
Y Melipona_melanoventer
ANOPU elipona_crinita
GNP Melipona_capitosa
GIAMYN elipona_rufiventris
GAO Melipona_lateralis
GOP Melipona_fulva
Melipona_solari
Melipona_panamica
Melipona_melanopleura
Melipona_costaricaensis
MO Melipona_fasciata
Melipona_colimana
APU Melipona_fuscopilosa
IANPU elipona_eburnea
GIAMYNU lipona_seminigra
GMYN elipona_scutellaris
M Melipona_capixaba
GIMYO elipona_marginata
M Melipona_bicolor
GAMYP elipona_amazonica
GIMYP elipona_illustris
GIYP Melipona_bradleyi
Melipona_micheneri
M Melipona_orbignyi
MY Melipona_mandacaia
MY Melipona_quadrifasciata
M Melipona_asilvai
GYO Melipona_favosa
GIMYOP elipona_compressipes
GMY Melipona_fasciculata
GIJAMYNPU pona_grandis
M Melipona_quinquefasciata
Melipona_triplaridis
Melipona_beecheii
M
MO
MN
AM
A
Y
25
20
15
10
5
0
Millions of years ago

Melipona M2

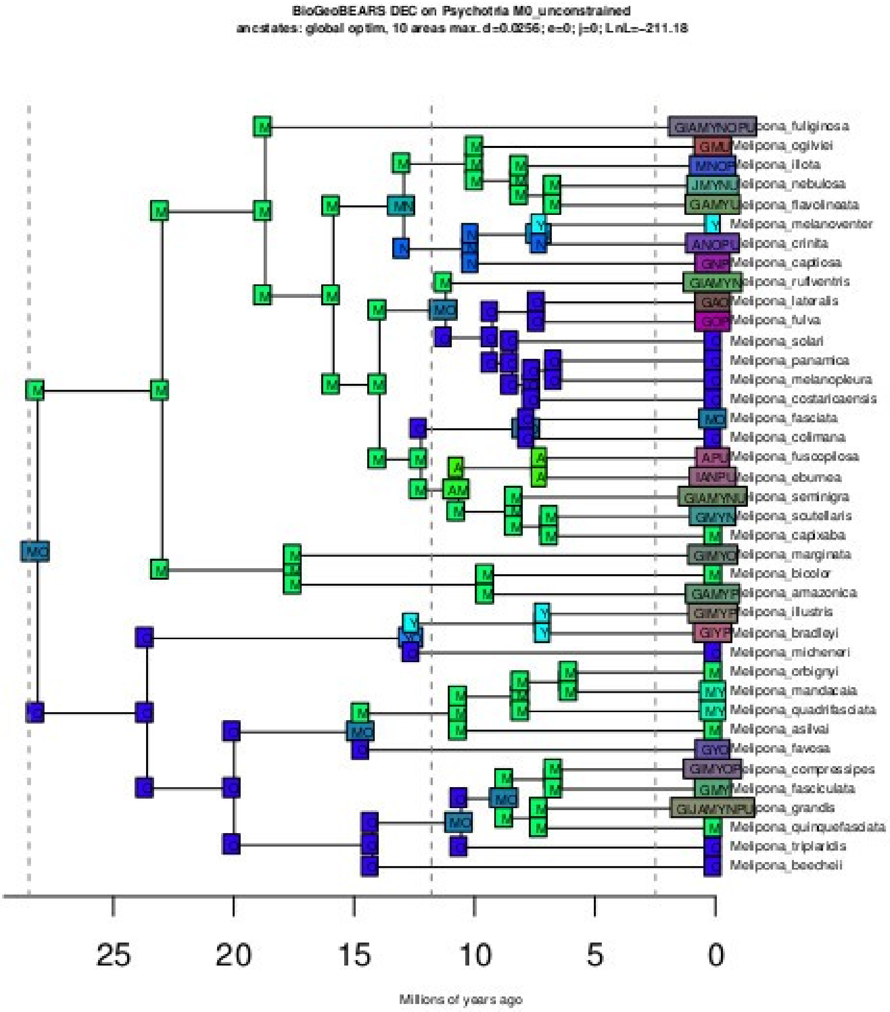
BioGeoBEARS DEC on Psychotria M0_unconstrained
ancstates: global optim, 10 areas max. d=0.0256; e=0; j=0; LnL=-211.18
GIAMYNOPU pona_fuliginosa
GMU Melipona_ogilviei
MNOP elipona_illota
JMYNU elipona_nebulosa
GAMYU elipona_flavolineata
Y Melipona_melanoventer
ANOPU elipona_crinita
GNP Melipona_captiosa
GIAMYN elipona_rufiventris
GAO Melipona_lateralis
GOP Melipona_fulva
Melipona_solari
Melipona_panamica
Melipona_melanopleura
Melipona_costaricaensis
MO Melipona_fasciata
Melipona_colimana
APU Melipona_fuscopilosa
IANPU elipona_eburnea
GIAMYNU lipona_seminigra
GMYN elipona_scutellaris
M Melipona_capixaba
GIMYO elipona_marginata
M Melipona_bicolor
GAMYP elipona_amazonica
GIMYP elipona_illustris
GIYP Melipona_bradleyi
Melipona_micheneri
M Melipona_orbignyi
MY Melipona_mandacaia
MY Melipona_quadrifasciata
M Melipona_asilvai
GYO Melipona_favosa
GIMYOP elipona_compressipes
GMY Melipona_fasciculata
GIJAMYNPU pona_grandis
M Melipona_quinquefasciata
Melipona_triplaridis
Melipona_beecheii
25
20
15
10
5
0
Millions of years ago

Melipona M3

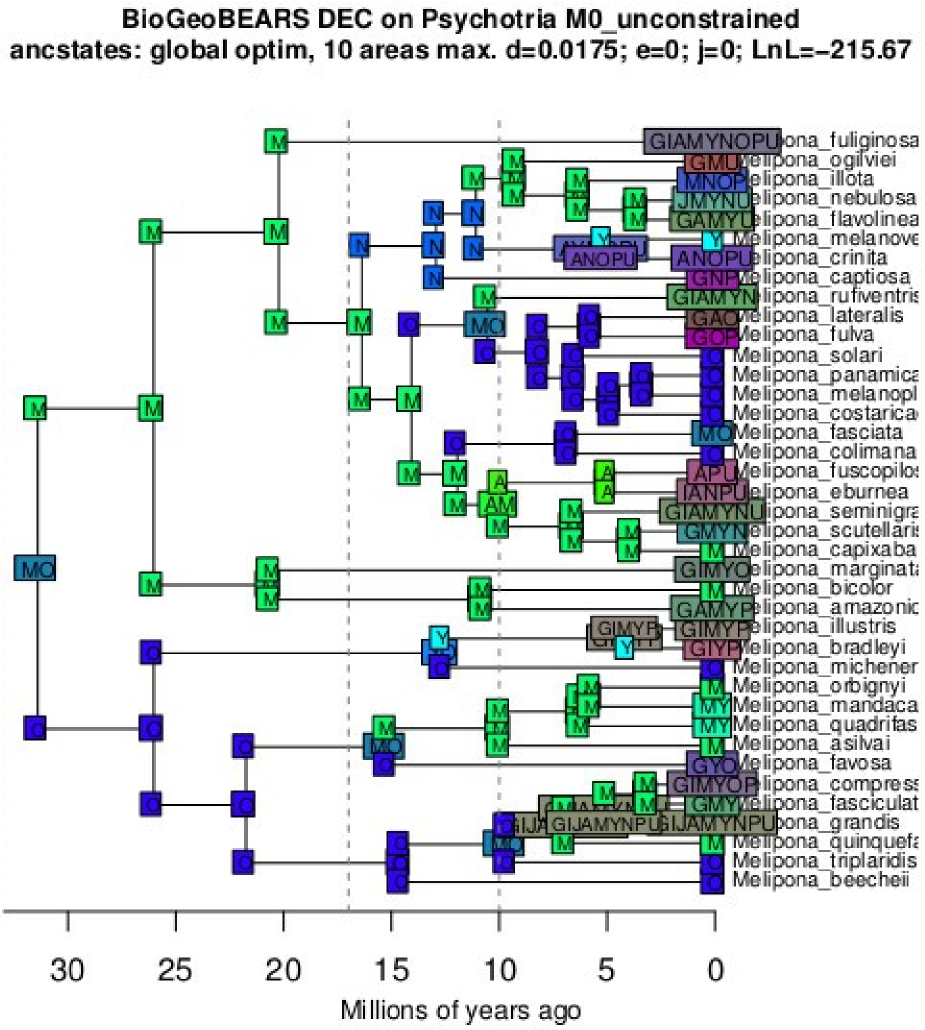
BioGeoBEARS DEC on Psychotria M0_unconstrained
ancstates: global optim, 10 areas max. d=0.0175; e=0; j=0; LnL=-215.67
GIAMYNOPU
ona_fuliginosa
GMU
elipona_ogilviei
MNOP
elipona_illota
JMYNU
elipona_nebulosa
GAMYU
elipona_flavolinea
Y
Melipona_melanove
ANOPU
elipona_crinita
GNP
elipona_captiosa
GIAMYN
lipona_rufiventris
GAO
elipona_lateralis
GOP
Melipona_fulva
Melipona_solari
Melipona_panamica
Melipona_melanopl
Melipona_costarica
MO
Melipona_fasciata
Melipona_colimana
APU
Melipona_fuscopilos
IANPU
elipona_eburnea
GIAMYNU
ipona_seminigra
GMYN
elipona_scutellaris
M
elipona_capixaba
GIMYO
elipona_marginata
M
Melipona_bicolor
GAMYP
elipona_amazonic
GIMYP
elipona_illustris
GIYP
Melipona_bradleyi
Melipona_michener
M
Melipona_orbignyi
MY
Melipona_mandaca
MY
Melipona_quadrifas
M
Melipona_asilvai
GYO
elipona_favosa
GIMYOP
lipona_compress
GMY
elipona_fasciculat
GIJAMYNPU
GIJAMYNPU
pona_grandis
M
Melipona_quinquefa
Melipona_triplaridis
Melipona_beecheii
30
25
20
15
10
5
0
Millions of years ago

Melipona M4

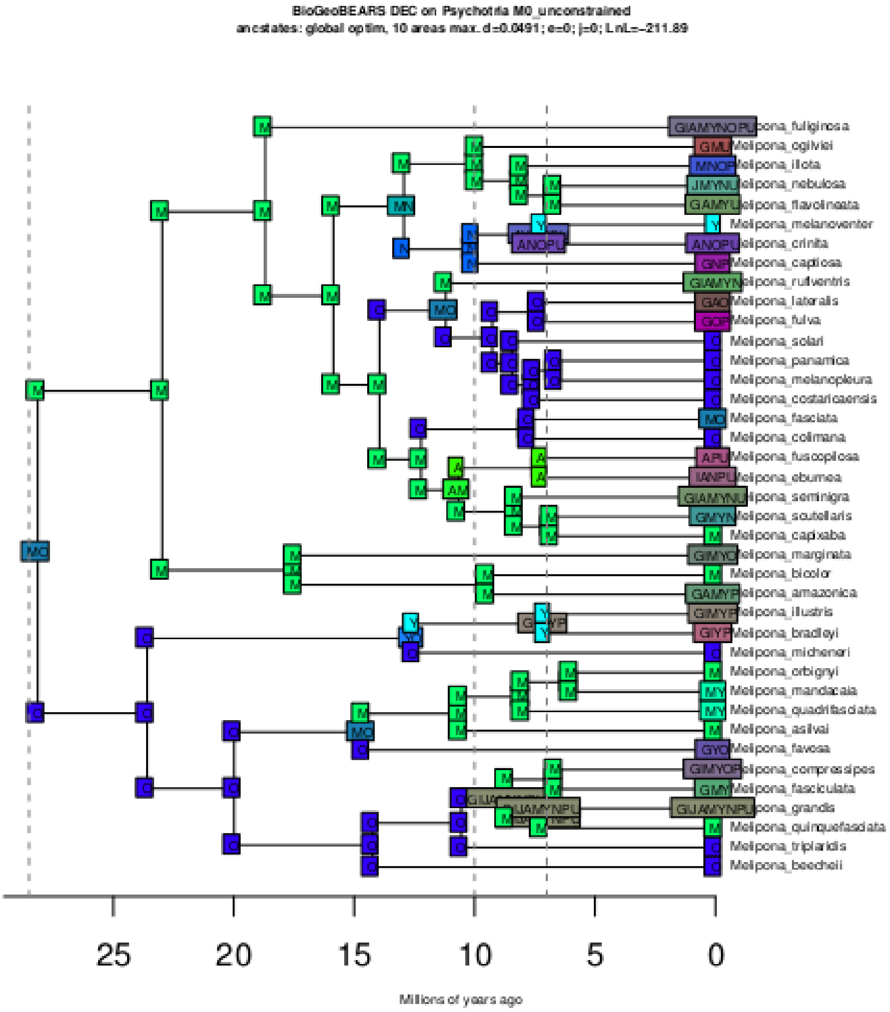
BioGeoBEARS DEC on Psychotria M0_unconstrained
ancstates: global optim, 10 areas max. d=0.0491; e=0; j=0; LnL=-211.89
GIAMYNOPU
pona_fuliginosa
GMU
Melipona_ogilviei
MNOP
Melipona_illota
JMYNU
elipona_nebulosa
GAMYU
elipona_flavolineata
Y
Melipona_melanoventer
ANOPU
elipona_crinita
GNP
Melipona_captiosa
GIAMYN
elipona_rufiventris
GAO
Melipona_lateralis
GOP
Melipona_fulva
G
Melipona_solani
Melipona_panamica
Melipona_melanopleura
Melipona_costaricaensis
MG
Melipona_fasciata
Melipona_colimana
APU
Melipona_fuscopilosa
IANPU
elipona_eburnea
GIAMYNU
lipona_seminigra
GMYN
Melipona_scutellaris
M
Melipona_capixaba
GIMYO
elipona_marginata
Melipona_bicolor
GAMYP
elipona_amazonica
GIMYP
elipona_illustris
GIYP
Melipona_bradleyi
Melipona_micheneri
Melipona_orbignyi
MY
Melipona_mandacaia
Melipona_quadrifasciata
Melipona_asilvai
GYO
Melipona_favosa
GIMYOP
elipona_compressipes
GMY
Melipona_fasciculata
GIJAMYNPU
pona_grandis
Melipona_quinquefasciata
Melipona_triplaridis
Melipona_beecheii
25
20
15
10
5
0
Millions of years ago

Stenodermatinae M0

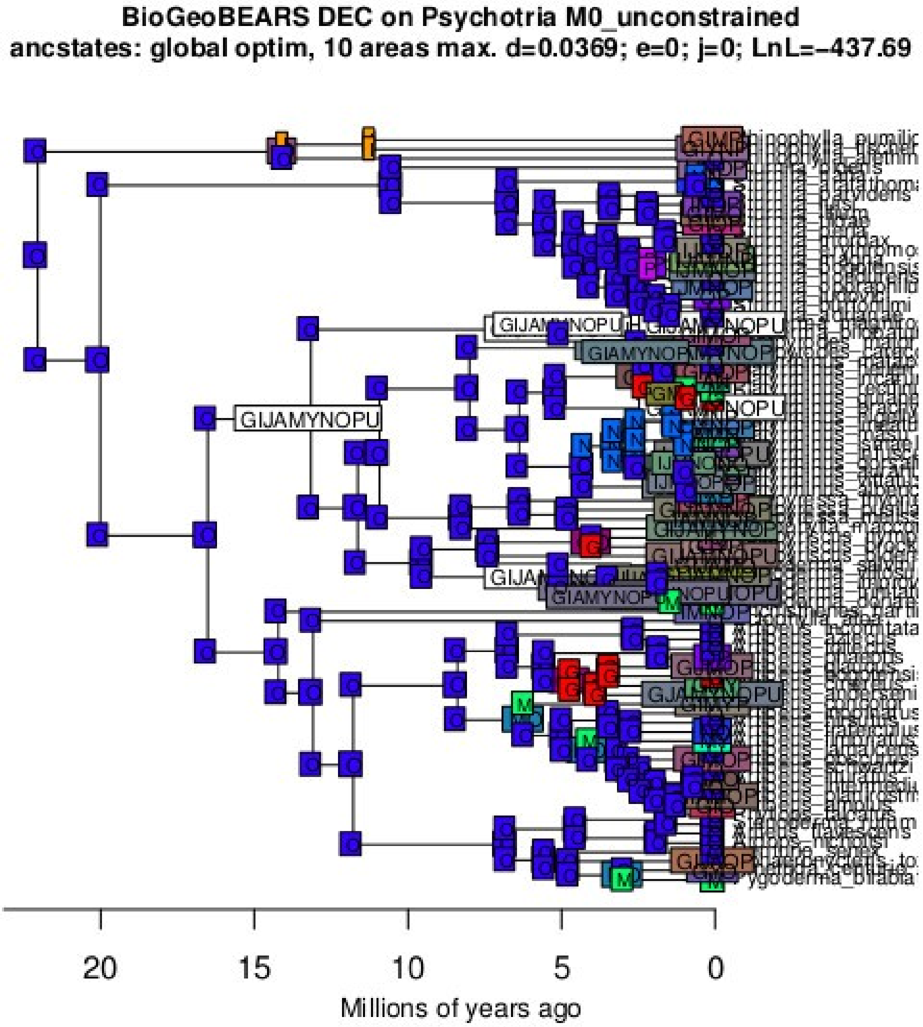

Stenodermatinae M1

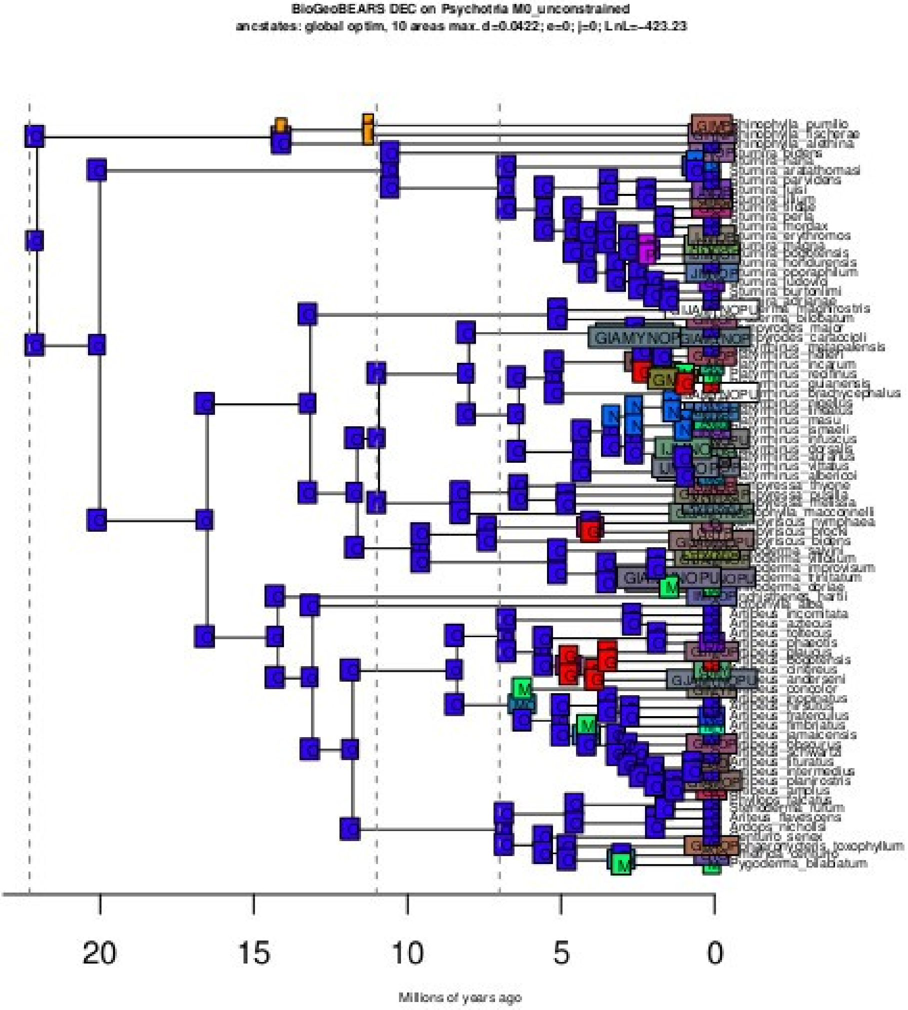

Stenodermatinae M2

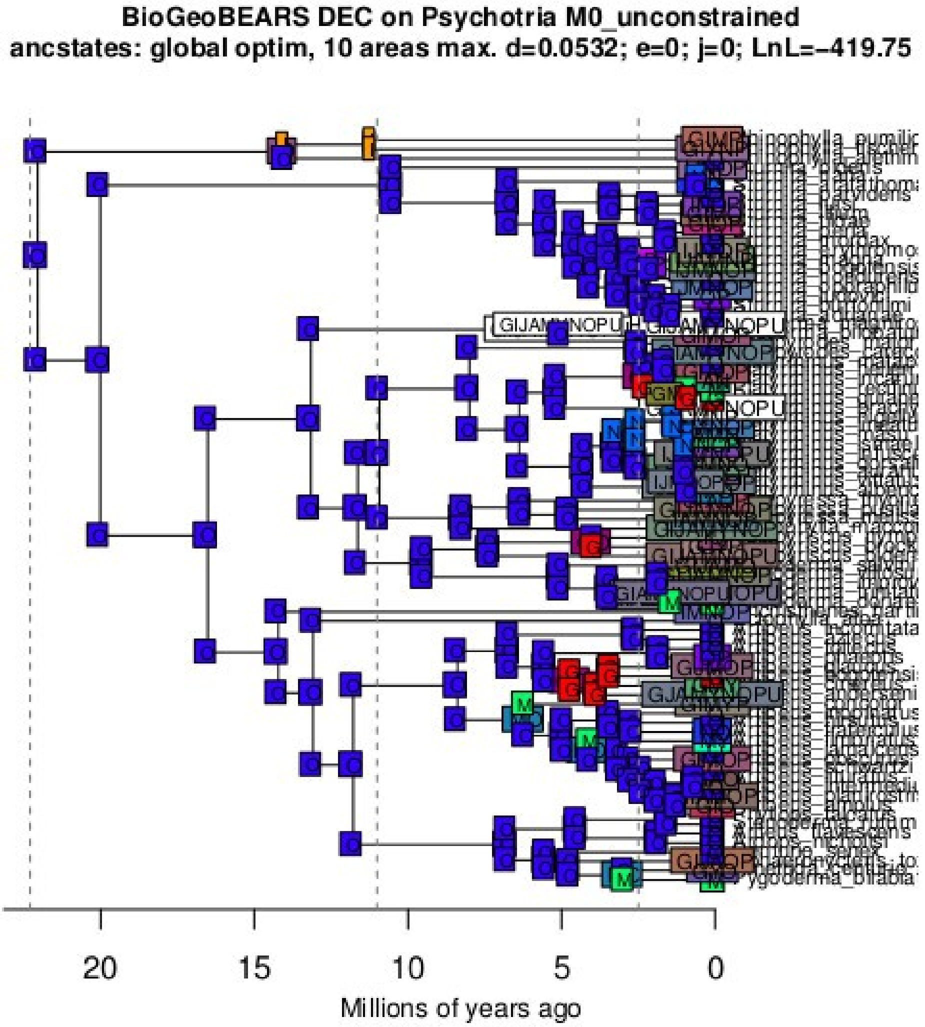

Stenodermatinae M3

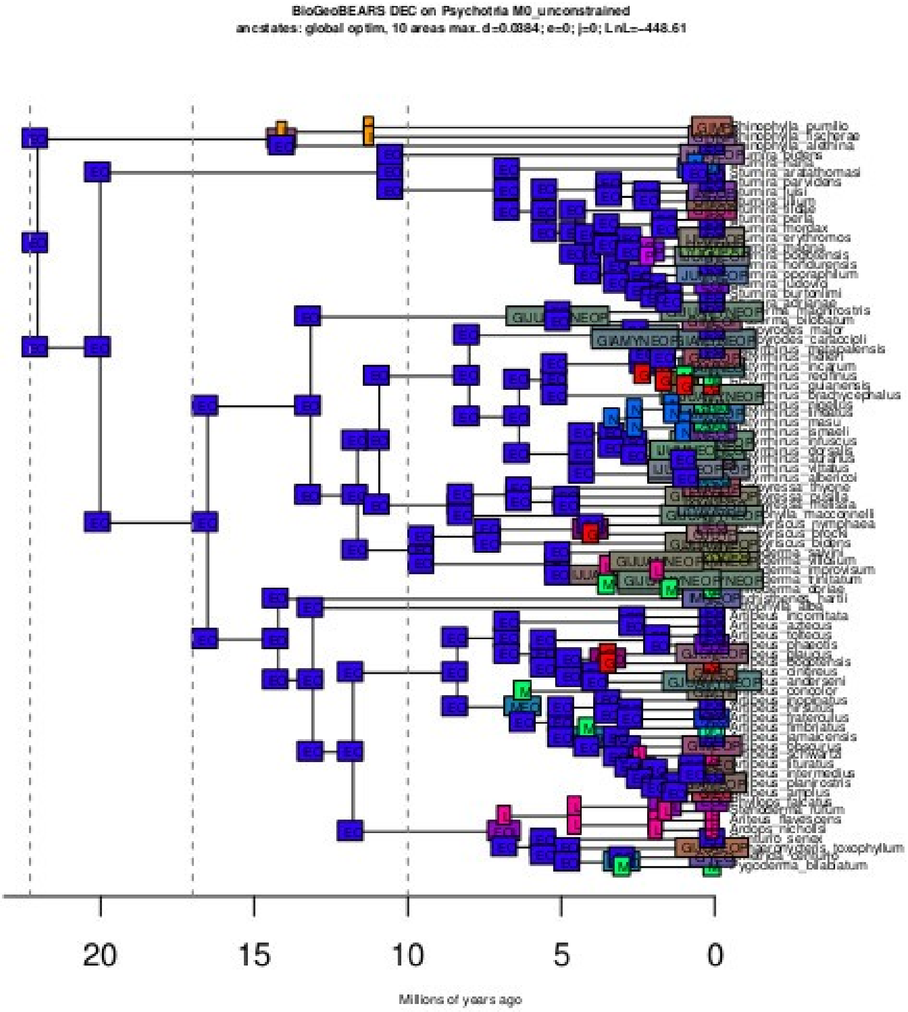

Stenodermatinae M4

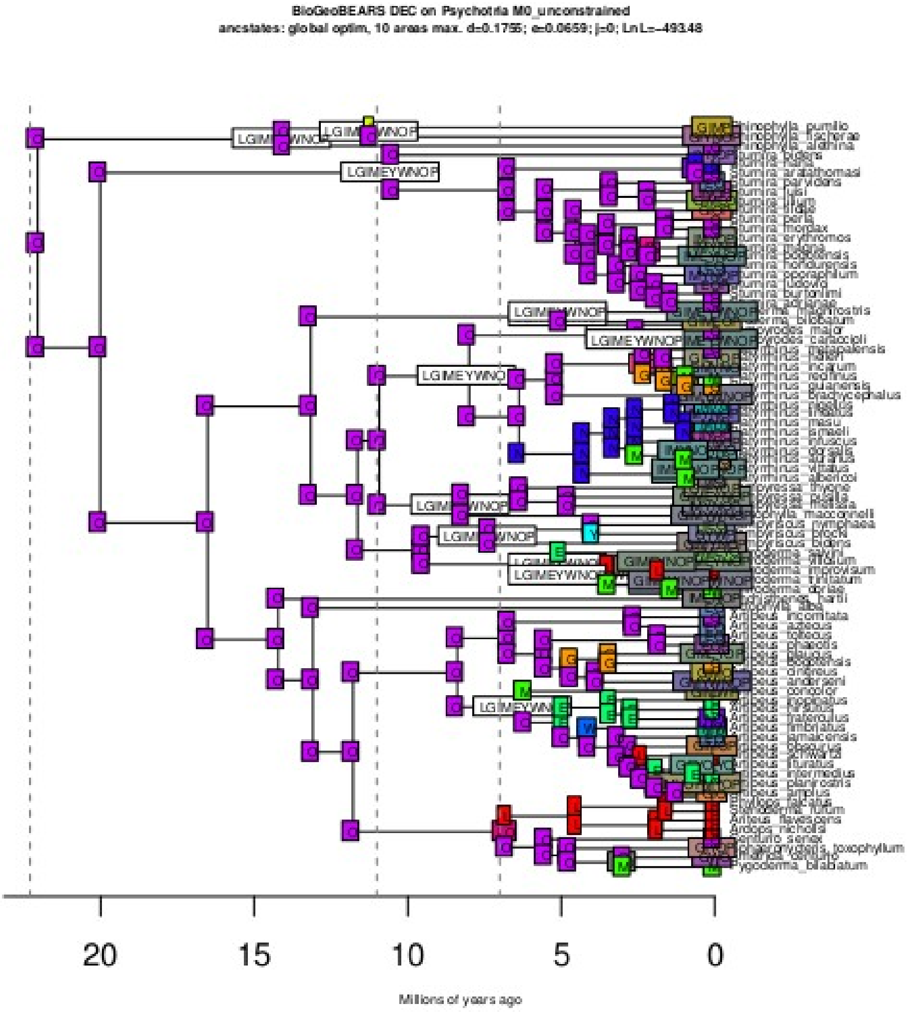

Echimyidae M0

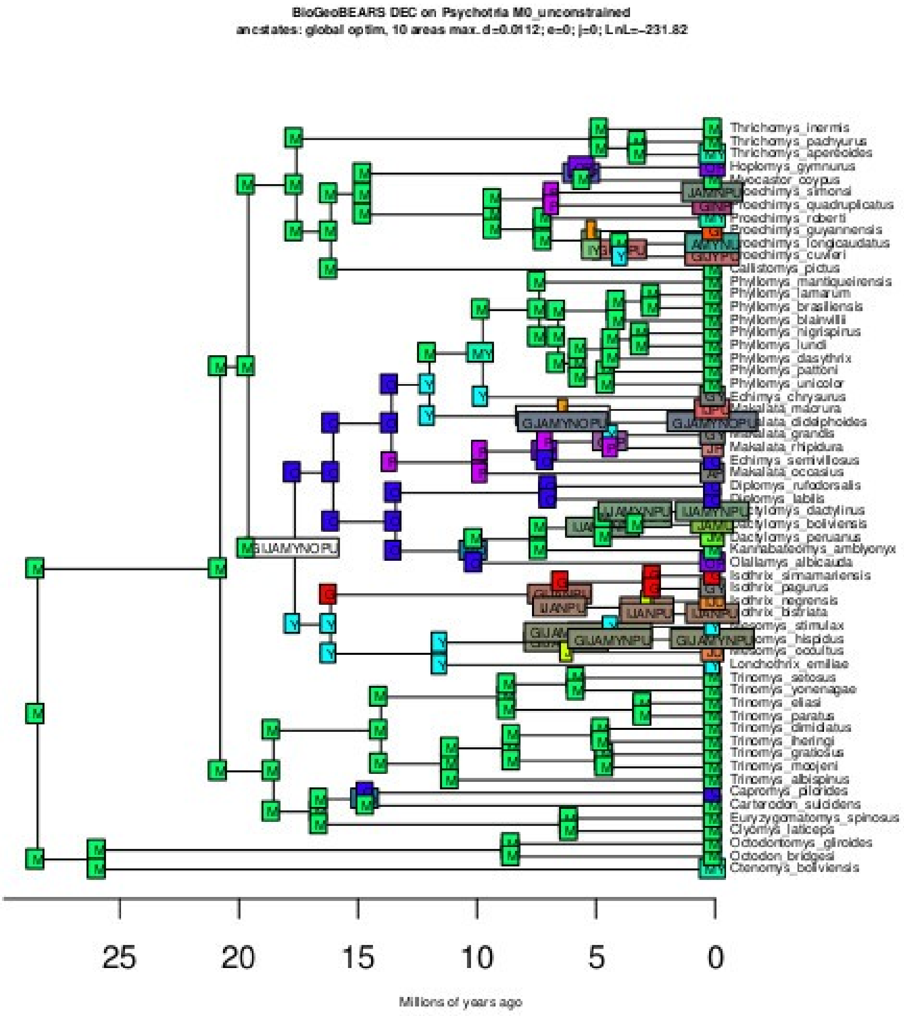

Echimyidae M1

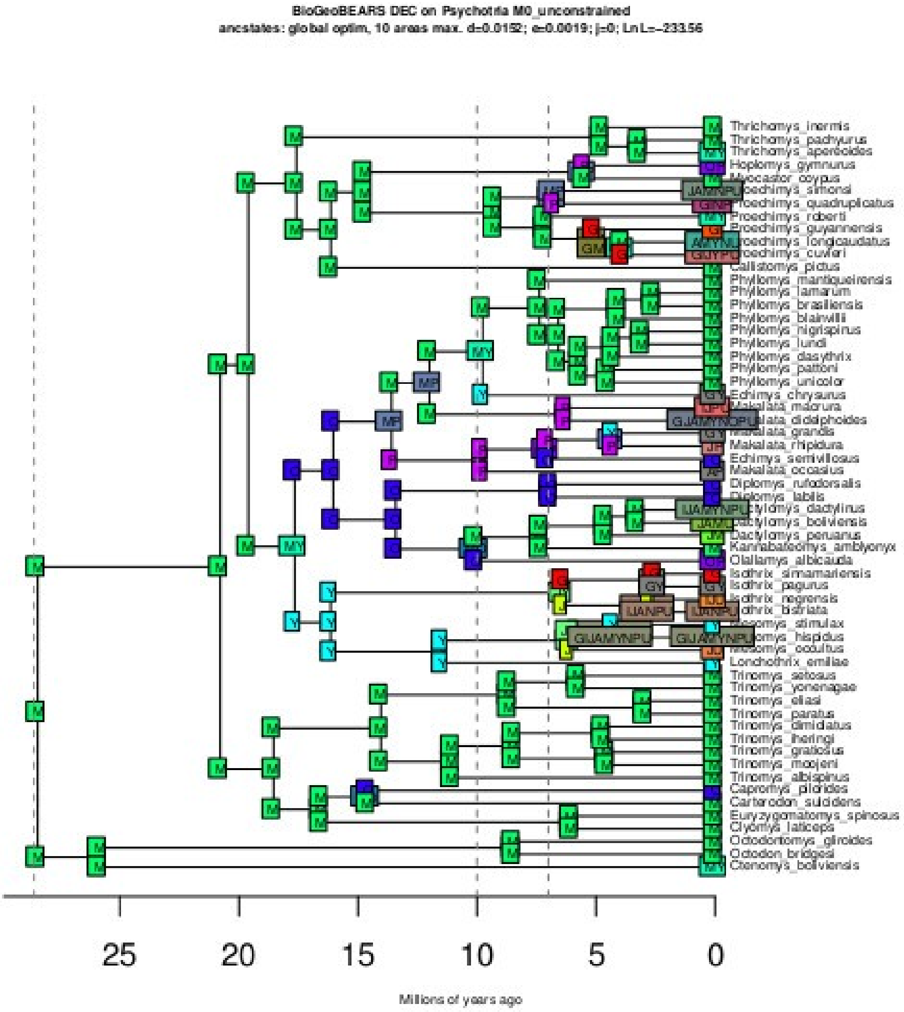

Echimyidae M2

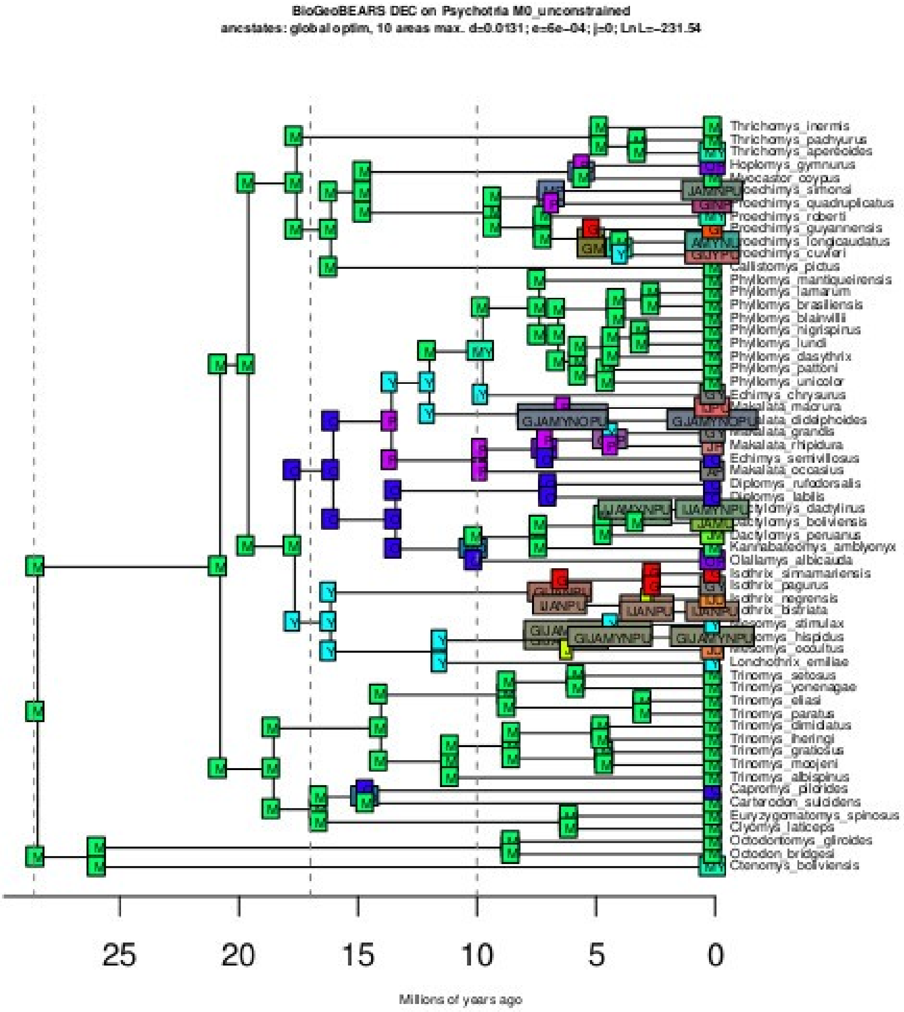

Echimyidae M3

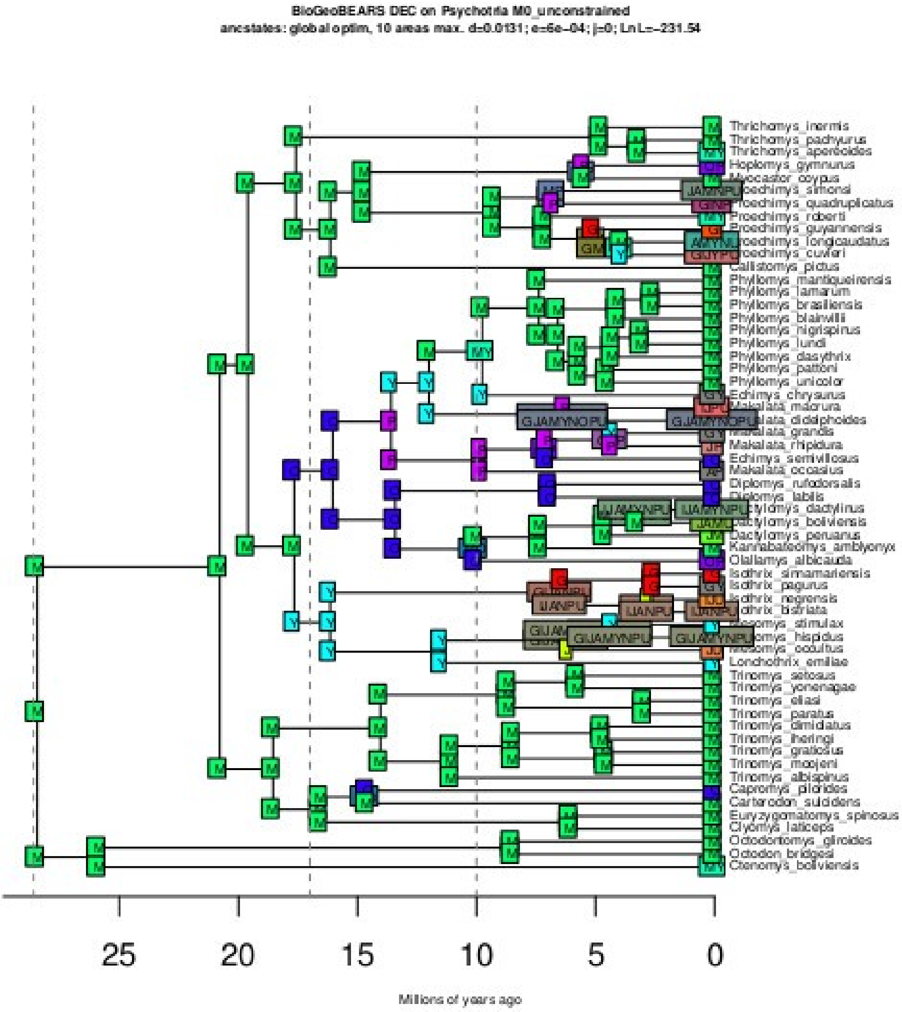

Echimyidae M4

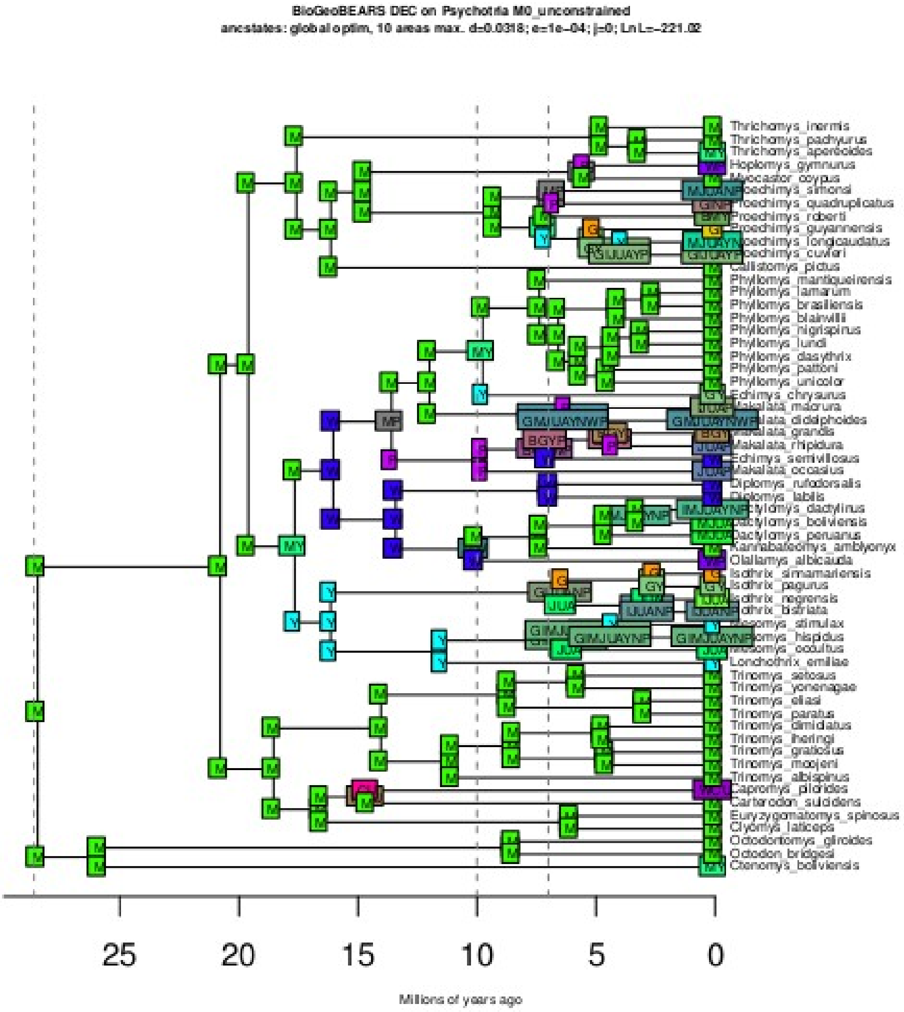

Appendix I

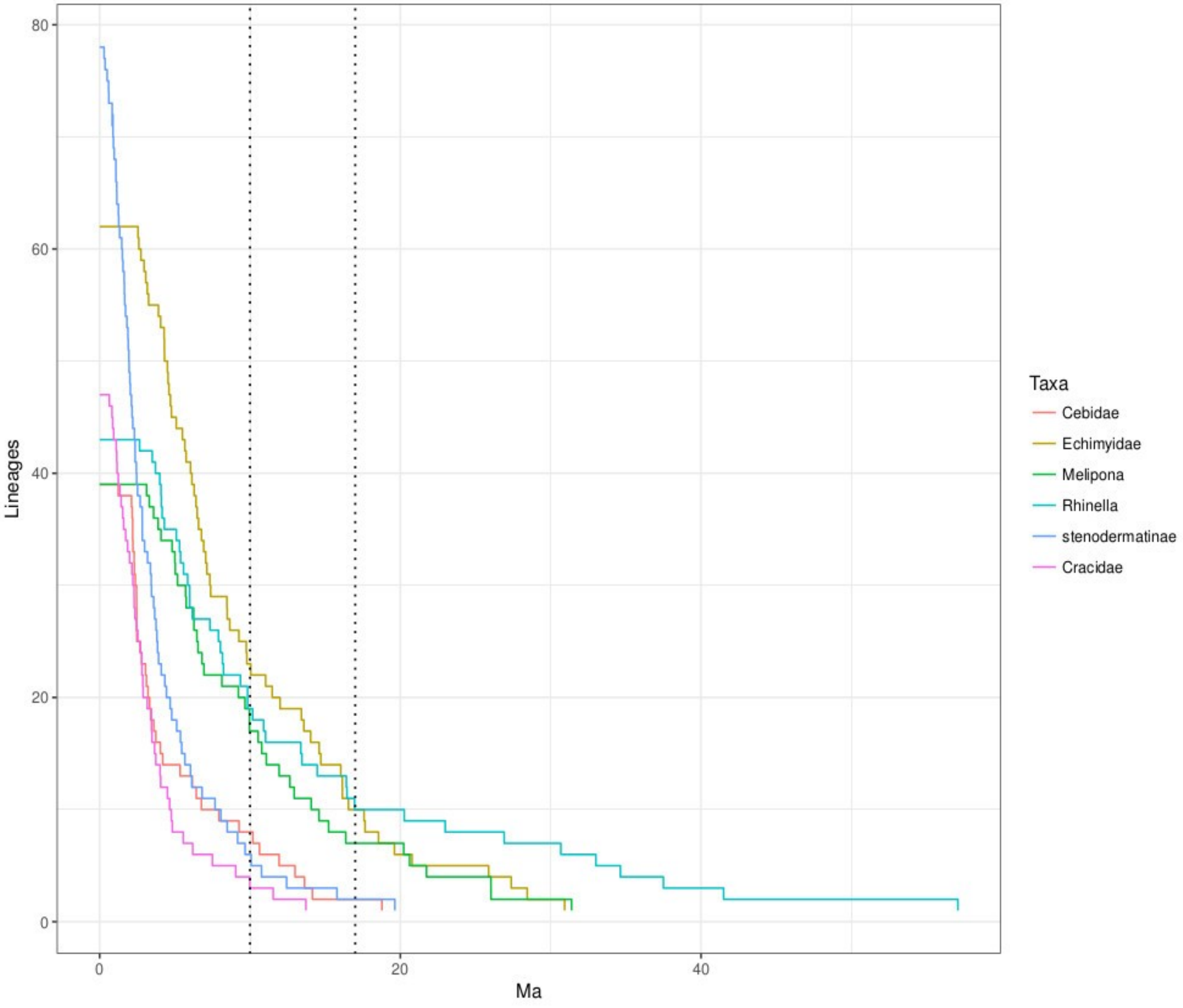

Lineage-through-time plot for all taxa